NASA SP-8093

NASA
SPACE VEHICLE
DESIGN CRITERIA
(CHEMICAL PROPULSION)

SOLID ROCKET MOTOR INTERNAL INSULATION

DECEMBER 1976

NATIONAL AERONAUTICS AND SPACE ADMINISTRATION

FOREWORD

NASA experience has indicated a need for uniform criteria for the design of space vehicles. Accordingly, criteria are being developed in the fellowing areas of technology:

Environment
Structures
Guidance and Control
Chemical Propulsion

Individual components of this work will be issued as separate monographs as soon as they are completed. This document, part of the series on Chemical Propulsion, is one such monograph. A list of all monographs issued prior to this one can be found on the final pages of this document.

These monographs are to be regarded as guides to design and not as NASA requirements, except as may be specified in formal project specifications. It is expected, however, that these documents, revised as experience may indicate to be desirable, eventually will provide uniform design practices for NASA space vehicles.

This monograph, "Solid Rocket Motor Internal Insulation," was prepared under the direction of Howard W. Douglass, Chief, Design Criteria Office, Lewis Research Center; project management was by Carl C. Ciepluch and M. Murray Bailey. The monograph was written by Sherwood E. Twitchell of Hercules Incorporated and was edited by Russell B. Keller, Jr. of Lewis. Significant contributions to the text were made by R. G. Knauer of Aerojet Solid Propulsion Company. To assure technical accuracy of this document, scientists and engineers throughout the technical community participated in interviews, consultations, and critical review of the text. In particular, R. L. Bailey, Jet Propulsion Laboratory, California Institute of Technology; R. F. Mulliken, Langley Research Center; and J. J. Pelouch, Lewis Research Center reviewed the monograph in detail.

Comments concerning the technical content of these monographs will be welcomed by the National Aeronautics and Space Administration, Lewis Research Center, (Design Criteria Office), Cleveland, Ohio 44135.

December 1976

GUIDE TO THE USE OF THIS MONOGRAPH

The purpose of this monograph is to organize and present, for effective use in design, the significant experience and knowledge accumulated in development and operational programs to date. It reviews and assesses current design practices, and from them establishes firm guidance for achieving greater consistency in design, increased reliability in the end product, and greater efficiency in the design effort. The monograph is organized into two major sections that are preceded by a brief introduction and complemented by a set of references.

The State of the Art, section 2, reviews and discusses the total design problem, and identifies which design elements are involved in successful design. It describes succinctly the current technology pertaining to these elements. When detailed information is required, the best available references are cited. This section serves as a survey of the subject that provides background material and prepares a proper technological base for the *Design Criteria* and Recommended Practices.

The *Design Criteria,* shown in italics in section **3,** state clearly and briefly what rule, guide, limitation, or standard must be imposed on each essential design element to assure successful design. The *Design Criteria* can serve effectively as a checklist of rules for the project manager to use in guiding a design or in assessing its adequacy.

The Recommended Practices, also in section 3, state how to satisfy each of the criteria. Whenever possible, the best procedure is described; when this cannot be done concisely, appropriate references are provided. The Recommended Practices, in conjunction with the *Design Criteria,* provide positive guidance to the practicing designer on how to achieve successful design.

Both sections have been organized into decimally numbered subsections so that the subjects within similarly numbered subsections correspond from section to section. The format for the Contents displays this continuity of subject in such a way that a particular aspect of design can be followed through both sections as a discrete subject.

The design criteria monograph is not intended to be a design handbook, a set of specifications, or a design manual. It is a summary and **a** systematic ordering of the large and loosely organized body of existing successful design techniques and practices. Its value and its merit should be judged on how effectively it makes that material available to and useful to the designer.

CONTENTS

LIST OF FIGURES

LIST OF TABLES

SOLID ROCKET MOTOR INTERNAL INSULATION

1 INTRODUCTION

Internal insulation in a solid rocket motor is a layer of heat-barrier material placed between the internal surface of the case and the propellant. The primary function of internal insulation is to prevent the case from reaching temperatures that endanger its structural integrity; in addition, the insulation performs important secondary functions:

- Inhibits burning on certain propellant grain surfaces on which burning is undesirable.
- Buffers the transmission of case strain into the propellant.
- Bars the migration of mobile chemical species within the motor.
- Prevents impingement of combustion products on the case.
- Seals the case, joints, and fittings to prevent loss of pressure and damage from hot combustion products.
- Guides combustion products into the nozzle in laminar flow to the greatest extent possible.

Most insulator materials fail to perform one or more of the secondary functions, but if the primary function is performed well, designers usually are able to modify the design or provide other parts or materials to ensure the performance of secondary functions.

Two examples of insulation failures illustrate the range of problems that occur in the desigii of internal insulation:

(1) Early Minuteman motors employed butadiene-acrylonitrile rubber (NBR) insulation with double-base (DB) propellant. Insulation erosion measured after static firing was several times the anticipated amount, and if the insulation had been pared to flightweight thickness, the erosion would have caused motor failure. The excessive erosion was attributable to the affinity of NBR for

nitroglycerin, the result being a material with high erosion rates. Substitution of butadiene-styrene rubber **(SBR),** which absorbs much less nitroglycerin, reduced the high erosion rates.

(2) Failures or severe problems in several large development booster motors (52-, 102-, and 156-in.* diam.) were attributable to solvent residue. The hand-layup method for fabricating the insulation required a rubber solvent at the interfaces of layers of rubber to produce adhesion. When insufficient drying times were allotted for each layer, the insulation produced was high in solvent content. Erosion during firing then was high, because the erosion rate increases as the solvent content of elastomer increases.

This monograph, drawing on the extensive design experience accumulated in the development of internal insulation for rocket motors, presents guidelines for avoiding critical problems and indicates the approaches that lead to successful design. The monograph is intended to be used in the design of insulators after the systems-integration and -optimization work has been completed. The document is written with concern only for design of the insulator itself, and is organized to correspond to the logical design sequence: selection of materials, evaluation of thermal environment, insulator design, insulator fabrication and processing, and design verification. Sufficient detail is provided to assist the designer in avoiding known design pitfalls, but no attempt is made to reproduce material that is covered adequately in the references.

*Factors for converting U.S. customary units to the International System **of** Units **(SI units) are** given in **Appendix A.**

2. STATE OF THE ART

The designer of internal insulation must perform the following tasks: (1) select the insulation material, (2) establish the insulation thickness throughout the motor, and **(3)** design flaps, joints, fillets, and inserts that are needed for proper insulator performance. Figure 1 illustrates many of the insulation design features in solid rocket motors. Figure 1(a) (aft section, multi-nozzle configuration) is typical of Minuteman motors; figure 1(b) (aft section, submerged nozzle) is typical of Poseidon motors. The conocyl* grain slot in the forward dome (nozzle is aft) of figure 1(c) (full section) is typical of Poseidon first stage. The propellant slots at the tangent lines of the full section are typical of large segmented motors. The heat-flux data in figure 1 present the rate at which heat is transferred to insulation near these special design features. The variation in insulator thickness illustrated in figure 1 is intended to allow for variation in time of exposure to the propellant combustion products, variations in local heat flux and in particle-impingement effects, and desired downstream flow patterns. Thicker insulation is needed in areas exposed to severe conditions and in areas where streamline or other specific downstream flow effects are desired.

Knowledge of insulator function is a prerequisite to both selection of material and thickness design. Most current insulators for solid rocket motors function as heat barriers primarily through the mechanism of ablation; i.e., the material absorbs heat by increasing in temperature and changing in chemical or physical state, the changes usually being accompanied by loss of surface material. The best current knowledge of the ablative insulation function divides the material into three zones (fig. 2): (1) virgin-material zone, (2) decomposition zone, and **(3)** reaction (or char) zone. The interfaces that separate these zones are somewhat indistinct, but even so the zones can be defined by the principal phenomena found in each.

In the virgin-material zone, the phenomena are relatively simple. The temperatures are low enough that changes in chemical properties of the material are negligible, and heat is transferred by simple conduction.

In the decomposition zone, energy is absorbed by the fragmentation and scission of molecules. **As** the temperature of the material increases, the decomposition reactions become more vigorous and cause a substantial polymer weight loss. Decomposition of some inorganic fillers also occurs, and occluded water is lost. Two energy-transfer modes are present in the decomposition zone: (1) transfer by conduction, and **(2)** transfer by pyrolysis and subsequent loss of hot combustion products. **As** the temperature of the reaction increases, a large percentage of the total energy accommodated in the overall ablation process is absorbed by cracking and heating of pyrolysis gases. The magnitude of the energy absorption depends on the chemical content of the materials involved and on the temperature at which the reaction occurs. In general, while a relatively small number of decomposition reactions may be exothermic, the large majority of the reactions are endothermic.

***Terms, symbols, materials, and abbreviations are defined or identified in Appendix B.**

Region	Heat flux, Btu/ft^2 - sec
A, A", B	300 → 800
A', C	200 → 350
D, E	75 → 200

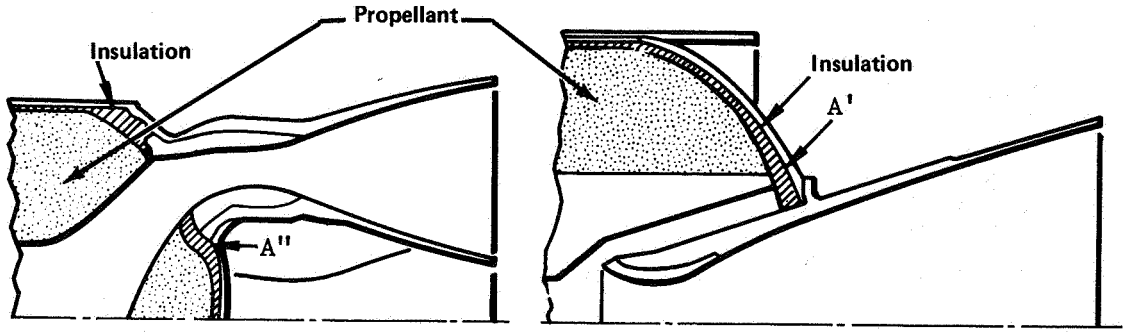

(a) Aft section, multi-nozzle

(b) Aft section, submerged nozzle

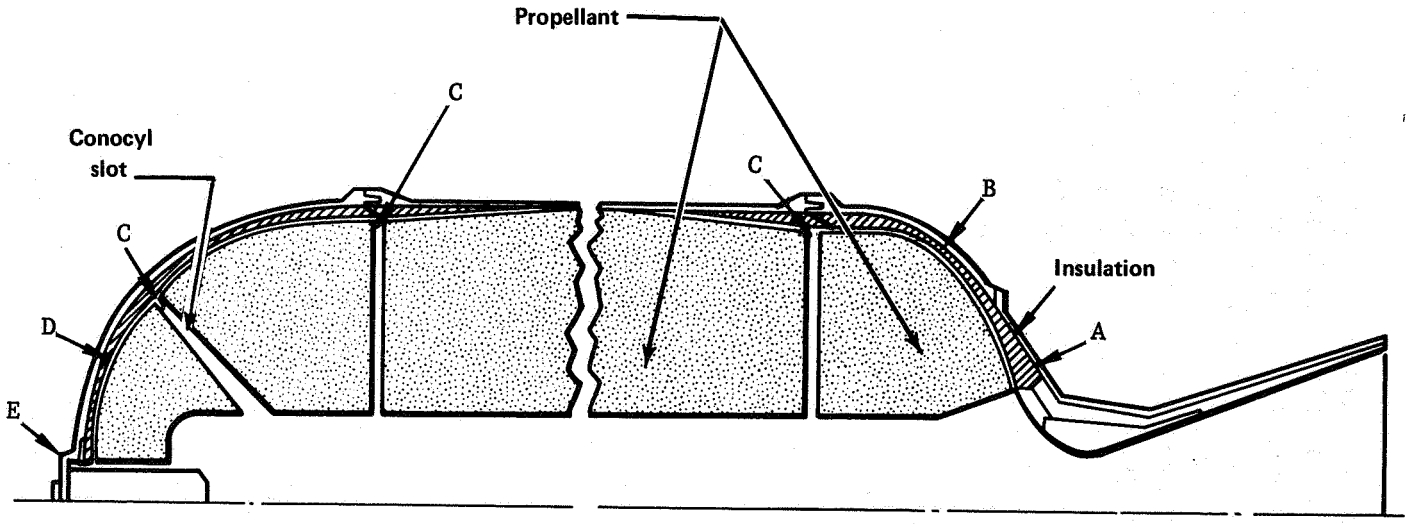

(c) Full section, conocyl/slotted grain, single nozzle

Figure 1. — Typical locations and relative thicknesses of internal insulation in a solid rocket motor.

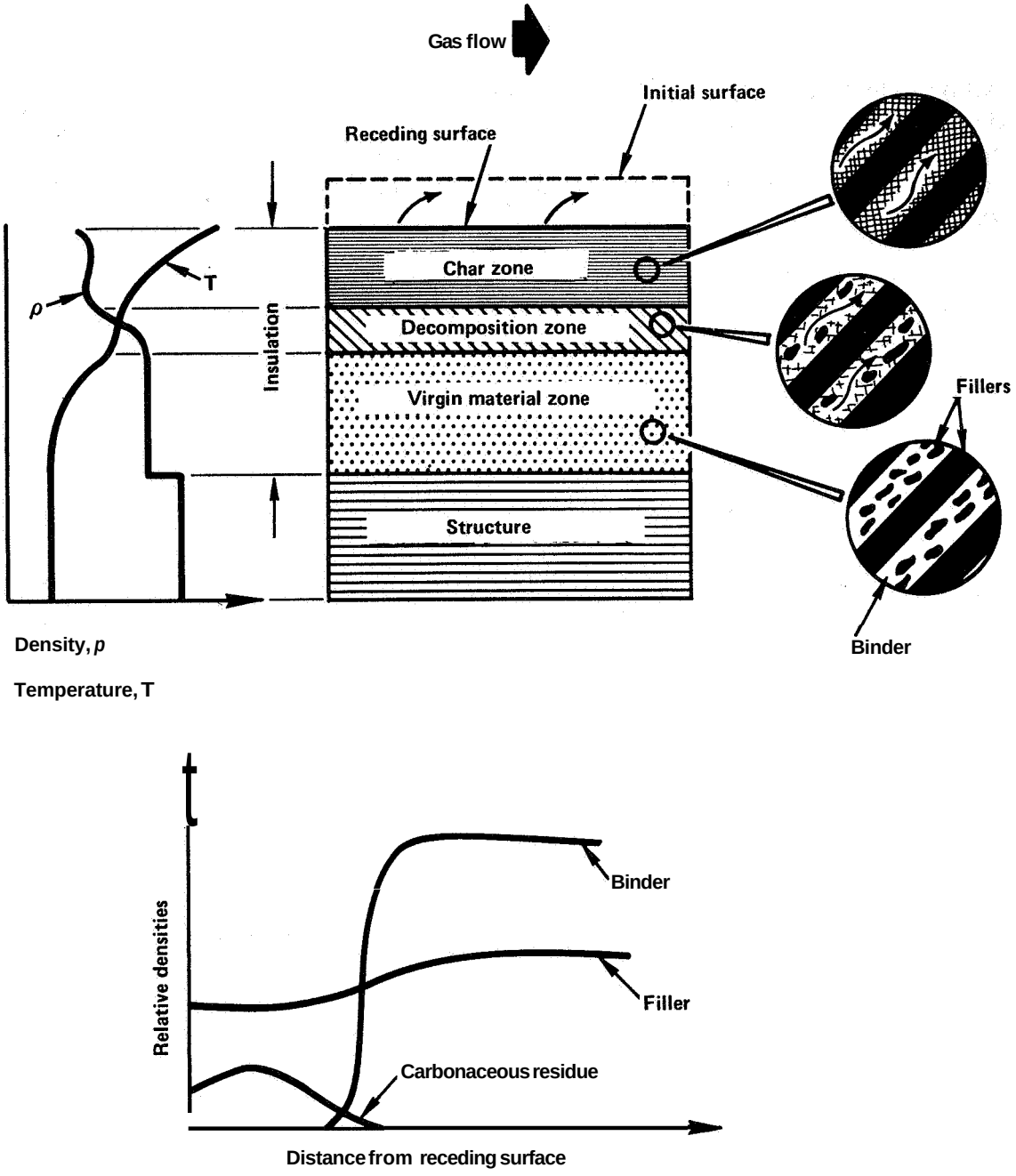

Figure 2. – Model of **ablating insulation.**

In the char zone, phenomena are similar to those in the decomposition zone, the principal difference being the particular reactions involved. The decomposition reaction produces a residue that continues to decompose and finally yields a residue that is primarily elemental carbon. Decomposition of inorganic components and pyrolysis gas cracking are also characteristic of this zone. Cracking of the low-temperature pyrolysis gas may result in the deposition of carbon within the char layer, the so-called "coking" effect. Static pressure, mass flowrate, composition of the pyrolysis gas, and rate of temperature rise – all vary with time in the char zone.

As exposure to the motor environment continues, surface material is eroded. The term "surface regression" is used to describe the total effect of various modes of surface loss. These modes include the following:

(1) Chemical effects:

- Surface chemical reactions of char-layer components with propellant gases and particles (usually liquid).
- Subsurface reactions (usually pyrolysis) in the char zone and the decomposition zone.

(2) Physical effects:

- Surface erosion due to particle impingement and shear stress imposed by skin friction.
- Thermal stress induced by heat transfer.
- Subsurface weakening due to mechanical and thermal stresses in the char layer and the decomposition zone; i.e., spallation due to internal pressure created by pyrolysis gas.

(3) Combinations of chemical and physical effects.

2.1 GENERAL CONSIDERATIONS

2.1.1 Design Approach

As with many design procedures in which highly complex physical and chemical phenomena are involved, insulator design is based on theory, observations, and measurements of material behavior and performance. However, the usefulness of material data depends on the

designer's ability to relate the data to different motor conditions. An example of this point was the redesign of the Scout vehicle. One of the proposed changes to an upper stage was reduction of the nozzle throat diameter. The result of this change would be higher chamber pressure, shorter burn time, and other conditions producing a more severe insulator service environment for a shorter time. The more severe environment suggested that the insulator should be thicker, but the shorter burn time lent some hope of compensating for the environment. A purely empirical approach to redesign would have required test firings to eliminate the uncertainty and determine the thickness needed. Instead, the semi-empirical design approach outlined in figure 3* was used to prove quickly that no changes to the insulator were necessary.

The design approach illustrated in figure 3 utilizes both theory and test history. The insulation material performance history referred to in the figure is firing and test history collected on the same material proposed for the insulator design. A discussion of the theoretical portions of this design approach is presented in section 2.3; the empirical portions are discussed in section 2.6. The marriage of theory and history takes place in the char-rate correlations discussed in section 2.4.1.1.2; thermal design occupies the balance of section 2.4.1. When thermal design requirements have been met, the thermal design must be evaluated for its structural adequacy; structural design is discussed in section 2.4.2. Postfire analysis is necessary to provide confidence in design adequacy and, in the event of overdesign or underdesign, to facilitate re-design; section 2.6.1 discusses the tools and methods used for postfire analysis.

When the prerequisites of the figure-3 design approach cannot be met because of data, funding, or schedule limitations, the designer must modify his approach. If large quantities of reliable data are available, the designer may make a somewhat less scientific but educated interpolation or extrapolation of known data to the material performance at design motor conditions. If little reliable data on the insulator material are available, the designer must assume a more nearly empirical approach: (1) design an ultraconservative (thick) insulator based on available information; (2) test fire a sufficient number of motors to evaluate insulator performance, and (3) trim the insulator design thickness to the thickness that will provide the desired thermal margin of safety (sec. 2.4.1.1). This last step is a vital part of reducing motor inert weight to a minimum.

2.1.2 Motor Application

The design approach must emphasize the specific requirements for which the rocket motor is to be used. For example, inert weight is more critical in upper-stage motors than it is in lower-stage or booster motors, because excessive inert weight in the upper stage more severely limits the range or payload capacity of the complete vehicle. The findings presented in reference 1, in which the performance of a specific vehicle was examined, are an excellent illustration of this fact. The results of the examination are shown in the following

*Symbols in figure 3 are defied in Appendix B.

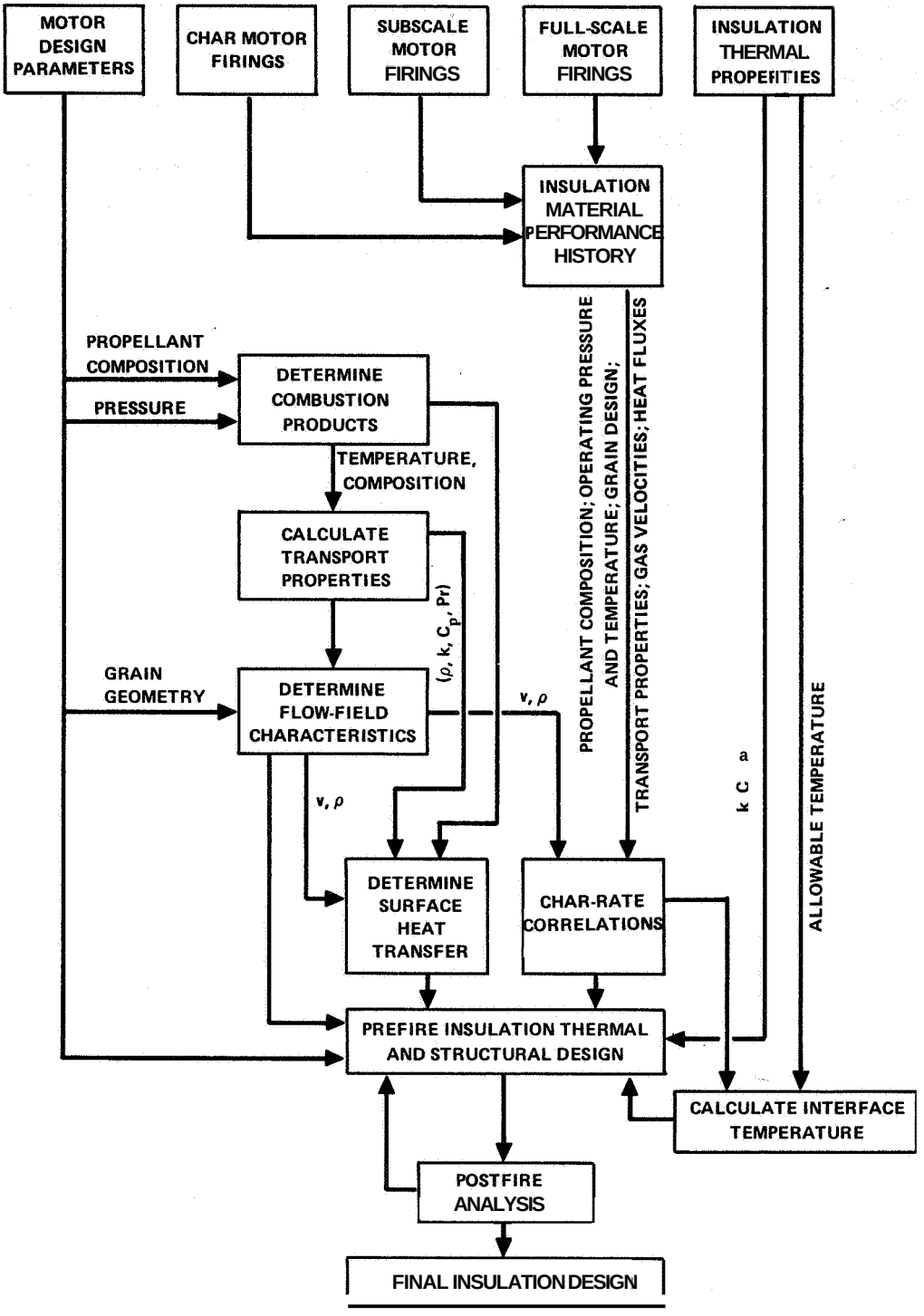

Figure 3. – Schematic of interrelated procedures in the design of an insulator.

tabulation, in which both the rate of change of payload with change in inert weight ($\Delta W_{PL}/\Delta W_{inert}$) and the rate of change of ideal velocity with change in inert weight ($\Delta v_{ideal}/\Delta W_{inert}$) are presented for a typical three-stage vehicle:

	Stage I	Stage II	Stage III
$\Delta W_{PL}/\Delta W_{inert}$, lbm/lbm	-0.0421	-0.2069	- 1.000
$\Delta v_{ideal}/\Delta W_{inert}$, ft/sec-lbm	-0.2382	- 1.1698	- 5.6524

As shown, both overall vehicle payload and ideal velocity in the third-stage are 24 times more sensitive to a change in inert weight than is the case in the first-stage motor. The overall payload would be reduced 1 lbm for each extra pound mass of third-stage inert weight, whereas the overall payload would be reduced only 0.04 lbm for each extra pound mass of inert weight in the booster stage. Standard practice in material selection and insulator design is to take into account this variation in sensitivity of performance to weight.

2.1.2.1 BOOSTER MOTORS

Since the performance of booster motors is relatively insensitive to extra inert weight, the cost of insulation material and its installation is deemed more important than insulation weight in booster insulator design. The currently preferred booster insulator materials are elastomers, both heat-cured materials and mastics (sec. 2.2.1). The heat-cured material has well-known performance characteristics, and processing methods for it have been well established; however, the hand-layup installation method frequently used in large motors is expensive, usually costing about 35 percent more than installed mastic insulation.

2.1.2.2 UPPER-STAGE MOTORS

Since the performance of upper-stage motors is so much more sensitive to inert weight than the performance of boosters, the insulator design that possesses the lightest possible overall weight is the most desirable, as long as performance is preserved. The designer chooses a material that combines performance and low density to produce the desired overall light weight. In addition, the Insulation configuration of upper-stage motors frequently is designed to provide the least allowable insulation thickness on every portion of the interior surface of the case. Such designs are based on the anticipated erosion and thermal requirements of the chamber at each location within the motor, and the resulting internal insulators continually vary in thickness (cross section). For example, the third-stage Athena X-259 motor has a propellant grain that is slotted at the aft end. As shown in figure 4, the

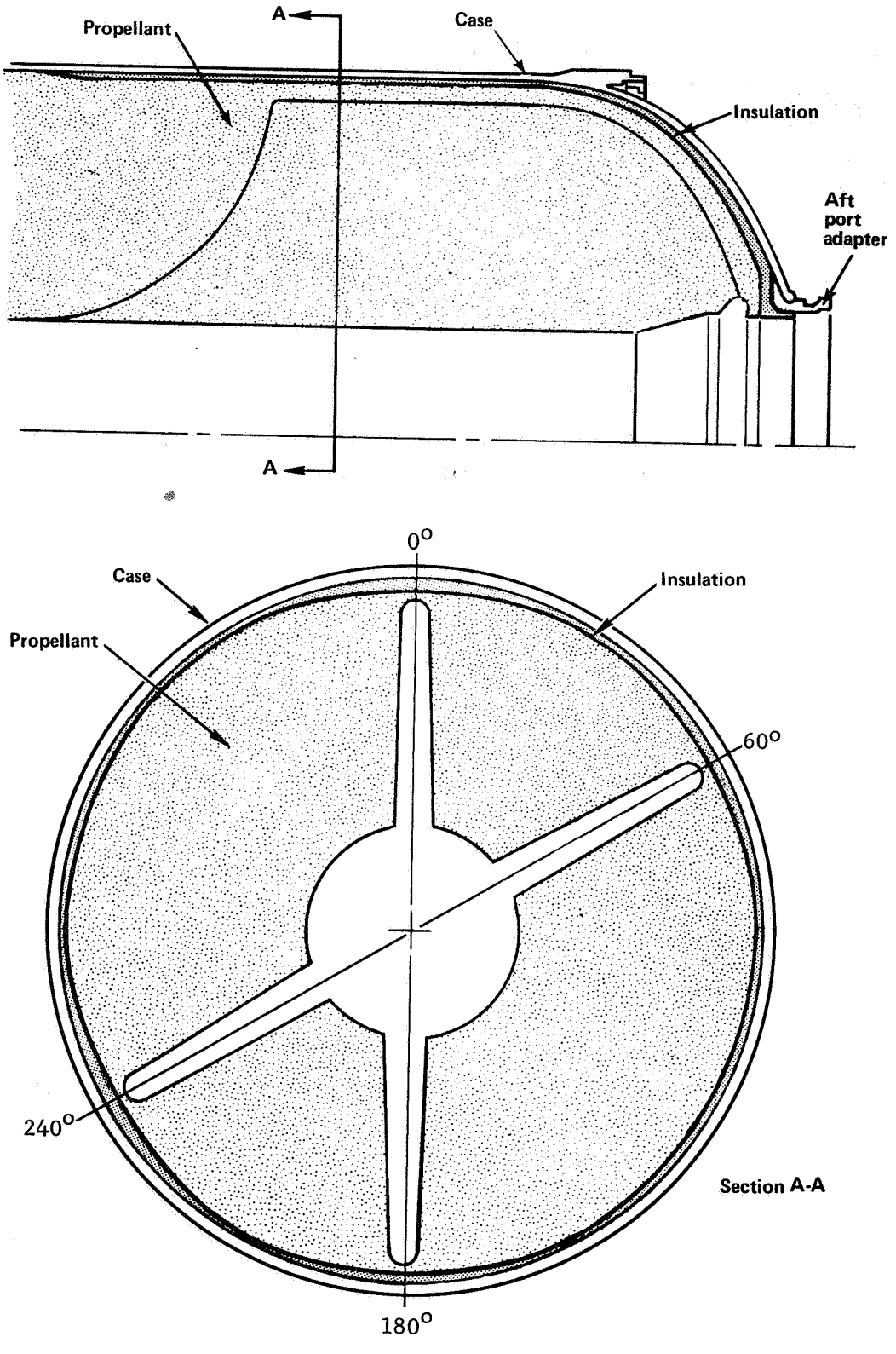

Figure 4. — Cross-section drawings showing increased insulator thickness at slots in propellant grain (Athena X-259 motor).

insulator is thicker near the slot tips than between the tips. Thicker insulation near the slot tip compensates for the longer exposure of the insulation to combustion products that .results from early propellant burnout in this region.

2.1.2.3 THRUST-CONTROL MOTORS

Thrust-control or pulse motors create a difficult environment for insulation materials. **A** service temperature range of –65" to +135°F at sea level and a much wider temperature range in space are typical applications. In the air-launched category, the off time between pulses is of very short duration, probably in the order of seconds. For space missions, the off time between pulses varies from seconds to months, all in the hard vacuum of space. Insulation materials must not be combustible, because during sea-level operation influx of air can ignite hot combustible insulation. In space operations, the material is degraded by outgassing. The only means of heat rejection in space is radiation; thus, all of the heat absorbed during the motor thrusting period must be conducted to an outside surface and radiated to space, the result being long heatsoak periods for the insulation. Sometimes the motor is restarted while the insulation is still hot from the previous thrusting period; this condition results in unusual thermal profiles and in thermal stress conditions not normally encountered in single-pulse rockets (ref. 2).

2.1.2.4 SPACE-OPERATIONAL MOTORS

Four space-environment phenomena affect rocket motor insulation (refs. 3 and 4):

(1) Ionization radiation

(2) Electromagnetic radiation

(3) Temperature extremes

(4) Vacuum.

Ionization results from energetic atomic particles (protons and electrons) that exist primarily in the earth's radiation belts; beyond the outer belt, the damage potential from ionization is much lower. Ionization damage is largely a surface phenomenon: the effects decrease exponentially from the exposed surface to the rocket motor interior.

Electromagnetic radiation (excitation) emanates from the sun, and the intensity varies inversely as the square of the distance from the sun. Degradation of rocket motor insulation results primarily from radiation in the ultraviolet range; in the vacuum environment of space

this degradation increases elastomer weight loss. As with ionization, the damage is a surface phenomenon. The effects of both types of radiation may be reduced or eliminated by compounding or by shielding. Shielding can be provided by paint or spray-on coatings. The motor case usually serves as a shield for internal insulation.

Temperature extremes in space occur both as a result of thermal cycling in pulse motors and as a result of radiation heat loss to space during storage. The low-temperature extremes may be encountered in multipulse motors during long delays between pulses. During such periods, nozzle components radiate heat to space, thereby cooling the internal insulation components. The problems created are thermal expansion and contraction, structural instability, and vulnerability to cracking during subsequent pulses.

Vacuum stability in space depends on insulator formulation and curing procedure. Insulators are organic-based materials consisting of a binder modified by plasticizers, processing aids, extenders, and curing agents, with filler material added principally as a reinforcement. In general, the tighter the degree of insulator cure (more highly chemically crosslinked), the better the stability in a vacuum; low-molecular-weight plasticizers in the formulation affect the vacuum stability adversely. Low erosion rates observed in plasma-arc ablation tests also indicate good stability in hard vacuum (ref. 5). One of the most obvious effects produced by hard vacuum on insulation materials is the loss of surface volatiles and entrapped volatiles, including moisture and low-molecular-weight materials such as plasticizers, lubricating oils, and nonbonded diluents. The loss may occur as a result of out-gassing, evaporation, or sublimation. Such weight loss does not significantly affect mechanical performance.

In summary, the effect of space environment does not appear to be exceptionally detrimental to shielded internal insulation materials; however, each mission encounters unique combinations of environments that may prove to be significant. Very limited data are currently available for assessing the effects of the space environment on insulator thermal and ablative properties; therefore, when unusual environments are predicted, the designer must carefully evaluate the possible effects.

2.2 SELECTION OF MATERIALS

2.2.1 Insulators

Materials used as insulators for solid rocket motors usually are identified by a hybrid name (e.g., asbestos/NBR) that identifies a filler or reinforcement material (asbestos) in a matrix or binder (NBR) (see fig. 2). Two classes of materials are used as binders for internal insulation: elastomers and thermosetting plastics.

Elastomers. – An elastomeric material has the following basic characteristics (ref. 6):

- It is relatively soft, and its elastic modulus is low.
- It will withstand very high strains, up to 900 percent.
- It will return quickly to its original length following strain.
- It is noncrystalline, and the glass transition temperature characteristic of the material is well below the normal operating temperatures at which it will be used.

Filled elastomers are useful in internal insulation both because their thermal properties are excellent and because their high strain capabilities allow the transmission of stress concentrations to be diffused from the case into the propellant. Typical char and decomposition patterns for three types of filled elastomers are illustrated in figure 5. Note the differences in the postfire appearance of these materials, particularly the lack of surface regression in figure 5(c).

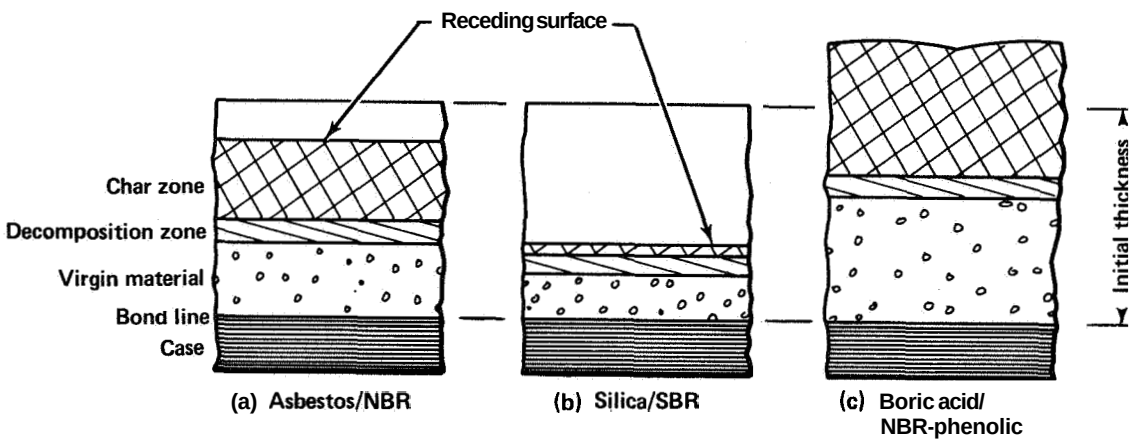

Figure 5. – Cross-section drawings showing appearance of three different insulators after firing.

Both the widely used heat-cured insulators and mastics are elastomers. The heat-cured elastomers are filled with silica or asbestos or both, are molded or laid up by hand, and are cured at approximately 300°F and 100 psi; the mastics, generally filled with asbestos, are cast or troweled in place and are cured at or near room temperature and pressure. Typical properties of filled heat-cured elastomers and mastics used as insulators are presented in table I.

Table I. – Typical Properties of Filled Heat-Cured Elastomers and Mastics Used as Internal Insulation on Solid Rocket Motors.

Composition		Thermal Properties		Physical Properties			Example of use
Binder	Filler	k, $\frac{\text{Btu}}{\text{ft-hr-°F}}$	C_p, $\frac{\text{Btu}}{\text{lbm-°F}}$	Tensile, psi	Density, lbm/ft^3	Elongation, %	
				Heat-cured elastomers			
CTPB*	Carbon black	0.12	0.43	275	60.5	350	Saturn ullage motors; Sidewinder/Chaparral
EPDM**	Asbestos	0.14	0.4	950	61.0	900	Phoenix
	Asbestos	0.13	0.45	260	74.4	400	Condor; Phoenix; Sparrow/Shrike
NBR	Silica	0.13	0.4	1700 to 2450	76.1	—	Poseidon 1S; Polaris A2 and A3, 1S; Minuteman 2S and 3S; 260 SL-1, -2, -3
NBR	Silica, asbestos	0.1[illegible]	0.41	2000	79.2	440 to 623	Poseidon 1S; 260 SL-1, -2, -3; TCC 100-in. demo Titan III strap-ons; Polaris A2 and A3, 1S
NBR-phenolic	Boric acid	0.17	0.41	800 to 1600	73.6	200 to 450	Polaris A3, 2S; Poseidon 2S
SBR	Asbestos	0.25	0.40	1000	87.3	400	Athena; Hibex; Sprint 1S and 2S
SBR	Silica	0.13	0.34	1900 to 4000	73.3	550 to 800	Minuteman 3S; Athena; Polaris A3, 2S; Poseidon 2S
				Mastics			
NBR-polysulfide-epoxy	Asbestos	0.[illegible]2	0.33	900	73.1	2 to 5	Titan III; Polaris A3, 1S; 260 SL-1, -2, and [illegible]
PBAA	Asbestos	0.28	0.36	175	83.1	1	TCC 156-in. demo
PBAA	Asbestos	—	0.34	884	81.1	38	Lockheed 100-in. demo
PBAN-epoxy	Asbestos	0.13	0.36	866 to 1640	87.8	69	260 SL-3

* Carboxy-terminated polybutadiene – aziridine cured.

* Terpolymer elastomer made from ethylene propylene diene monomer – peroxide cured.

TCC = Thiokol Chemical Corp.

1S = 1st stage

2S = 2nd stage

3S = 3rd stage

Heat-cured insulators have been fabricated from binders of NBR, SBR, butyl, EPDM, polysulfide, silicone, and urethane in combination with a wide variety of fillers. The base polymers generally are used with propellants in the following combinations: NBR with composite propellants; SBR- or NBR-phenolic with double-base propellants; and butyl, silicone, or EPDM elastomers in low-temperature applications with either type of propellant.

The mastic-type insulators gained wide attention during the development of the large solid motors. Mastic materials developed, evaluated, and used in these booster motors (refs. 7, 8, and 9) usually employed PBAA, PBAN-epoxy, and NBR-polysulfide-epoxy as binder systems. The fillers were primarily asbestos and carbon black.

Ablative performance of a typical mastic insulation material is illustrated in figure 6, and for comparison, the performances of a silica-loaded NBR, an asbestos-loaded NBR, and a silica/phenolic insulator are included. These curves indicate that the mastic insulator performs about the same as the standard heat-cured elastomeric insulator (asbestos/NBR) for a combustion-products mass flux range of 0.3 to 0.7 lbm/in.^{2}-sec. At higher and lower mass flux, the mastics compounded thus far have exhibited ablation rates lower than those of the heat-cured elastomers.

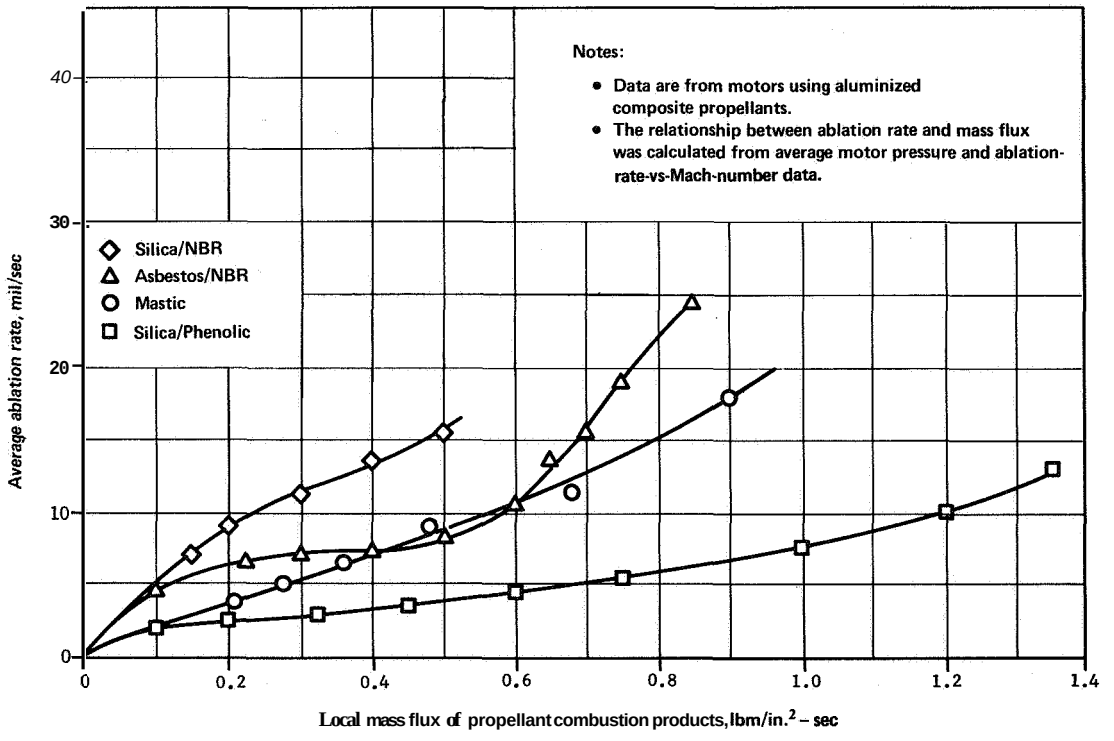

Figure 6. – Average ablation rates for typical insulators as a function of mass flux of combustion products.

Thermosetting plastics. – The second class of material used for internal insulation is reinforced thermosetting plastic. The binder resin used in this application is usually a high-temperature phenolic, although phenylsilane and polyamide-modified phenolic have also been used. The resin typically is filled with silica, asbestos, nylon, carbon, or glass cloth or fiber. Typical properties of filled plastics used as insulators are shown in table 11.

Because shear forces applied by high-velocity flow of combustion products can mechanically remove the char layer, the shear strength of the insulation char layer is an important design consideration. For high-mass-flux conditions ($\geqslant$ 1.3 lbm/in.^{2}-sec), the strength of the char layer is vital. Char-layer strength in turn is greatly dependent upon the orientation of reinforcement material with respect to combustion-products gas flow. Randomly oriented reinforcement material produces relatively weak char, while a reinforcement material oriented perpendicular to the gas flow produces a strong char because each fiber is continuous through the transition zone and is individually anchored to virgin material (ref. 10).

Reinforcement materials may be asbestos, nylon, carbon, or zirconia in the forms of bulk fiber, batt, cloth, sleeving, yarn, flakes, or felt. The reinforcement may be built up by lamination or molding. Various schemes are used to orient reinforcement materials so that optimum thermal properties may be obtained. These include (1) rosette layup, (2) parallel-to-centerline layup, (3) tape wrap, and (4) 3-D weaving. In comparison with elastomers, the reinforced plastics are hard and brittle, but a more flexible product can sometimes be produced if modifiers are added to the binder resin. Elongations in reinforced thermosetting plastics range from 0.02 percent to 50 percent, the value depending upon degree of modification of the base resin. The ablation rate of reinforced plastics generally is lower than that of the elastomers (fig. 6), and the plastics are more dense. Plastics are in limited use for internal insulation, but are valuable in applications where insulators will be exposed to gases at relatively high temperatures (2000" to 6000°F) and to high local mass flux of combustion products ($>$ 1.3 lbm/in.^{2}-sec); for example, protrusions or irregular features of the internal motor surface are best insulated by reinforced plastics. The use of reinforced plastics in current rocket technology is discussed in detail in references 11 and 12.

In addition to weight and cost considered as discussed previously, other factors that are involved in selection of insulator materials are thermal properties, mechanical properties, compatibility with other rocket motor materials, and relative performance in screening tests. Each of these subjects is covered in the paragraphs that follow.

2.2.1.1 THERMAL PROPERTIES

Several phenomena are involved in insulation thermal performance: (1) energy transfer from the combustion-gas/particle cloud to charred insulator surface, (2) energy absorption capacity of insulation material, (3) mass transfer of pyrolysis products, (4) energy transfer

Table II. – Typical Properties of Filled Thermosetting Plastics Used as Internal Insulation on Solid Rocket Motors.

Composition		Thermal Properties		Physical Properties			Examples of use
Binder	Filler	k, $\frac{\text{Btu}}{\text{ft-hr-°F}}$	C_p, $\frac{\text{Btu}}{\text{lbm-°F}}$	Tensile, psi	Density, lbm/ft^3	Elongation, %	
Phenolic	Asbestos	0.2	0.28	1000	95.0	1.0	Redhead, Roadrunner, Redeye
Phenolic	Asbestos	0.40	0.27	1200 to 6600	110	0.5	Poseidon 1S, 2S; Minuteman 3S; Nike Zeus 1S
Phenolic	Carbon cloth	0.48	0.23	2500 to 22 000*	89.9	—	Redhead, Roadrunner
Phenolic	Carbon fiber	0.17	0.3	2000	78.0	0.25	Early Phoenix
Phenolic	Glass cloth	0.15	0.23	5900 to 100 000*	116.7	—	Sparrow/Shrike
Phenolic	Glass (chopped fiber)	0.26	0.25	5000	115.4	—	Saturn ullage motors
Phenolic	Nylon	0.10	0.31	2500 to 4400	74	—	Minuteman 3S

*Range of values is function of orientation of reinforcement.

from char surface into uncharred insulation, (5) energy conduction through uncharred insulation, and (6) the adherence of char layer to uncharred material. The energy transfer from the gas cloud to the insulator surface is discussed in section 2.3.2. Simple conduction of heat through a material is discussed in a number of textbooks on heat transfer (e.g., ref. 13).

As noted, insulation absorbs energy by the following mechanisms: (1) heating of the material, (2) phase changes in the material, **(3)** pyrolysis of the material, and (4) heating of the gaseous products of both pyrolysis and phase changes. Energy-absorbing phase changes are melting, vaporization, and sublimation. Heats of melting, vaporization, and sublimation are measured by standard calorimetric methods, differential thermal analysis (DTA), and thermogravimetric analysis (TGA) (ref. 14). Pyrolysis is the thermal decomposition of polymers and fillers. Pyrolysis is studied by determination of heat dissipation (Btu/lbm), identification of decomposition products, studies of reaction kinetics, and studies of solid residues produced from a sample in an arc-image furnace (ref. 14).

Most of the material properties and tests listed above are used in research and development on new materials. Insulator design, however, is not often based on research data. Design data usually come from subscale or full-scale firings. Data correlations used for design relate surface regression rate to thermal diffusivity, emissivity, and density of the insulator and to combustion-gas conditions (pressure, temperature, velocity, and emissivity). Thermal diffusivity χ is defined as follows:

$$\chi = \frac{k}{C_p \rho} \tag{1}$$

where

χ = thermal diffusivity, ft^2/hr

k = thermal conductivity, Btu/(ft-hr-°F)

C_p = specific heat at constant pressure, Btu/(lbm-°F)

ρ = density, lbm/ft^3

Thermal conductivity k and specific heat C_p are measured by standard calorimetric methods. Emissivity (i.e., total hemispherical emissivity) is the adjustment made to the Stefan-Boltzmann equation for radiators that are not black bodies (sec. 2.3.2.2); emissivity values are obtained by methods such as those described in reference 14.

2.2.1.2 MECHANICAL PROPERTIES

Mechanical properties of insulation materials are a measure of the behavior of the material in response to applied forces. Knowledge of these properties is required for structural analysis of insulators. Material evaluation, processing studies, and quality control specifications also require data on mechanical properties. Appropriate physical-property tests conducted as specified by ASTM* or ICRPG** are used for different classes of materials. Physical-property tests for both propellant and propellant-to-insulator bond system (case bond) are conducted because data for each are required for structural analysis of the insulator.

The specific data on insulation-material mechanical properties used for structural analysis of the insulator depend on both the degree of sophistication of the analytical technique and the specific insulator design being investigated; e.g., stress-relaxation testing of materials is performed only when viscoelastic stress analysis of the insulator is to be performed, and "poker-chip" testing (ref. 16, sec. 4.5.5) of bond systems is applicable only when features that create stress concentrations in the insulator are absent.

Data on propellant properties used for structural analysis of the insulator include results from constant-crosshead-rate tensile tests, stress-relaxation tests, and bulk-modulus measurements. Metal-case data needed to analyze insulation performance include tensile modulus and Poisson's ratio; composite-case data needed are two tensile moduli (axial and transverse), Poisson's ratio, and shear modulus.

Uniaxial and triaxial tensile tests in addition to shear and peel tests are used to evaluate bonded interfaces such as the chamber-to-insulator bond surface. Thermal-expansion tests provide data used to calculate thermal stresses within the material.

Additional information on solid propellant structural integrity analyses is presented in reference 17.

2.2.1.3 COMPATIBILITY OF MATERIALS

An insulation material is selected only after thorough investigation of its chemical compatibility with both the propellant and sealants that are to be used together during motor fabrication and throughout the life of the motor. Compatibility in two general areas is considered: (1) the case-bond regions where one insulation surface is bonded to the case and the other is bonded to the propellant, and (2) the flap regions of the motor where one insulation surface is bonded to the case or propellant and the other is exposed to the storage environment. In the case-bond regions, each component must be compatible with every

*,**ASTM test methods are listed in reference 15.
ICRPG test methods are described in reference 16.

other component it contacts. In the flap regions, each component must be compatible with its substrate and, in addition, the combination must be compatible with the local atmosphere.

Compatibility of materials in and around case-bonded insulators is significant either because of potential migration of propellant plasticizers or burning-rate modifiers to the insulation or because of reactions between contaminants, migrating ingredients, and other components (ref. 18). These phenomena contribute to several failure modes, including reduction of bond strength and deterioration of insulation thermal and physical properties. For example, when double-base propellant and cellulose acetate (CA) are in physical contact or even in vapor-phase contact (e.g., when sealed in the same motor), plasticizers will migrate between the two polymer phases until partition equilibrium is established. Thus, nitroglycerin (NG) ultimately will appear in the CA, even though it was present originally only in the propellant, and dicarbitol phthalate will appear in the NG phase even though present originally only in the **CA** phase. The deleterious effects are degradation of the specific impulse of the propellant and degradation of the physical properties of the CA. Cellulose acetate and NG are compatible in the sense that they do not present a thermal instability problem, but they are less than compatible in the sense of being free of problems that affect ballistics and physical properties. Cellulose acetate is not used in thin sections, and its use in intermediate thickness sections is carefully analyzed.

Nitroglycerin is absorbed by other ester-type polymers used in motors (e.g., NBR, seam-sealing compound, polyurethanes, and polyesters). Polaris and Minuteman motors were plagued with a sticky brown liquid formed by deterioration of polyurethane potting compound. The potting breakdown was caused by a complex reaction involving zinc and was complicated by the migration of NG.

Typically, SBR is selected for use with highly plasticized double-base propellants because of resistance to NG migration (ref. 19). Migration-inhibiting barrier coats are used with both composite and double-base propellants.

Long-term-aging studies indicate that the minimum standard for compatible propellant/insulation systems is that insulation degradation must be negligible for at least five years, as shown in both motor tests and laboratory programs (ref. 19). Accelerated-aging tests are conducted at elevated temperature, and propellant/insulator compatibility is evaluated by use of the Arrhenius relationship (as described for solid-propellant aging in ref. 16, sec. 7). This method allows for extrapolation to ambient-temperature aging, and the results are in general agreement with the corresponding long-term-aging results.

During installation and storage, insulators are degraded by reaction with ozone in the atmosphere. The effect has been especially prevalent in regions of high ozone concentration such as Los Angeles. Numerous studies indicate that moderately strained elastomers

(elongation < 10%) and unvulcanized stock are not attacked by ozone. The important factors affecting stressed vulcanizates are exposure environment, polymer type, compounding variables, state of cure, and protective agents (ref. 20).

The two failure modes associated with degradation during storage are (1) deterioration of both mechanical and thermal properties, and (2) cracking of insulation that may result in both exposure of the propellant in the flap region and exposure of the case in case-bonded areas. The primary problem encountered is insulator cracking during the fabrication and installation sequences in high-ozone regions.

To prevent deterioration caused by ozone, antioxidants such as diphenylamines, waxes, cresols, quinolines, alkylated phenols, and phosphites sometimes are compounded into the elastomer. Strain is precluded by using contoured shipping supports. Protective coatings and sacrificial packings are widely used for protection during shipment and storage, but processing in high-ozone environments is avoided. The selection of either silicone rubbers or ethylene-propylene rubbers ensures resistance to storage-environment aging due to the presence of ozone. Numerous laboratory aging programs and motor test programs attest to the adequacy of currently used elastomeric insulators when exposed to air for periods up to 5 years (ref. 19). On a relative basis, the performance of commonly used materials in resisting ozone attack is (from best to worst) silicone, **EPR, EPT,** butyl, **NBR,** and **SBR** (ref. 21).

2.2.1.4 SCREENING OF MATERIALS

Candidate insulation materials are screened by oxyacetylene torch tests (ref. 22), plasma-arc tests (ref. 2), and subscale motor tests. The first two methods are adequate for preliminary screening of insulators and for early evaluation of adhesives and sealants, but subscale motors are used for final screening and for evaluation of material thermal and ablative properties for design purposes.

In subscale motor tests, material samples are placed inside a test motor at locations that represent as closely as possible the expected use environment. One such test motor is illustrated in figure 7. The motor has test specimens bonded into asbestos/phenolic holders designed to expose the specimens at least three levels of exhaust-gas velocity. Nozzle throat size, internal pressure, and firing duration are adjusted to approximate the full-scale motor conditions.

Figure 7 also illustrates two basic problems with subscale test motors: (1) samples located in the test section ablate and change the gas composition and temperature to which downstream samples will be subjected; and (2) a poor material in the test section will erode quickly and leave a step, which in turn disturbs flow so that other samples erode more quickly.

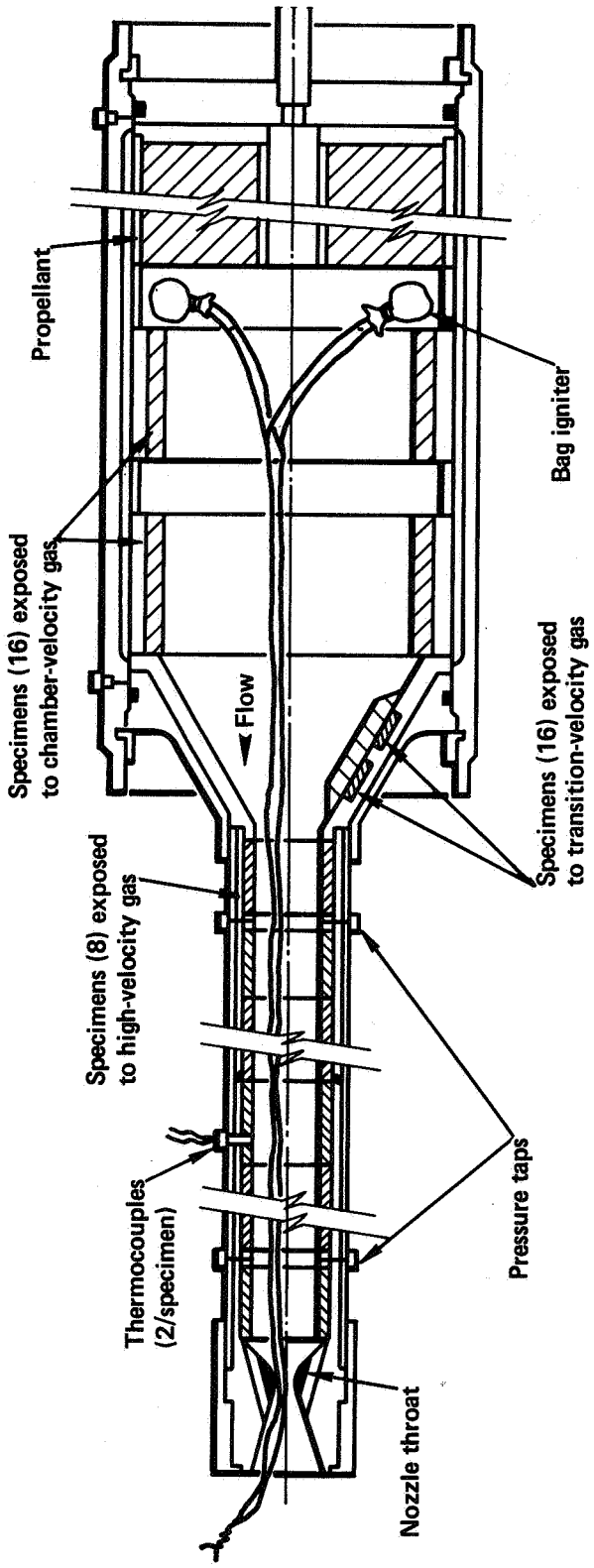

Figure 7. – Typical test motor for screening and evaluating candidate insulation materials.

Other examples of subscale motors are presented in figures 8 and 9. The motor in figure 8 is designed specifically for obtaining particle-impingement data; the design in figure 9 emphasizes comparative data on the effects of high and low gas velocity. The motor burn time in figure 9 is adjusted by changing the length of the grain.

Subscale tests yield relative values of erosion and char losses that are suitable both for screening candidate materials and for providing a basis for design of the full-scale insulation system. However, subscale data do not always correlate well with the performance in full-scale motors, so that full-scale testing of relatively new insulation materials or unusual designs is necessary in order to verify the adequacy of the insulationsystem design.

2.2.2 Adhesives, Liners, and Sealants

An adhesive is a material applied between components to bond the components together structurally; a liner is a thin layer of adhesive specifically used to bond the propellant to the case or to the insulator. A sealant is a liquidsolid mixture installed at joints and junctions of components to prevent gas flow. Careful selection of these materials is an important part of insulator design; the characteristics of each material required for successful use are discussed below.

2.2.2.1 ADHESIVES

An adhesive performs the following functions (ref. 23):

(1) An adhesive wets the substrates at the time of application by being sufficiently fluid to come into intimate contact with the adherends.

(2) An effective adhesive "sets" or hardens to give a bond line that is both strong and tough. Strength depends on the adhesives being transformed from the fluid state (which counteracts adherend roughness and absorbed boundary layers) into a structural solid. Toughness is a more complicated property; it is the work done to failure and is a function of tensile strength and elongation. Toughness may be measured as impact strength under a high rate of loading.

(3) A useful adhesive is noncorrosive to a metallic substrate. However, the proper primer can effectively block the action of a corrosive adhesive on a metallic substrate.

In selecting an adhesive for either fiberglass or metal rocket motor cases, a number of important parameters that relate to the specific application are considered. These

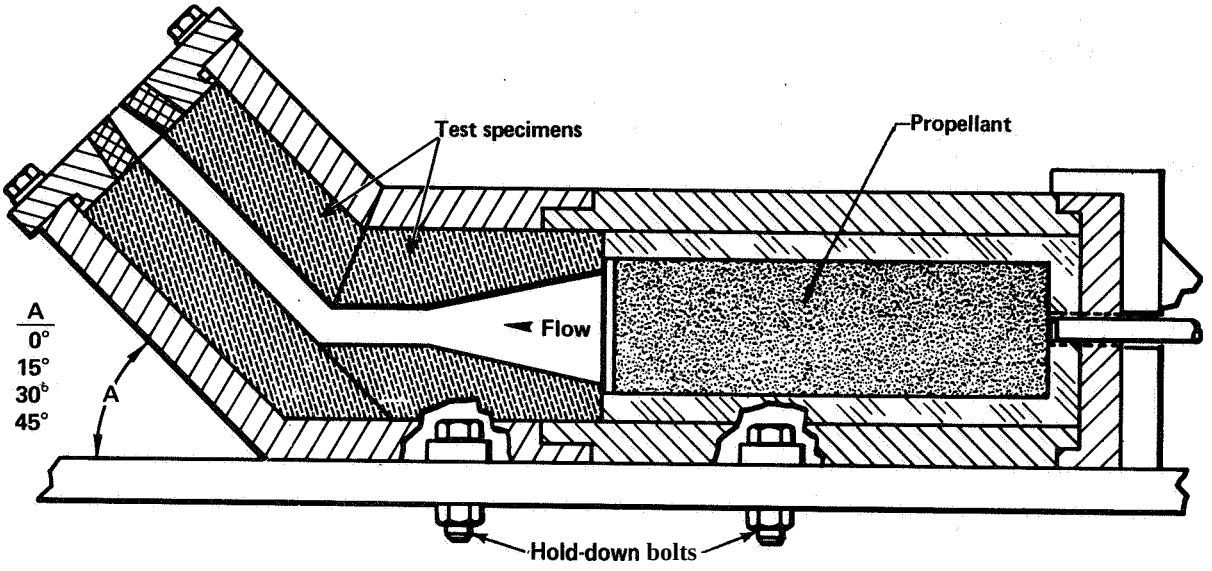

Figure 8. — Test motor for evaluating effects of particle impingement on candidate insulation materials.

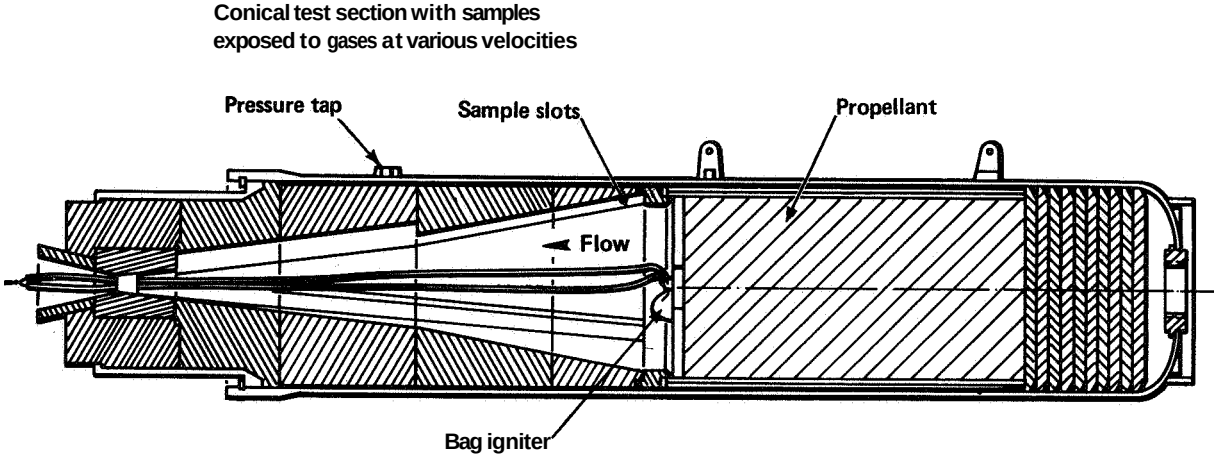

Figure 9. — Test motor for evaluating effects of varying exhaust-gas velocity on candidate insulation materials.

parameters are (1) strength requirements and mode of stress application to the bonded joint, **(2)** temperature requirements, **(3)** processing requirements, (4) availability of tooling and facilities, and *(5)* use environment.

The strength requirements of an insulator joint depend not only on the adhesive but equally as much on joint geometry and the mode for stress applications. Generally, thermosetting adhesives are not greatly extensible, but are considerably stronger than the elastomeric adhesives.

If the stresses imposed on the bond are shear or tensile, the thermosetting plastic outperforms the elastomers under ideal conditions, especially at high temperatures. However, bending moments imposed on the structural-type bond grossly and adversely affect insulator joint strength, because the nonextensible adhesives do not permit an equal distribution of peel forces as do the elastomers. If the principal load is in the peel mode, or if considerable bending moments are imposed on the bonded configuration (ref. 24), the heat-cured elastomer is the better of the two types.

The requirement for performance at relatively high temperature generally favors selection of thermosetting adhesive, primarily because the thermosets are extensively cross-linked systems in comparison with the elastomers, and they retain a greater degree of internal cohesive strength. The nature of the thermosets, in addition, renders them infusible, not prone to run or soften to the same extent as elastomers.

Insulator processing requirements include careful surface preparation, control of the pot life of the adhesive, and control of bondline thickness. These factors are evaluated for any adhesive application and become the basis for processing specifications. The creation of an effective bond is accomplished by compliance with the foregoing requirements. However, it is also important to assess processing capabilities realistically under normal shop conditions, which may not allow application of the entire laboratory bonding procedure. **As** an example, process-variables studies, as reported in references 25 and 26 for an epoxy adhesive, indicate that joint strength depends greatly on bondline thickness as well as on cleanliness and service temperature.

The insulator layup process includes (1) applying layers over a mandrel, **(2)** stitching layers together with special tools and rollers, **(3)** installing vacuum bag and bleeder cloth, and (4) curing in an autoclave. With the layup process, not only are the layers cured in proper alignment but also the amount of entrapped volatiles is lessened. Large insulator parts that cannot be accommodated by an autoclave or small areas in need of repair may be more conveniently and practicably joined by room-temperature-curing thermosetting adhesives, provided, of course, that the mechanical and bond properties achieved with a room-temperature cure are commensurate with the thermal and mechanical stress requirements of the assembly.

The bonding of elastomeric insulation to metal cases is complicated by extreme variation in the chemical and physical properties of the elastomers. Inclusion of processing aids, plasticizers, and antiozonants in the elastomer weakens the bond or even renders the bonding of some materials improbable. Therefore, the adhesive used must readily wet the metallic substrate and yet contain reactive species common to or compatible with the elastomer. Generally, bonding NBR to metal motor cases is less complicated than bonding neoprenes, SBR, or butyls. Elastomers newer to rocket motor applications (e.g., butyl, EPDM, or silicones) may present formidable bonding problems not yet encountered.

Chemical compatibility problems resulting in material migrations also complicate bonding of insulation to fiberglass rocket motors cases. Here the difficulty arises from the chemical incompatibility between the resin used in the fiberglass composite and the elastomeric binder. Therefore, the migration of reactive species usually is evaluated. In addition to the migration problem, bonding studies of glass cases have shown that cured elastomers are harder to bond than uncured; elastomer surface preparations are more critical than those for metal cases; and the bondline strain is significantly higher than that with metal cases. The majority of insulators, therefore, are abraded and bonded to the glass case. In some instances, a coupling agent consisting of the same resin used in the glass composite is sprayed over the insulator before fiberglass strands are wrapped onto the insulator.

The adhesives most frequently used in insulator fabrication are epoxies and elastomer-based materials. Because most adhesive bonding is done on the backside of the insulator next to the case structure, the operational temperature requirements of an adhesive used in rocket motor internal insulation usually are less than 250°F. If the adhesive at the backside is exposed to a temperature greater than 250°F, the insulator has failed to protect the case structure. Therefore, epoxies, because they are useful at 250°F or less, are the most "frequently used adhesives. The most commonly used epoxy hardeners are aromatic amines and cyclic anhydrides. Other resins occasionally are blended with epoxies to obtain special properties. For example, epoxy-polysulfides often are used as insulator materials because they combine the toughness and elasticity of polysulfide with the strength of epoxy. It should be noted, however, that most of the insulator materials are compounded with an adhesive matrix and therefore do not require the use of additional adhesive to secure an adequate bond to the case.

Nitriles and neoprenes frequently are used as a base for elastomeric adhesives, usually where considerable elongation is required. One type of elastomer adhesive is created by masticating the elastomer and dissolving it with an appropriate solvent such as methyl ethyl ketone or toluene; such adhesives cure by solvent evaporation. Other adhesives, however, are cured at elevated temperature after the addition of a sulfur-bearing compound that promotes polymerization (vulcanization). Vulcanized adhesives frequently are used in splicing or bonding rubber-to-rubber joints.

2.2.2.2 LINERS

Most current solid rocket motors are case-bonded, which means that, for support and control of the burning surface, propellant is bonded to the case through the insulation. Some propellants are bonded directly to selected insulation materials, but the achievement of composite propellant/insulation bonds of adequate strength generally requires the use of a thin, intermediate adhesive layer called a liner. The liner/propellant bond must be strong enough to withstand all anticipated stresses including the stresses induced by thermal cycling, normal handling and storage, and rapid pressurization on motor ignition. The liner, in areas where the insulator is very thin, is subjected to strain essentially equal to the strain that the case' undergoes. The failure of any significant area of the propellant-to-insulator bond can introduce an unprogrammed propellant burning surface, the result being abnormal ballistic performance or, even worse, rupture of the case as a result of overheating or overpressure. Therefore, selection of a liner for a given motor application is not made without consideration of all elements of the bonding system (i.e., case, insulation, liner, and type of propellant).

Although a vast amount of effort has been expended to improve the strength and reliability of propellant-to-insulator bonds, only a limited understanding of the basic chemical factors that influence solid propellant adhesion currently exists. An *a priori* selection of a liner for a particular motor application generally is not possible (ref. 27). Most motor programs therefore include a liner selection effort.

Ideally, it is desirable from the standpoint of simplicity and reliability to bond the propellant directly to the insulation without using a liner. The feasibility of this practice normally is evaluated as the first step in the selection of internal motor insulation.

There is general agreement that the strength of all bonded interfaces in the bonding system should exceed the cohesive strength of the propellant (refs. 24 and 28). If this condition cannot be achieved by the direct bonding of propellant to insulation, an evaluation of liners to promote adhesion is undertaken. The two factors considered in assessing the adequacy of a liner are (1) bond performance in all environments, and (2) ability of the liner to survive motor-processing steps without damage.

The best composite propellant bonding generally is obtained by using a liner based on the same polymeric binder used in the propellant in question. Processing, cure, and mechanical properties of the liner are controlled by the addition of relatively small amounts of powdered fillers. Colored fillers sometimes are used to aid in determining uniformity of application; thixotropic fillers frequently are used to provide resistance to sagging. The method of liner application influences the selection of filler type and content because different flow characteristics are required for trowelling, spraying, spinning, and other operations. For instance, tape fillers are an illogical choice of filler for an insulation material applied by spraying but may be acceptable for filler in a pressure-cured insulator. Long-fiber asbestos may be acceptable in a trowelable insulation formulation but troublesome in

castable materials. Generalizing, finelydivided fillers are acceptable in any insulation material; woven or long-fiber fillers, however, are best in material-application methods for which flow characteristics are not critical.

The physical properties of a liner are dependent on the curing-agent concentration and filler type and content. Both hard, fully-cured liners and soft, semicured liners are used in the industry. As yet there is no consensus as to which type is more effective in creating the strongest bond. Semicured liner bonds are developed during simultaneous cure of propellant and liner, but the life of the exposed1iner usually is limited. The liner therefore may require a supplementary wash coat in the event of an unexpected delay in casting.

The state of cure of the propellant immediately adjacent to the propellant/insulator interface is one of the more important conditions contributing to bond strength. Two methods of insuring a good propellant cure at the bond interface are (1) the use of wash coats that consist of curing agents with or without a catalyst, and (2) the incorporation of a propellant cure catalyst directly into the liner (ref. 27).

Double-base (DB) or composite-modified, double-base (CMDB) propellants, unlike composite propellants, normally are not used with an elastomeric liner. Although DB or CMDB propellants will bond to some elastomeric liners, the chemical stability of the bond is not satisfactory because the plasticizers and solvents used in such propellants migrate into the liner and cause degradation. The two most common methods currently used to bond DB or CMDB propellants to insulation are the powder-embedment technique and the coupling-layer technique. In the powder-embedment technique (ref. 29), a layer of casting powder granules is bonded to the insulation with an epoxy resin. The motor is then filled with casting powder and the casting solvent is introduced. The propellant-to-insulation bond is formed as the propellant cures, and the embedded casting powder becomes a part of the propellant grain. The epoxy resin used to bond the casting powder to the insulation also serves as a barrier to inhibit plasticizer and solvent migration across the bond interface into the insulation. In the coupling-layer technique, the insulator is chemically bonded (coupled) to the propellant (ref. **30).** The chemical bond is obtained by applying a thin layer of polymer to the insulator prior to propellant casting. One such method utilizes a triple layer of polymers. A layer of triisocyanate primer is applied to the insulator, followed by a layer of neoprene and then a layer of vinylchloride/vinyl acetate copolymer. This triple coupling layer, which is about four mils thick, provides not only bonding but also resistance to plasticizer migration. The coupling-layer technique is simpler than the powder-embedment process; in addition, it decreases the inert component weight and volume and also provides better low-temperature properties.

2.2.2.3 SEALANTS

A seam-sealing compound functions as a potting compound (filler) between insulation and propellant shrinkage liner and, as such, must possess sufficient ablation resistance to prevent

localized high erosion on the surface when subjected to the rocket motor environment. Adequate mechanical properties also are important in preventing joint separation. The important properties in selecting a sealant are ablation characteristics, tensile and tear strengths, elongation at tensile failure, adhesive quality, and chemical stability. The requirements for these properties are determined from stress analysis of the joint that is based on the assumption that the most stringent conditions exist.

In general, highstrength sealants such as polyurethanes, polysulfides, and epoxies are used only where subsequent disassembly and inspection of the interface is not a requirement and will not likely occur. The materials most frequently used as sealants are a noncuring chromate putty and the room-temperature-vulcanizing (RTV) silicone rubbers. Like the primary insulators, such compounds must have low ablation rates. Allowable ablation rate is determined by the insulation with which the sealant is used. Noncuring chromate sealant, sometimes referred to as a vacuum-bag sealing compound, is a blend of a synthetic resin and asbestos, titanium dioxide, and yellow chromate fillers compounded into a nonhardening material that retains its physical characteristics over a wide temperature range and resists ablation well (ref. 31). The RTV silicones, which perform better than the chromate sealants, are characterized by good adhesion to most surfaces (400 to 500 psi bond tensile), moderate tear strength (50 to 130 psi), low shrinkage, and excellant low-temperature and environmental-resistance properties.

2.3 EVALUATION OF THERMAL ENVIRONMENT

The insulator designer must know the internal thermal environment of the motor before he can begin his design effort. In particular, he needs to know the composition, temperature, viscosity, and thermal conductivity of the combustion products. Armed with this information, he can determine not only flow fields and heat-transfer rates but, ultimately, the insulator thickness needed at all internal locations to thermally protect the rocket motor case.

2.3.1 Combustion-Products Analysis

2.3.1.1 TEMPERATURE AND COMPOSITION

The equilibrium temperature and composition of the complex mixture of combustion products in a rocket motor chamber are calculated with the use of thermochemical information obtained from references 32 and 33. Each chemical species that is formed from the propellant ingredients and for which thermochemical data are available normally is included in the equilibrium calculation. Additional data used in equilibrium studies are average chamber pressure, propellant formulation, and ingredient heats of formation. The

chamber pressure is averaged over the total burn time or any segment thereof. Most commonly, equilibrium conditions are calculated by minimizing the Gibbs free energy for the spectrum of chemical species present and using the method of steepest descent (ref. **34).** Because of the many species present in solid-rocket combustion chambers, this calculation is performed on a digital computer. Examples of computational methods are given in references 35 and 36. After equilibrium composition is calculated, other properties such as molecular weight, density, specific heat, and specific-heat ratio usually are determined by summing the weighted contributions of each species in the mixture. These calculated propertics are used, along with combustion-product temperature, in subsequent calculations of transport properties, gas flow, and heat transfer.

2.1.3.2 TRANSPORT PROPERTIES

Transport properties of the combustion gases are used in calculating local convective-heat-transfer coefficients. Transport properties are gas viscosity and thermal conductivity at the temperature and pressure of the combustion products in the chamber. Such properties are determined for each gas species by using collision integrals for the Lennard-Jones potential (ref. 37) and tabulated force parameters (ref. 38) together with the Chapman-Enskog kinetic theory of gases (ref. 39). This theory has been extended by Curtiss and Hirschfelder (ref. 40) to include multicomponent gas mixtures. However, an adequate approximation usually is made by using the semi-empirical formula of Wilke (refs. 41 and 42). The condensible combustion products have a negligible effect on the convective-heat-transfer coefficient because their volume is less than one percent of the total gas volume; therefore, these products are not included in the transport-property calculations.

2.3.1.3 FLOW FIELD

A flow-field analysis of motor chambers is conducted to define local mass fluxes. Mass flux of combustion products, the product of local density and velocity, is required information for convective-heat-transfer coefficient and flow-field particle trajectory calculations. Two methods commonly are used to calculate local subsonic flow conditons. The first method, an analytical solution of the equations defining potential flow in a system, is the usual method for flow-field analysis. The general flow equations are simplified mathematically (ref. 43) for subsonic velocities by assuming that flow is inviscid and irrotational. With such a simplification, the equations can be solved for twodimensional axisymmetric or planar flow by numerical methods. Analysis of end-burning motors with a length-todiameter ratio greater than three (frequently found in test motors) is valid when the general flow equations further simplified to one-dimensional flow are used. Flow near logitudinal propellant slots, regions near multiple nozzles, and other geometrically complex locations are not adequately defined by two-dimensional analysis, but require a three-dimensional mapping for accurate

description. By the assumption of incompressible flow, the general flow equations reduce to Laplace's equation for velocity potential, which is solvable in three dimensions. The assumption of incompressible flow introduces an error of less than five percent for Mach numbers up to **0.3.** State-of-the-art potential-flow solutions and conservation-equation solutions provide streamlines, Mach numbers, temperatures, and pressures for the flow in the entire chamber.

The second method that has been used to define the chamber flow field is cold-flow modeling, an experimental technique for analyzing complex flow. To define local flow conditions, scale models representing the particular grain and chamber design are constructed and instrumented with thermocouples and with static and dynamic pressure probes. Usually it is impossible to adjust flow conditions in the model to simulate both the Mach number and the Reynolds number of the full-scale motor while keeping conditions within the limitations of laboratoryscale equipment; therefore, the designer chooses (1) the Reynolds number when boundary-layer flow is of principal importance, or (2) the Mach number when flow outside the boundary layer is to be examined. Compressed air is fed through the model at the temperature, static pressure, and mass flowrate that will adjust the chosen parameter to the desired value. Local velocities then are calculated with the use of the experimentally determined temperatures and pressure. This method does not depend upon assumptions of irrotational, inviscid, and incompressible flow. Its accuracy is limited by the motor characteristics that cannot be reproduced in the model, e.g., the effect of heat losses in the motor and the variation of model air input distribution from the gas distribution produced by the burning propellant.

2.3.2 Heat-Transfer Analysis

Heat-transfer mechanisms in a rocket-motor combustion chamber are affected by the chamber heating environment, chamber geometry, and type of insulation material selected for thermal protection of the case structure. The chamber heating environment is defined in terms of gas transport properties, operating pressure, flow-field patterns and velocities, and gas particle distribution and behavior. When these parameters are adequately defined, the heat-transfer rate from the gas/particle mixture in the chamber to the insulator (wall) may be calculated.

The basic mechanisms by which heat is transferred to the insulator are as follows:

(1) Convection from the gas/particle mixture, $\dot{q}_{con}$

(2) Radiation from the metal-oxide particles, $\dot{q}_{rad}$

(3) Impingement and deposition of the burning metal **and** metal-oxide particles, $\dot{q}_{par}$

The total rate of heat transfer $\dot{q}_{tot}$ from the chamber-gas/particle mixture per unit area of insulator wall is the sum of the convective, radiative, and particle heat-transfer rates per unit area (heat fluxes):

$$\dot{q}_{tot} = \dot{q}_{con} + \dot{q}_{rad} + \dot{q}_{par} \quad (2)$$

where all heat fluxes are expressed in Btu/(ft² - hr).

The total heat flux thus determined is used either directly or indirectly in calculations to determine temperature rise at the insulator/chamber bondline and through the chamber Wall.

Various methods of analysis are used in the industry to evaluate each of the three modes of heat transfer. These methods are discussed in the following paragraphs.

2.3.2.1 CONVECTION

The'convective heat flux often is needed to evaluate heat transfer from the gas/particle mixture to the insulated chamber wall. In satellite motors or start-stop motors, convective boundary conditions are required for determining postfire equilibrium conditions. In either case, the convective-heat-transfer rate per unit area usually is written as the product of the heat-transfer coefficient and a driving potential (which is defined for rocket-motor chamber conditions as the difference between the temperature of the wall of the insulated chamber and the theoretical temperature of the combustion gas):

$$q_{con} = h_{con} (T_g - T_w) \quad (3)$$

where

h_{con} = convective-heat-transfer coefficient, Btu/(ft² - hr - °F)

T_g = theoretical temperature of combustion gas, "F

T_w = temperature of chamber wall (i.e., the insulator), "F

With the driving potential defined, all that is necessary to complete the determination of the convective-heat-transfer rate is a method for predicting the convective-heat-transfer coefficients. Results from references 44 and 45 show that convective heating at various locations in a rocket motor may vary by a factor of two or more, the variation depending on

complex iiiteracting phenomena such as chemical reaction, mass flow, turbuleiice, secondary flow, flow nonuniformity, and surface discoiitiiiuities – all of which influence the chamber convective heat transfer. An analytical solution that treats each of these conditions has not been feasible. However, by considering the dominant nature of certain of these phenomena, which depend on motor geometry and chamber heating environment, and by relating them to experimental data, it has been possible to develop prediction methods that produce satisfactory results.

The simplest and most extensively used method for predicting convective-heat-transfer coefficients is the equation given in reference 44, which was developed by relating axial variation of heat flux to mean mass flux at each axial location. This equation is not valid in regions of undeveloped, secondary, separated, or vortex flow. Heat-transfer coefficients calculated for regions of subsonic flow by the equation of refereiice 44 generally are lower than measured values (refs. 44 and 46). Other modifications to the equation of reference 44 are (1) correction for undeveloped-flow length, and (2) use of hydraulic radius for noncircular flow areas such as finned ports. Much of the data in reference 46 is correlated with the use of a Staiiton number. The evaluation of Staiitoii number in combustion chambers is discussed in reference 12, which also contains criteria for evaluating laminarization of the boundary layer.

A more rigorous method of predicting heat-transfer coefficients in the chamber is the boundary-layer-growth method derived in reference 47. Although this procedure was developed for axisymmetric nozzle flow, it is applied to chambers wheii the chamber envelope forms a continuous upstream extension of the nozzle. Thus, this method is not applied directly to any chamber that has complex geometrical features such as nonerodiiig grain restrictioiis, submerged nozzles, or iiisulation discontinuities.

A more sophisticated method of predicting heat-transfer coefficients in a rocket motor chamber is presented in reference 48. This work included modeliiig and modeling aiialysis; the development of a heat-transfer and ablation computation method with various analytical techniques and geometry inputs arranged into computer programs; and the applicatioii of stress analysis to the concentric cylinder configuration of the nozzle throat area aiid the aft-closure shell. Modeling and computations were confined to 55-in.- and 100-in.-diameter motors. The area of interest was from the graiii end through the aft closure to just beyond the nozzle throat. The reference-48 method is based on the problem approach outliiied in references 49 and 50 and can be used with either axisymmetric (e.g., single nozzle) or two-dimensional (e.g., four nozzle) geometries.

Areas of separated or vortex flow often occur in motor geometries involving submerged nozzles (ref. 11), multiiiozzle configurations, or insulator surface discontinuities. Predictions of heat-transfer coefficient in these areas require special methods. Methods for determining the effect of surface cavities on heat-transfer coefficients are outliiied in references 51 and

52. Where separated flow occurs, as across a step or surface discontinuity, the heat-transfer coefficient is increased to account for the increased local velocity (ref. 53). Motor geometries involving submerged nozzle throats or multinozzle configurations produce regions of separated or vortex flows for which local heat-transfer coefficients are, in general, difficult to predict by present analytical techniques. However, in such areas, scaling techniques based on velocity measurements from cold-flow modeling have been used successfully. Chambers with submerged nozzle throats have large areas aft of the nozzle entry plane where vortex flow is developed (refs. 11, 54, and 55). Convective-heat-transfer coefficients in these regions are determined by using the standard flat-plate theory after flow conditions have been defined by flow-field analysis (sec. 2.3.1.3).

The type of insulation material selected for use in the rocket motor chamber also is a factor that must be considered in the determination of heat-transfer coefficients. The ablating characteristics of the material affect the overall heat-transfer coefficient. High surface temperatures that develop in some insulators reduce the total rate of heat transfer; other effects such as transpiration cooling by the vaporizing gases also effectively reduce the total rate of heat transfer (refs. 56 and 57).

2.3.2.2 RADIATION

The difficulties in obtaining reliable values for the emissivity and absorptivity of the propellant combustion products and the insulator present formidable difficulties in calculating rates of radiant heat transfer in rocket motors. The insulator char layer generally is assumed to be a black body, but for the occasion that may require it, emissivity of the char is measured by standard methods (e.g., those described in ref. 14).

The addition of metals such as aluminum to a solid propellant results in a dispersion of a metallic oxide (alumina in this case) cloud in the form of liquid droplets or solid particles distributed throughout the chamber. The effect of this second phase on radiation heat transfer is analogous to the increase in radiation that occurs in a furnace gas that contains a concentration of soot (carbon particles) (refs. 13 and 58). The usual method for analysis of an isothermal particle cloud is to treat the system as a gray body and to define the effective emissivity in a semi-empirical equation of the form

$$\epsilon_{cl} = 1 - \exp(-aQ) \tag{4}$$

where ϵ_{cl} represents the emissivity of the gas/particle cloud, a is a function of particle size, density, and concentration, and Q is the mean beam path length for radiative transfer, all in a consistent set of units. A discussion of this relationship is given in reference 59.

The relationship in equation (4) predicts unit emissivity in large chambers for almost all high-pressure motors with solid propellants that contain reasonable percentages ($\approx$ 15%) of

aluminum. Both gray-body emissivity predictions and actual measurements (ref. 60) have indicated low values of emissivity (0.2) in small motors with relatively high (21%) aluminum content but operating with short radiant-beam path lengths and at low pressure (< 300 psi). Within the rocket motor chamber, the contribution of radiation has been measured to be 2 to 3 times greater than that of convective heating (ref. 60), the amount depending on operating pressure, radiant-beam path length, and aluminum content.

If the view factor within the rocket motor chamber is considered to be unity and the wall (insulator) emissivity ϵ_w is assumed to be equal to the insulator absorptivity, the interchange factor $\epsilon_{cl\text{-}w}$ between the gas/particle cloud and the insulator is given as (ref. 61)

$$\frac{1}{\epsilon_{cl\text{-}w}} = \frac{1}{\epsilon_{cl}} + \frac{1}{\epsilon_w} - 1 \tag{5}$$

The radiant heat flux to the insulator $\dot{q}_{rad}$ then is defined as

$$\dot{q}_{rad} = \epsilon_{cl\text{-}w}\, \sigma (T_{cl}^4 - T_w^4) \tag{6}$$

where

σ = Stefan-Boltzmann constant, 0.1713×10^{-8} Btu/(hr-ft^2-°R^4)

T_{cl} = temperature of gas/particle cloud, °R

2.3.2.3 PARTICLE IMPINGEMENT AND SLAG DEPOSITION

Impingement occurs when a chamber boundary intercepts a particle trajectory. Particle trajectories in the two-phase flow field are calculated by use of the equation of motion of a particle. The usual procedure is to first approximate the gas flow field by one of the previously discussed methods (potential flow analysis and cold-flow modeling). Then, with the use of Newton's second law of motion together with the acceleration forces and appropriate drag law, the velocity and direction of individual particles are traced through the chamber. Stokes' law (ref. 62, pp. 59, 191-193) is widely used to approximate the drag because it is simple and reasonably valid for the low slip velocities found in a rocket motor chamber. Burning droplets have been found to have two or more times the drag of inert particles (ref. 63).

The size of the particle is a necessary parameter for making trajectory calculations. Reference 64 summarizes the effect of chamber size, location in chamber, and chamber

conditions on metal-oxide particle size. The size of burning metal agglomerates as they leave the burning propellant surface is determined experimentally with window/bomb techniques (refs. 65 and 66). It is necessary to determine the reduction in size of these particles as a function of time in transit through the flow field. **A** burning-rate equation presented in reference 67 generally is used for this calculation.

In a solid-propellant rocket motor, the particles arriving at insulated wall surfaces generally have releasable heat and chemical energy in addition to kinetic energy. Normally a large portion of all this energy is transferred to the chamber wall (refs. 68 and 69), the result being locally increased regression of the insulator surface.

The insulated wall surface is subjected to localized particle impact, accompanied by heat flux, and by chemical attack when the surface temperature becomes high enough. Usually only one of these attack modes is dominant at a particular time. The response of the surface depends greatly on the nature of the material. The results may be failure by mechanical abrasion, thermal shock, chemical corrosion, or melting. Should propellant slag deposition or puddling occur, the insulation is exposed to very high heat fluxes in a small area. Conversely, carbon deposition may protectively coat the material.

Experiments have indicated that when aluminum oxide droplets from a solid-propellant gas flow impinge on a wall, the droplets lose heat to the wall only until they have changed phase and then are swept away (ref. 68). Some experimenters assumed also that the particles cooled completely to wall temperature before being swept away; but in reconciling the test data the experimenters reduced their calculated heat flux by an arbitrary "impaction efficiency" (ref. 69). The experimental findings of reference 68 probably are closer to the actual condition, but the approach of reference 69 is used more often because it produces conservative design.

Test data presented in reference 70 show that impinging droplets that were at or close to the wall temperature had no observable effect on heat transfer.

Impingement of particles of burning metal fuel on solid propellant rocket insulation and nozzle surfaces usually is accompanied by severe erosion and heating (ref. 71), unless the wall is cold enough to extinguish the particle. The deposited metal produces abnormally high heat fluxes as it continues to burn on the surface. These high fluxes occur because the heating potential of the droplet, due to its unspent heat of combustion, is two to five times greater than that of the oxide.

Impingement has also been observed to cause reduction of heat flux. In such cases the deposits are nonburning and form protective layers that effectively shield the surface (ref. 72).

The forward and aft domes are the principal locations affected by burning-metal impingement. Burning fuel is deposited on both the forward dome and igniter and on the aft

dome and nozzle backside (in submerged-nozzle systems). In all cases, the burning fuel may run down into semistagnant crevices, concentrating large heat fluxes on thinly insulated areas and creating potential burnthrough areas (refs. 65 and 73).

Insulator thickness requirements for protection against particle impingement and slag deposition are determined empirically. After analysis both the areas of particle impingement and the number of particles striking a unit area per unit time can be predicted (ref. 65). The effect of this impingement on the insulator surface regression rate must be known from previous experience or determined experimentally in subscale testing.

Some design approaches that minimize the impingement problem are (1) selection of a propellant whose exhaust products will burn completely before they reach the insulated surfaces, **(2)** aerodynamic design of the motor internal surfaces so that abrupt turns of flow occur only at low velocities and gradual turns exist where there are high velocities, and **(3)** avoidance of ridges and obstacles of any kind in regions of high-velocity flow.

Slag Deposition. – Insulation ablation caused by the accumulation of metal slag on insulator surfaces also is determined empirically. Although theoretically the energy released from burning-metal agglomerates and molten oxide droplets can be calculated and the effect on the insulator determined, in practice the amount of deposition, the deposition areas, and the nature of material being deposited (ratio of metal to oxide) cannot be calculated with enough accuracy for design use.

The literature (refs. 74, 75, and 76) contains information on the metal slag problem, including the effect that propellant composition has on the formation of metal agglomerates, the results of research on the mechanisms of slag deposition on nozzle materials, a description of the influence of motor geometry on slag accumulation, and details of studies on the evaluation of several insulation materials in contact with slag.

Axial acceleration forces tend to eliminate the accumulation of slag during motor flight (refs. 65 and 77). Radial accelerations, as incurred by spin stabilization, tend to increase the accumulation of slag (ref. 78). In some cases, slag deposition may cause excessive insulator ablation during static firings only. Slag flow into stress-relief cavities during static firing has been eliminated by static firing the motors in a vertical rather than horizontal position (ref. **77).**

Specific design provisions are effective in reducing slag deposition. Flow of deposited slag into cavities can be eliminated by the use of flow deflectors or by filling the cavities with potting materials.

2.4 INSULATOR DESIGN

The insulator designer, having selected the insulator material and evaluated the thermal environment, then proceeds to design the insulator. Insulator design may be subdivided into

thermal design and structural design. Thermal design is the determination of material thickness for each point of the insulator and flaps. Structural design is the generation of design features that will accommodate the loads, stresses, and failure modes that will occur in fabrication, storage, handling, and operation of the motor.

2.4.1 Thermal Design

2.4.1.1 INSULATOR THICKNESS

Three basic methods currently are used for calculating insulation thickness: (1) Q* (effective heat of ablation) analysis, (2) char-and-erosion-rate correlations, and (3) ablation analysis. Each method provides a solution of the same problem, and the choice of method usually depends on the degree of accuracy desired and the insulator data available. Whatever the method of calculation, the designer must take care to use material properties representative of the conditioning temperatures anticipated for motor firing, since the regression rate of the insulator surface is dependent on conditioning temperature. For example, most insulation materials lose thickness more rapidly after conditioning at +170°F than they do following -60°F conditioning. A motor to be fired under a temperature span such as -60°F to +170°F would necessarily be sized for the higher temperature.

Q* analysis is a simplified approach that is also the least expensive of the three methods. The method predicts temperature gradients within the insulation material.

Char-and-erosion-rate analysis, by which the greatest accuracy can be obtained, is the use of subscale and full-scale firing data to predict thickness requirements. However, temperature gradients cannot be predicted by this method – only char and erosion rate.

Ablation analysis is a computerized simulation of regression mechanisms that also predicts temperatures throughout the material thickness. This method is the most complex and time consuming (expensive). Some designers have reservations about its accuracy.

Many successful insulator designs have been based exclusively upon the char-and-erosion-rate method because the motors were to function under familiar operating conditions and only small changes in pressure or action time were expected. A change in propellant formulation or insulation materials frequently causes the designer to use the ablation-analysis method to predict material response to the new (unfamiliar) propellant-exhaust environments. Frequently, more than one method is employed in order to provide confidence in decisions. In some instances, all three methods have been used concurrently to predict an insulator thickness for a motor designed for unfamiliar operating conditions.

Provision for insulation char and erosion is only part of the total insulator thickness requirement. The designer usually provides additional insulation thickness primarily to ensure that the structural integrity of the motor will not be jeopardized by (1) heat conduction through the remaining uncharred insulation, (2) variation in internal ballistics from motor to motor, or (3) variations in behavior of insulator material. Another purpose for additional insulation arises in spacecraft that have temperature-sensitive instrument packages adjacent to a solid rocket motor. Postfire heat soak is limited so that the outside surfaces of the rocket motor and attached nozzle do not exceed prescribed maximum temperatures; thus radiation heat transfer to adjacent instrument packages is prevented or controlled.

The heat tolerance of the substructure is calculated, and from this result, the thickness needed for conduction insulation is calculated (refs. 79 and 80). Variations in motor internal ballistics and materials are determined by testing. Adequate thicknesses are provided to protect the combination of "worst cases" of each set of variations. Thus both the most severe internal ballistics and the poorest material performance are assumed for design purposes.

When the worst-case thickness has been calculated, a thermal margin of safety is applied. The thermal margin of safety is the percentage by which the thickness of the insulator exceeds the necessary thickness. Thus, an insulator 1.25 times as thick as that determined to be necessary by design methods would have a thermal margin of safety of 25%. The application of a margin of safety to worst-case thickness requirements may result in overly conservative design, especially where the required thickness is large. When the volume of data is large enough to be statistically sound, the use of a statistical variation analysis permits the designer to select the degree of conservatism desired while eliminating questionable data.

A thermal margin of safety of 25 to 50% generally is allowed for insulation design for a new motor. This thickness is added to the thickness calculated for each insulator location, and the locus of points is then smoothed to provide a contour that is free of sudden bumps, steps, or other contour discontinuities. This practice results in an insulator design that ranges from a minimum margin of safety of 25% at some locations to one many times as great at other locations.

2.4.1.1.1 Q* Analysis

The Q* method used for insulation design is based on a mathematical simplification of the complicated ablation process that occurs as the result of heat transfer from propellant exhaust products to the chamber wall. The total heat flux $\dot{q}_{tot}$ as expressed in equation (2) represents the amount of heat that is incident on a nonablating, nonreacting surface. The surface temperature or "effective ablation temperature" T_a usually is assumed to be constant and is taken to be the temperature at which surface decomposition begins. The local ablation rate $\dot{x}_a$ is taken to be the linear rate of movement of T_a into the insulator.

The insulator density ρ is taken as the density at room temperature. In this manner, the over-all ablation process is simplified by defining the effective heat of ablation Q* as

$$Q^* = \frac{\dot{q}_{tot}}{\dot{x}_a \rho} \tag{7}$$

where

Q^* = effective heat of ablation, Btu/lbm

$\dot{x}_a$ = local ablation rate, expressed as ft/hr

Values of Q* must be determined experimentally by measuring ablation rates at known heat fluxes, determined calorimetrically, or obtained from the literature. When Q* is known, the local ablation rates in a rocket motor are calculated for the local total heat flux. The local total heat flux varies both with motor burn time and with position within the chamber. The total heat fluxes can be calculated from the combustion-products transport properties, velocities, and heat-transfer mechanisms previously discussed.

With the use of a computerized version of an explicit finite-difference solution of the partial differential equation representing one-dimensional heat transfer (ref. 13, p. 34), temperatures are calculated for nodes within the insulator/case system. (One-dimensional methods generally are adequate, since insulators are relatively thin in comparison with chamber diameters.) As a temperature rise based on $\dot{q}_{tot}$ is calculated for the surface node and subsequent interior nodes, comparisons are made with the ablation temperature of the material for each calculation interval. When the surface node reaches the ablation temperature, it is held at that level (unless a loss of heating occurs). The amount of heat calculated, represented by the temperature rise (or loss), for each calculation interval is summed and compared with the effective heat of ablation. When this integrated heat equals or exceeds the effective heat of ablation, the node is removed from further consideration. In this manner the total ablated insulator depth and the insulator/case temperature profile during motor burn time are calculated.

The assumption of a constant ablation temperature implies that the heat of ablation is absorbed isothermally, and the insulator temperature can never rise above the ablation temperature. This assumption is misleading in relation to insulator materials that form a hard high-temperature char layer and can lead to significant error in calculating temperature profiles.

The basic assumption of the Q* method is that the insulator ablation rate is proportional to the total heat flux. This assumption does not lead to serious error if the experimental conditions under which Q* is determined are similar to the environment for which the new insulator is being designed.

2.4.1.1.2 Char-and-Erosion-Rate Correlations

The prediction of internal insulator thickness often is based on empirical equations for insulator char-and-erosion rate. These equations relate char and erosion data to the variables associated with rocket motor operation. Although it would seem that only erosion of the insulator is of concern, in practice both char rate and erosion rate (and of course char depth and erosion depth) are important in success or failure of the insulation. For example, as shown in figure 5(c), an insulator can develop an extensive char layer but undergo no surface erosion (regression) at all. Therefore, in this monograph, the expression "char and erosion" will be used to identify the total material behavior. For simplicity in symbols, the subscript ch (for "char") is used to indicate the charring and/or eroding condition.

When only a limited quantity of data was available, the resulting char-and-erosion correlations were simple and of the form (ref. 81)

$$\dot{x}_{ch} = C_1 P^a T_{cl}^b v^c \tag{8}$$

where

$\dot{x}_{ch}$ = char rate, in./sec

P = local pressure, psia

v = local gas/particle velocity, ft/sec

C_1, a, b, c = empirical constants fitted to the data for char rate

Such equations are determined specifically for a particular insulation material; for similar materials, the equations differ only by the constant C_1.

When larger amounts of data became available, correlations were developed that related char to more of the variables believed to influence the complex phenomenon of insulator charring and erosion (ablation). The relative importance of the different variables that influence char rate is not known, and rigorous mathematical models that quantitatively account for all variables have not been developed. As a consequence, dimensional analysis has been employed to indicate a logical grouping of the significant variables (ref. 82); these variables are related to gas/particle flowrates adjacent to the insulator surface, gas transport properties, motor geometry, insulator thermal properties, and thermal radiation from the insulator surface to the propellant gas/particle mixture. These complex relations are illustrated in the following equation using dimensionless groups:

$$Lu = C_2\ Re''\ Fo^b\ Bi^c \left(\frac{r}{\dot{x}_i}\right)^d \left(\frac{\chi_i}{\chi_{cl}}\right)^e \epsilon_{cl}^f \qquad (9)$$

where

$$Lu = \text{Luikovnumber} = \frac{r\dot{x}_{ch}}{\chi_i}$$

$$Re = \text{Reynolds number} = \frac{\rho\, v\, r}{\mu}$$

$$Fo = \text{Fourier number} = \frac{\chi_i\, t}{r^2}$$

$$Bi = \text{Biot number} = \frac{hr}{k_i}$$

r = radius of flow channel (i.e., ½ chamber inner diameter at a given location)

x_i = total insulator thickness

h = overall coefficient of heat transfer from the exhaust gas to the insulator

t = time

μ = absolute viscosity

thermal diffusivity of insulator

χ_{cl} = thermal diffusivity of gas/particle cloud

C_2, a, b, c, d, e, f = new constants for this equation fitted to the data on Lu

In order to achieve maximum confidence in such correlations, char and erosion data usually are obtained from a variety of rocket motors that vary in size, operating conditions, and propellant composition. The data often pertain to more than one kind of insulation material. The size of the motors from which data have been obtained ranges from small

subscale (about 10 lbm propellant) to large (over 40 000 lbm propellant). Operating conditions have varied from low pressures (≈ 200 psi), low combustion-products flow velocities (≈ 20 ft/sec), and short exposure times (a few seconds) to high pressures (≈ 1000 psi), high flow velocities (> 3000 ft/sec, ≈ Mach 1) and long exposure times (> 100 sec). Statistical concepts have been used to determine the confidence limits of the data near the least-squares regression line for the set of data being investigated. Char and erosion rates for new designs are predicted from an upper confidence line that is often selected so that, at a 95-percent confidence level, there is a 95-percent probability that the prediction will produce a conservative design.

The dimensional-analysis approach has been adequate and effective in preliminary design of insulator thickness for new motors when the accumulated data were extensive and valid or conversely when no firing data were available. However, it must be emphasized that final design is based on direct postfire measurements on full-scale motors and, where necessary, on empirical correlations of the form given in equation **(8)** as developed for a specific motor.

2.4.1.1.3 Ablation Analysis

The most sophisticated technique used to calculate insulator thickness is finite-difference boundary-layer/charring-ablator analysis, in which the detailed mechanisms of charring and erosion are considered. The most widely used method of this type that has been adapted to the digital computer is described in references 68 and **83.** While this procedure has been used primarily for the analysis of ablative nozzle materials, it can also be used for the analysis of internal insulators. Reference **84** describes the application of the method to ablative nozzle materials, and reference 2 describes the use of the method for insulators and extends the method for application to multiple-restart applications.

When this method is employed, the insulator is modeled in three zones: (1) a char or residue zone at the surface, (2) a pyrolysis zone, and **(3)** a virgin-material zone (fig. **2).** The decomposition of the virgin material by chemical reactions occurs in the pyrolysis zone, leaving a char or residue at the surface. This decomposition yields a pyrolysis gas that percolates through the pyrolysis zone and the char zone to the surface where it reacts chemically with the boundary-layer gas. The surface of the char zone also reacts with the boundary-layer gas, and often it is mechanically eroded.

Analysis is carried out in two phases. First, the diffusion-limited chemical interaction among the surface char, the pyrolysis gas, and the boundary-layer gas is calculated as a function of wall temperature and rate of pyrolysis-gas evolution, and a tabular solution is obtained. Second, the in-depth transient-heat-transfer analysis of the insulator is made, and the solution is determined iteratively, with the use of the previously determined tabular results of surface reactions. In addition to analysis of chemical reactions, the evaluation of

boundary conditions at the surface includes analysis of mechanical erosion, radiative heat transfer, and convective heat transfer corrected for flowing of the pyrolysis gas. The two important results of the calculation are the total surface erosion and the temperature distribution within the insulator as a function of time. A procedural outline and the required input data for several well-known insulators are presented in reference 48.

2.4.1.2 STRESS-RELIEF-FLAP THICKNESS

The remaining problem in insulation design is to determine the thickness required for grain restrictions such as the propellant-shrinkage liner, commonly called the stress-relief flap. Heat conduction of sufficient magnitude through the stress-relief flap will heat propellant to the autoignition level. The thickness of the stress-relief flap, therefore, depends on both the flap-cavity heating environment and the exposure time as well as on propellant autoignition temperature and flap material properties. When the insulator-flap cavity is filled with a suitable potting compound (sec. 2.2.2.3), the flap surface is not exposed to a heating environment, and the flap thickness depends only on structural and manufacturing considerations. It is only necessary to ensure that the regression rate of the potting compound is not appreciably greater than the propellant burning rate. If the insulator-flap cavity is not potted, the cavity heating environment is considerably less severe than the chamber heating environment unless slag accumulates in the cavity (sec. **2.3.2.3).**

Unlike the chamber thermal environment, which changes relatively slowly with time, the thermal environment in the unpotted stress-relief-flap cavity changes rapidly with time. The cavity, initially empty, fills with hot combustion products during initial pressurization. The hot-gas/particle mixture filling the cavity transfers heat to the insulator flap surfaces and rapidly cools off. As the mixture cools, additional gases flow into the cavity to maintain pressure equilibrium between the flap cavity and the chamber. The cavity temperature is, therefore, a maximum at ignition and decreases thereafter with time. The rate of cavity-temperature decrease depends on the cavity dimensions, thermal properties of the gas/particle mixture, and the degree of turbulence within the cavity (ref. 85). The flap cavity dimensions depend on the initial propellant temperature (lower temperatures produce larger cavities), the propellant slump, and the case expansion during pressurization – all of which increase the cavity volume. Propellant slump typically occurs in motors with stress-relief flaps in either the forward or aft closure. The slump creates a relatively large gap between the boot insulator near the top of the motor but no gap at the bottom of the motor. A motor of such a configuration also will develop a variable circumferential gap if it is static fired in the horizontal position. Higher ablation rates and higher case temperature then result from the differential in gap width.

The exact size of the insulator flap cavity seldom can be calculated accurately. The degree of cavity turbulence and, therefore, the convective-heat-transfer coefficients also are difficult to predict accurately. Similarly, radiation heat transfer from the cavity-gas/particle

mixture can seldom be calculated accurately, because the emissivities and absorptivities generally are not known as a function of temperature. If emissivity and absorptivity data are available, flap-temperature profiles can be calculated by the method presented in reference 85, which assumes that heat is transferred by radiation only. This procedure, which is an iterative process, involves the assumption that flap-cavity wall temperatures are a function of cavity-gas temperature and calculates the cavity-gas temperature as a function of time. The heat-transfer rates to the cavity walls then are calculated and used as boundary conditions for the one-dimensional heat conduction equation to determine wall-temperature profiles. The wall surface temperatures then are compared with the assumed wall surface temperatures used to calculate the gas temperature. If agreement is poor, the procedure is repeated, the calculated wall surface temperature being used to determine a new gas temperature-time history.

When little data are available, the initial flap design may be analyzed by calculating the flap temperature profiles as a function of time and assuming "reasonable" or "maximum feasible" values of the heat-transfer coefficients. If the cavity volume and gas composition are constant, then according to the perfect gas law the product of gas mass and the gas temperature is a function only of cavity pressure. Hence, if the chamber pressure is reasonably constant, the product can be assumed to be constant. Heat balance for the cavity can then be expressed as follows:

> heat in with fresh gas minus heat lost to flap and insulator equals change in sensible heat of cavity gas.

The cavity temperature-time history can be calculated by using the relation between gas temperature and cavity-gas mass derived from the perfect gas law, simplified flap-cavity geometry, and assumed heat-transfer coefficients for calculating the heat loss to the flap and insulator surfaces. The cavity temperature history then can be used to calculate temperature profiles within the flap, and therefore, the flap/propellant interface temperature. The magnitude of the flap/propellant interface temperature determines whether or not propellant autoigniton will occur.

Preliminary design thicknesses generally are based on previous experience. The current procedure is to use flaps ranging in thickness from 0.05 to 0.1 in. except on very large motors where insulation fabrication requirements dictate thicknesses up to 0.25 in. (ref. 9). Flaps are, in general, uniform in thickness except near the motor centerline, where heating is higher and the flap thickness is correspondingly increased, and near the propellant-bond termination point, where a thicker section is necessary to reduce the case-to-propellant transition stresses.

2.4.2 Structural Design

2.4.2.1 LOADS

Environmental. – Both the loads applied to a solid propellant rocket motor and the environment in which the motor is placed have a significant effect on the structural integrity of the insulator and, hence, on insulator performance. The environment alters the mechanical properties of the insulator and also places loads upon it. Storage, transportation, and handling environments generally produce the highest nonoperating loads on the insulator. Thermal loads are imposed by transportation and storage. Impact loads occur during handling and transportation. Generally, the shipping and storage containers protect the insulator from both thermal and impact loads, and environments are kept within thermal tolerances during shipping and storage by means of air conditioning.

Processing. – Insulator and motor processing operations affect insulator mechanical properties and cause residual stresses in the insulator. Molding, layup, and other insulator manufacturing operations also cause stresses in the insulator. Both fiberglass-chamber winding and subsequent cure have a significant effect on the insulator structural behavior. Filament winding normally causes compressive stresses in the insulator by squeezing it against the winding mandrel. However, such stresses are much smaller in magnitude than the compressive stresses developed during the high-temperature cure cycle for the chamber. The coefficient of thermal expansion of the insulator is significantly higher than that of the case and mandrel; this differential can cause high compressive stresses in the insulator at the 300°-350°F cure temperature. It is not unusual, moreover, for the insulator to flow under the combination of sustained high temperature and compressive stress; hence, the locations of splices and joints may change during chamber cure. Therefore, changes in mechanical properties (chiefly strain capability) resulting from chamber cure are significant (fig. 10). Because of the viscoelastic nature of elastomeric materials, the relative change in mechanical properties varies with loading rate and temperature and, hence, a recharacterization using samples that have been subjected to the chamber cure cycle often is required.

Because the maximum cure temperature of most propellants normally is less than 150°F, the mechanical properties of the insulator generally are not affected by the processing cycle for the propellant grain. The temperature at which composite propellant grains are free of stresses normally is about the same as the cure temperature. When the grain is cooled to a 70°-80°F level, residual tensile stresses in the grain, insulator, and motor case are created. So that little or no residual tensile stress occurs in the motor at the end of manufacture, most double-base propellant grains are pressurized during cure and are cured at approximately 120°F. Hbwever, compressive stresses developed in the grain and insulator during processing can become as large as 300 psi.

Operational. – The most severe operational loads on an insulator generally occur during motor firing at low temperature, where the combined effects of thermal shrinkage, motor

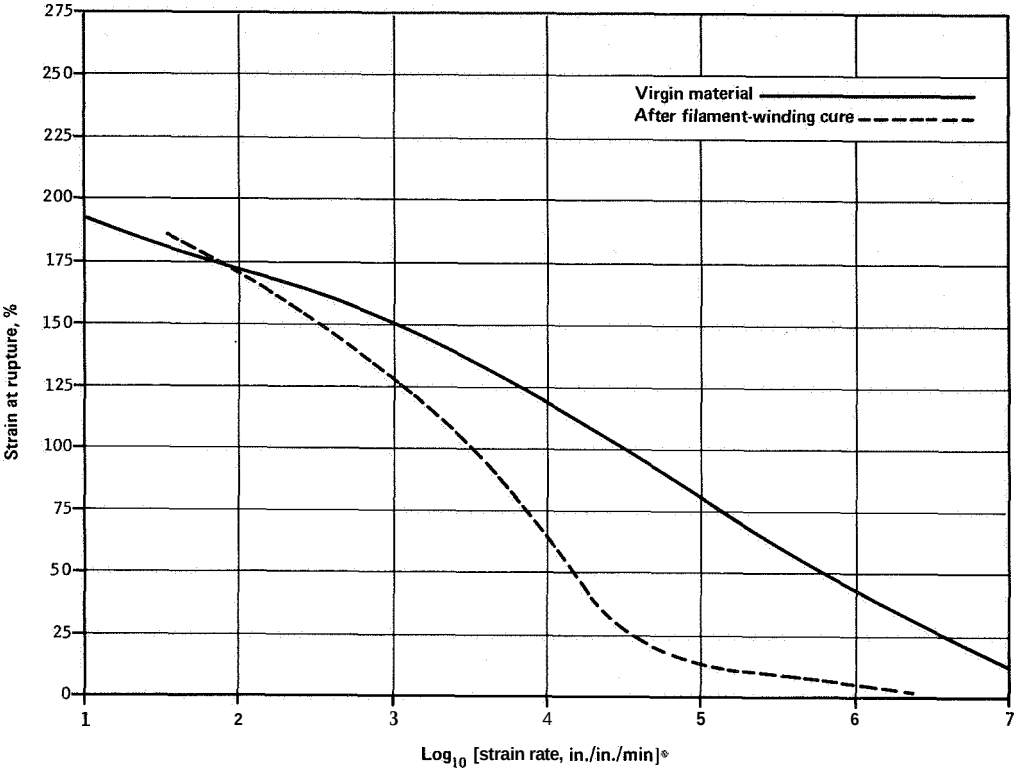

Figure 10. – Strain-at-rupture vs strain-rate for boric acid/NBR-phenolic insulation before and after cure of the filament-wound case.

pressurization, and flight acceleration are present. Under pressure loading, differential movement of the grain and case is higher in motors with glass cases than it is in motors with metal cases. Hence, insulator shear/tensile stresses and strains generally are higher in glass-case motors during motor pressurization. On the other hand, in many motors with metal cases, the failure-producing components of thermal stresses and strains developed in the insulator and propellant grain most often are larger than those of the stresses and strains developed as a result of motor pressurization.

2.4.2.2. STRESSES

Preliminary Analysis. – The major portion of an insulator usually is subjected to small (< 2%) strains during motor processing, development, and operation; i.e., insulator strains are no greater than those imposed upon the case. At a distance of (i.e., equivalent to) only a few insulator thicknesses from bond terminations of the grain, the insulator is in essentially a

uniform hydrostatic state of stress. Propellant and insulator stresses are, therefore, more directly related to the dilatational stiffness (bulk modulus) rather than the distortional stiffness (shear modulus) of the insulator. Most insulator stresses are not only compressive as a result of motor pressurization but also tensile as a result of propellant shrinkage. The compressive stresses usually do not strain the material beyond its capability, but tensile thermal stresses can be large enough to cause the insulator to separate from the case or from the propellant or both (ref. 17).

One-dimensional stress solutions (ref. 86) are used to obtain an estimate of the average insulator stresses for both thermal and acceleration loads. However, there are no simple stress analyses that provide accurate predictions of the local stress levels at the critical bond terminations.

Parametric studies have revealed the following useful trends in changes to insulator stresses and strains at bond terminations under thermal and pressure loads:

(1) Insulator stresses for both thermal and pressure loading are proportional to the tensile modulus of the propellant, within the effective modulus range for most motors. Thus, a motor with a high-modulus propellant is more likely to experience insulator-to-flap structural failures than the same motor with a low-modulus propellant.

(2) Failure-producing components of insulator stresses resulting from pressure loading are proportional to the case strain. Motors with composite cases therefore are more likely to experience insulator structural failure during firing than motors with metal cases.

(3) In motors with simple port configurations, stresses and strains at bond terminations are related to the stresses and strains at the grain center port. The proportion of bond-termination stresses and strains to center-port stresses and strains increases as length-to-diameter ratio (L/D) decreases (refs. 87 and 88).

Refined Analysis. – Numerical analyses such as the finite-element method (ref. 89) are used to calculate stresses and strains in the insulator of a solid propellant rocket motor. It is a relatively common practice to include the insulator in mathematical models used for stress analyses of the propellant grain (ref. 17), particularly near the bond terminations. The insulator is assumed either to be incompressible or to have an elastic bulk modulus. However, insulation materials filled with fibrous materials often have directional properties that should be considered in the structural analysis.

The theory of linear viscoelasticity (ref. 86), normally applied to the propellant grain, is also applied to the insulator for analysis of the distortional stiffness. Effective moduli for transient loading conditions usually are based on the quasi-elastic approximation; i.e., the

approximate step-loading solution uses the value of the tensile and/or shear relaxation modulus at selected time intervals after application of a load. Superposition (ref. 90) then is used to obtain the general time-dependent solution.

Large geometrical changes and high local insulator strains at bond terminations greatly reduce the applicability of the linear numerical model. In fact, such linear solutions are highly unreliable at the bond termination and theoretically should predict infinite stresses. The best method at present for dealing with this situation is fracture mechanics (ref. 91). This discipline employs a balance of the energy that creates new insulator surface, the elastic energy released in the motor as the insulator tears, and the work exerted by external forces. Nonlinear effects in material are approximately contained in material parameters relating to the creation of new surface energy.

2.4.2.3 STRENGTH ANALYSIS

A strength analysis is performed to define the structural capability of a material in relation to the predicted stress and strain values determined by the stress analysis. The strength of an insulation material is a function of five factors: (1) the rate of loading, (2) the directions in which the loads are applied, **(3)** previous loads and environments experienced by the material, (4) material age, and (5) temperature. Elastomeric insulation materials obey the superposition principle (ref. 90), an equivalence of temperature and strain rate that is useful both in comparing properties of different materials and in predicting structural response of a material at conditions other than those tested.

Stress, plotted as a function of temperature and reduced strain rate, increases with increasing strain rate, but maximum capability of the insulator to strain without fracturing occurs at some intermediate strain rate (ref. 86). Different allowable properties apply to uniaxial tension, biaxial tension, shear, and compressive loadings. This dependence of strength on direction of loading usually is expressed by a relation between allowable properties and state of stress. Examples of commonly used failure theories for insulation materials are maximum principal strain, maximum shear strain, and maximum principal stress (ref. 89).

Previous loadings (e.g., from chamber processing) introduce residual stresses and strains in insulator material. Chamber and grain cure cycles produce chemical and mechanical changes in the insulator. Aging alters the material strength and strain capability, as previously explained.

In a strength analysis, allowable properties for the appropriate strain rate, temperature, state of stress, loading history, and material age are compared with the results from the stress analysis. From this comparison, an appropriate factor of safety being used, a prediction of the structural integrity of the insulation is made. Structural factors of safety are used to

account for uncertainties in the loads, analytic methods, and material property variablility. **A** commonly used structural factor of safety is 1.50, but the exact value depends upon the amount of material performance history available and the accuracy of the analytical procedures. When reliable material property data and proven analytical procedures are used, the factor of safety may be as little as 1.25. When the material data and analysis procedures are not well proven, the factor of safety may be as high as 2.00. Strength analyses are made of bonded interfaces'as well as of the insulation material itself. Local increases in insulation thickness, at such locations as flap terminations, can provide significant reductions in the propellant-to-flap bond stress, even though no reduction may occur in the maximum insulator stress.

The insulator structural integrity is evaluated by examination of the structural margin of safety:

$$MS = \frac{1}{R} - 1 \qquad (10)$$

where

MS = structural margin of safety

$$R = \frac{\text{design stress}}{\text{allowable stress}}$$

The design (i.e., computed) stress value includes the structural factor of safety.

When the MS is either negative or too large positively, the designer substitutes materials or changes the design to adjust the MS to either zero or a small positive number, but preferably zero. Large margins of safety are reduced primarily to minimize inert weight, but reduction of expensive insulation material costs can be a strong consideration.

2.4.2.4 FAILURE MODES

Metal cases and fiberglass-reinforced composite cases have some failure modes in common. In both, insulator cracking and slump can occur during insulator and insulated-case processing. Moreover, during motor operation, separations between insulator and flap, case, or propellant, in addition to insulator cracking, may develop.

Relative importance of the failure modes varies wtih motor environment, design, manufacture, and case materials. During storage, long-term aging/viscoelastic effects cause bond separations and subsequent propellant slumping or cracking. Propellant ignition also

causes bond separations that result in exposure of the case to gases and heat. The primary result of insulator/propellant separation is the creation of additional propellant burning surface that, in turn, causes premature exposure of insulation, or, if the separation is large enough, enough extra pressure to cause case failure. It has been established by X-ray studies that additional propellant surfaces created by the insulation or flap separation ignite as soon as one edge of the propellant surface is exposed to the flame front (ref. 92). Several effects may occur, the nature depending on the void length perpendicular to the burning front. The separation may simply expose the insulation prematurely and cause the insulation to ablate at the normal rate but for a longer time. However, if insufficient vent area for the separated area exists, then the pressure and gas velocity will increase in the slot created by the separation. This "tunneling" has led to an order-of-magnitudeincrease in insulation ablation rate. A confined site of combustion can also cause inward grain fracture that results in nozzle or port blockage. Insulator/propellant separations often are identifiable as large anomalies on the motor pressure-time curve, but if the tunneling becomes severe enough, the separations can result in localized failure by insulator burnthrough.

The shear and peel structural requirements for the bond between insulation and case are quite similar to those for the bond between insulation and propellant, and the stress levels allowable for storage and firing are determined in tests similar to insulation/propellant bond tests. Insulator-to-case separations are not as readily identified with a failure mode as are the insulator-to-propellant separations. In testing, motors have historically performed successfully with extemely large case-to-insulator separations. The primary failure mode results from the passage of gas between the case and insulation, which eventually leads to a case burnthrough. Knowledge of this phenomenon has led to the current industry practice of requiring all insulation terminus points to be free of voids.

All failure modes postulated for metal-case motors are also common to glass-case motors. The tensile modulus of glass is about 3.5×10^6 psi, whereas the tensile modulus of steel is about 29×10^6 psi. At the same pressure level, strains in the fiberglass case are at least triple those in steel cases. The higher strain in glass cases has caused or contributed to failures at (1) the insulator/case interface, where bond failure leads to case burnthrough; (2) the insulator-to-insulator joints, where adhesive or sealer strain capability is exceeded; and (3) the insulator surface, where mechanical strain accelerates erosion rate. A critical structural condition usually exists adjacent to the port adapters because of differences in the stiffnesses of the port adapter and the case. The pressurized case expands much more than the adapter, thus pulling the case back from the adapter. A flexible rubber insert usually is placed between the case and the adapter, allowing the case to strain without destroying its bond with the adapter. -Moreover, sufficient insulator thickness usually is maintained under the adapter tip to reduce strains at the insulator/propellant interface to a level compatible with the propellant strain capability.

Maximum principal strains at the level of 50 percent have been observed in insulators adjacent to bond terminations. The usual precautionary design feature is additional insulator

thickness to reduce strains. **A** rubber insert sometimes is used to provide a fillet at the termination of the stress-relief-flap bond.

In high-strain regions such as adapter tips and flap terminations, or in any area where principal strain exceeds 2 percent, special care must be taken in insulator design. Insulator splices (and repairs) are not made in highstrain regions. Barrier coats are formulated with attention to anticipated strains, because cracks originating in barrier coats have been known to propagate themselves in insulation and propellant.

2.5 INSULATOR FABRICATION AND PROCESSING

In order to produce a reliable, conservative design, the designer must have at his disposal a rather sizable reservoir of reliable material performance data. He therefore runs a risk in utilizing new materials, although sometimes the risk is justified by potential gains in material performance. The designer generally eliminates the risk of insufficient or misleading information by utilizing well-known materials. Compounding specialized elastomeric insulator material for a specific design is the special province of the rubber technologists, who by changing ingredients, altering recipes, or changing compounding methods have produced insulation materials with specific properties designed for the needs of a specific motor. The insulation designer thus must be familiar with the nomenclature and jargon used by rubber technologists. Reference **93** provides a glossary of terms and descriptions of rubber properties.

2.5.1 Compounding

The process of blending ingredients together to produce an insulation material is termed "compounding." The insulation material consists of an elastomer, the classes of which were previously discussed, and a filler material that is added to enhance certain thermal or physical properties. Char characteristics, tensile strength, elongation, aging resistance, hardness, thermal conductivity, and ablation rates – all can be altered by variation in filler type and amount added. Extenders and diluents are, like fillers, materials added to the elastomer to create specific desirable changes in physical properties.

Fillers. – Fillers are compounding ingredients added to elastomers to improve elastomer physical or thermal properties, change the hardness, or extend or dilute the elastomer (i.e., increase its volume). Certain materials enhance tensile strength and thus reinforce SBR, NBR, and silicone rubbers. In SBR, a synergistic reinforcement effect is produced by the combination of coumarone resin and mineral fillers. In NBR, carbon black produces this reinforcement. Silicone rubbers are reinforced by fine-particle silica. Other reinforcing fillers

are zinc oxide, lignin, and clay. Materials that improve the insulating properties of elastomers are silica, asbestos, and inorganic hydrates such as boric acid or potassium titanate.

An extending filler produces an increase in material volume without a commensurate decrease in physical properties of the product. **A** diluent, on the other hand, is used to dilute the rubber hydrocarbon, and in this operation a loss of physical properties is anticipated. Vulcanized vegetable oils, mineral rubber, pitch, vegetable oils, natural rubbers, synthetic elastomers, petroleum derivatives, and resinous materials are used as extenders or diluents.

Quality and uniformity of fillers is as important to product quality as is the quality and uniformity of the base elastomer itself.

Mixing. – The mastication or milling of rubber stocks is the method by which vulcanizing agents, fillers, pigments, accelerators, and other additives are blended into the rubber stock. Careful milling is necessary to produce uniform, well-mixed insulation material that performs as anticipated. For instance, excessive milling of asbestos-filled insulation material chops up the asbestos fibers and reduces insulation thermal performance. The outstanding performance of one well-known insulator is due in large measure to the manufacturer's ability to mill the elastomer without breaking up asbestos fibers. Inadequate milling produces insulation materials that do not perform uniformly, eroding at widely varying rates from spot to spot. Some early upper-stage motors, for example, failed because filler materials were not dispersed throughout the insulator. Soft spots, which eroded rapidly to bring failure, occurred at localized areas with low filler content. Other failures in motor insulation have been attributed to excessive variations in the recipe for compounding the insulation material. Perhaps many operational failures of insulation can be explained by the fact that largemixers and mills are much less efficient than laboratory-scale mills in producing uniform quality.

2.5.2 Fabricating

Insulators normally are made from unvulcanized sheets of elastomer either by compression molding or by hand layup. Insulators also are manufactured by machining the part from a vulcanized block of convenient shape. **In** the case of mastics, the insulation is applied by troweling. The quantity of the parts to be produced, the dimensional tolerances required of the end product, and the time available for fabrication are considered in determining the method of fabrication for any particular insulator. Products made by compression molding, hand layup, machining, troweling, and by combinations thereof have performed at the same level in comparable tests.

2.5.2.1 MOLDING

The usual method of fabrication, once the insulator design is firm, is to compression mold the parts in matched metal dies. When large numbers of parts are required, compression molding produces parts at the lowest piece cost, at the maximum reliability, and at good dimensional uniformity; however, tooling costs for this method are the highest. **A** molded insulator is made from an unvulcanized rubber preform that is extruded, calendered, or pattern-cut from rubber stock. The preform is necessary in some large moldings to ensure that elastomer flows into all parts of the mold cavity before vulcanization takes place. The various elastomers used in insulator molding are very different from each other in their ability to flow into the mold cavity recesses. The combination of mold design and mold preform therefore often is established by trial and error. When layup preforms are used, the grain of the material is oriented parallel to the propellant side of the preform, and the plies are stitched together in the manner described for the hand-layup method.

Three methods of loading a compression mold are illustrated in figure 11. Molding variables, mold charge, pressure, temperature, and time are controlled to produce optimum insulator vulcanization. The weight of the preform slug is not permitted to vary more than ± 10 percent from the desired weight of the molded insulator. Molds are closed slowly during the prevulcanization operations. Removal of entrapped air is accomplished by "bumping" (repeated release and application of pressure to the mold). Mold pressures range from 500 to 900 psi, and temperatures from 200 to 350°F. The mold and insulator are cooled to 180°F before the molded insulator is removed from the mold. Insulators produced from molded or laidup NBR will shrink approximately 2 to 3 percent where the shrinkage is unrestricted by insulator geometry. This shrinkage is anticipated by designing the mold so that the insulator falls within dimensional specifications following shrinkage. Dimensional tolerances on finished molded parts usually are ± 0.010 to ± 0.020 in., although some compounds may be molded to tighter tolerances (ref. 21).

2.5.2.2 HAND LAYUP

Final products may be made by hand layup when the quantity of parts required is small, when the design of the end product is subject to change, when the cost of permanent molds is prohibitive (e.g., because of size), or when the time available for fabrication will not permit the procurement of permanent tools. The installed costs for hand-layup parts are high, usually approximately **2** to 5 times the cost for comparable compression-molded parts or for troweled mastic. However, temporary, inexpensive, and readily fabricated tools are adequate for hand-layup production. The thickness tolerance for hand-layup parts must be large, usually ± 0.050 in., because the dimensions of the finished part depend on the skill of the technician. The functional reliability of parts produced by hand-layup procedures can be the same as that for parts produced by any other method of fabrication (ref. 94).

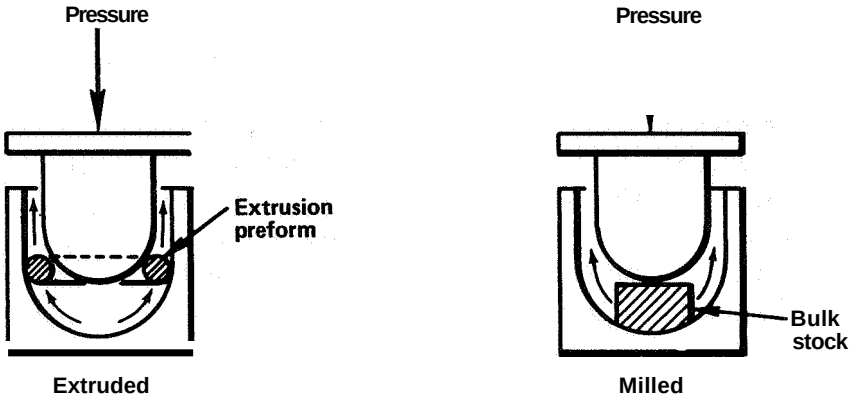

(a) Slug loading

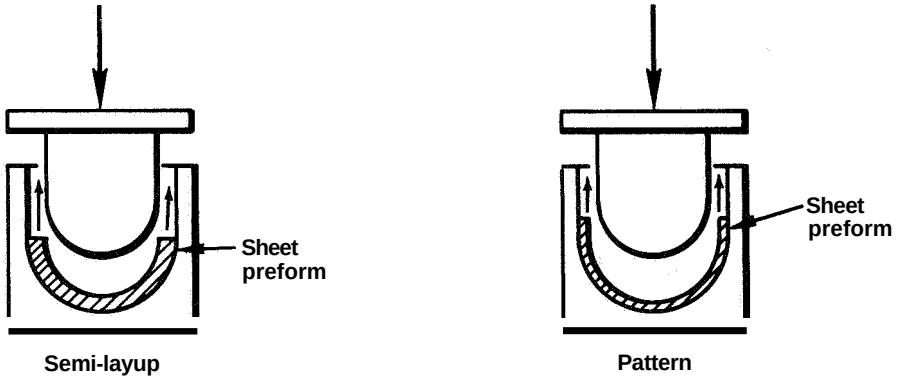

(b) Layup loading

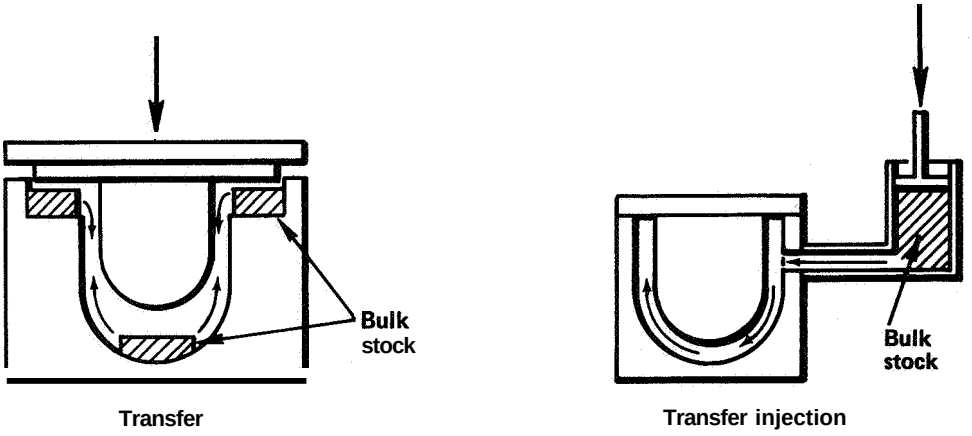

(c) Transfer loading

Figure 11. – Three methods of loading a compression mold with elastomeric material.

The layup procedure consists of applying pattern-cut pieces of unvulcanized elastomer over a form or inside the motor case so that the largest patterned pieces will be the first exposed to the motor chamber environment (ref. 95). When **NBR** or **SBR** is used, all surfaces and edges of patterned elastomer pieces are scrubbed with clean cloths that are "wet but not dripping" with methyl ethyl-ketone (MEK) and simultaneously or immediately thereafter scrubbed with a brush. After all traces of MEK have evaporated, the patterned pieces are laid in place and stitched together with standard rubber-working tools after the rubber is softened with a solvent. As noted, failures have occurred because of inadequate evaporation of MEK between application of rubber layers. High MEK content in the insulator results in general softening of the insulator and resultant high erosion rate, ply delaminations caused by the release of volatiles from absorbed MEK, and undercuring and increased erosion.

A small ($\leqslant$ 5%) amount of natural rubber in the recipe creates sufficient tack for hand layup. Otherwise, an adhesive, usually one based on natural rubber, is used to produce good layer-to-layer adhesion. Cure of hand-layup insulators generally is accomplished with a vacuum-bag device being used to compress the elastomer laminate.

2.5.2.3 TROWELING

In the use of mastic insulators, three application techniques have been used: rotating chamber (ref. 9), pump extrusion (ref. 96), and spray. In the first method, the chamber is rotated as the mastic is troweled on in layers of a specific critical thickness determined by the slump characteristics of the material. The insulation is gelled after application of each critical thickness. Following the final application, the assembly is cured at about 135°F for five days. Thickness control is maintained by the sweep templates. Product dimensional tolerance has been demonstrated to be 0.17 to 0.25-in. thickness for one pass with a trowel designed for a 0.25-in. thickness (ref. 97). Thicker applications or multiple passes require wider tolerances. The pump extrusion technique uses cartridge guns or hoses and a hand-troweling finish operation. Thickness control is maintained either by guides or templates or by final machining. Spray methods apply 0.07 to 0.09 in. per pass. The minimum practical thickness for mastic insulation is 0.25 in.

A common problem encountered in compounding mastic insulation is controlling slump during application. Three process-formulation philosophies to control slump have been used to date: (1) the use of thixotropic agents, which allows a long working life; (2) application of insulation to an isolated section on each pass, taking advantage of a short pot life; and (3) application of mastic in thin layers and gelling before proceeding with the next layer. Sometimes all three methods must be used simultaneously to prevent slump.

The primary problem with mastics is void inclusion, which is encountered with all of the mastics (refs. 8 and 9). Compounding variations are used to control the voids created by thixotropic materials. The voids are identifiable by various techniques, but still remain a major problem.

Elastomeric mastics in general and many thermosetting-plastic insulators require a liner to limit migration of plasticizers and moisture. Where flaps are required in a motor in which mastic is to form the insulator, a material other than mastics usually is used for flap fabrication.

2.5.2.4 MACHINING

The final insulator may be machined from a vulcanized block of convenient dimensions and shape, or from material cast, troweled, or laid up somewhat oversized. The machining is done by programming the movement of the insulator past a belt sander or rotating abrasive tool; conventional lathe or milling operations are not used. Usually, it is desirable to machine the final product when the number of parts required are so few that accurate permanent tools or compression molds cannot be justified. It is sometimes necessary to produce a portion or all of the end product by machining when the required dimensional tolerances are extremely close.

2.5.3 Processing

The designer must consider all rocket motor processing steps and their effect on the materials used for insulation, liners, and adhesives. The temperature, pressure, moisture, and time spent in each motor production step must be evaluated for their possible effects on the insulator. The inverse viewpoint must be considered also; i.e., the designer must examine the effect that his choice of insulator material would make upon the complexity and subsequent cost of motor processing. Successful design is achieved when the motor requirements can be met with maximum cost effectiveness. The relation of solid propellant processing factors to rocket motor design is treated in detail in reference 29.

An excellent example of how processing factors. affect final design can be seen in the experience with a boric acid/NBR-phenolic insulator selected for the Poseidon second stage. The material provides excellent thermal protection, is lightweight, and seemed to be the best candidate. However, two major processing problems – the need in manufacture for elaborate mandrels, and the difficulty in preventing degradation of the boric acid during the cure of the filament-wound case – were continual production headaches. These problems eventually resulted in the decision that the insulator material should be replaced.

The degradation of insulator materials generally is caused by moisture absorption, aging, or damage in processing. Many adhesive systems are degraded by absorption of moisture, and they must be thoroughly dried prior to propellant casting. The drying cycle varies from zero time to three days at 180°F. The detrimental effect of moisture on one adhesive system is shown in figure 12 (adptd. from ref. 98). The effect of moisture normally is explored during development of the liner, preferably before final selection of insulator material.

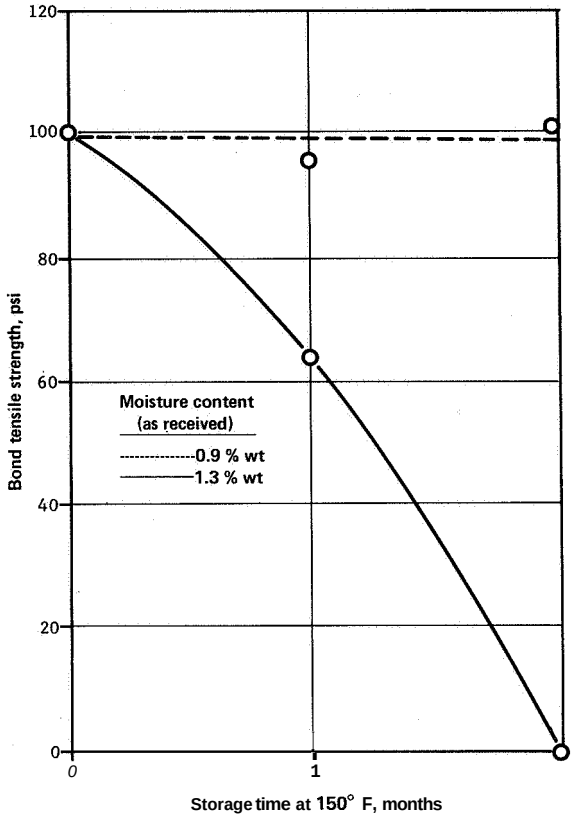

Figure 12. – Effect of insulation moisture content on insulation/liner/propellant bond strength during storage (adptd. from ref. 98).

Polyurethanes, polyesters, polysulfides, cyanoacrylates, epoxy-polysulfide, and epoxy-nylons are subject to degradation by moisture.

Materials that are quickly degraded by ozone or sunlight aging (e.g., NBR, **SBR,** or natural rubber) must be protected from exposure to ozone and sunlight. It is common practice to place cotton with the insulation to seal it from air (ozone) circulation, and to'store insulated cases or insulation material in the dark to prevent aging by sunlight. Silicones, fluorosilicones, polyurethanes, EPDM (under 200°F), polysulfides, and Hypalon (chlorosulfonated polyethylene) elastomers are resistant to ozone attack and aging by sunlight.

Only an extremely small number of large insulators (> 30 in. diam.) free of voids, nicks, cuts, scratches, or thin spots have been manufactured. All others have required rework or repair. Through the stress analysis described in section 2.4.2.2, zones of the insulator where strain is too high to permit repair are identified. Any area that is strained over 2 percent is

considered an area worthy of detailed analysis. Strains over *25* percent generally are considered too high to permit repair.

Repair methods depend on the severity of the damage; i.e., the size and shape of the damaged area and its location in bond line, insulator, or substrate. Damage to the substrate must be evaluated with respect to the structural integrity requirements. Where insulator or bondline damage is apparent, the repair usually consists of cutting out the entire damaged area and vulcanizing an insulator patch over the damaged area. New adhesive is applied to the substrate, the removed insulation is replaced by unvulcanized stock of the same composition, and the patch is vulcanized in place under pressure of about 100 psi (ref. 99). Less severe damage, which neither compromises structural integrity by creating a stress concentration nor poses a threat of thermal failure due to insufficient insulation, may be repaired with adhesives or potting compounds to which the casebond system will adhere. **A** thin (0.030 in.) insulator sheet sometimes is bonded over the repair area in order to facilitate case bonding.

2.6 DESIGN VERIFICATION

Verification of design by testing and inspection of insulators is a vital part of development programs. The designer must know that materials, geometry, and integrity of the insulator match design assumptions before the test data become meaningful. Test data are useful to the designer in evaluating the performance of his design. Zones shown to be marginal and unsatisfactory by static-fire test data can be redesigned. Thin areas are made thicker, and overweight sections are trimmed.

Most preliminary insulator designs are ultraconservative in order to prevent loss of test data pertaining to other motor components during early program test firings. **As** confidence in the material performance and insulator design increase, the insulator is trimmed to the configuration that yields desirable margins of safety. This empirical design approach provides high reliability and high confidence in the finished design.

Destructive testing is used throughout the insulator development program. Complete insulators are cut. up to verify that materials and dimensions are within the design tolerances. Samples cut from finished insulators are given the same thermal tests to which preliminary material samples were subjected to detect any changes produced by the manufacturing process.

2.6.1 Full-Scale Testing and Evaluation

A quantitative verification of the insulation design usually is made during the motor development test phase to determine whether insulator thickness is marginally adequate or

unnecessarily conservative. Such assessment of the design requires a carefully prepared program of physical measurements and hardware examination to determine insulator performance. Usually the chosen material is tested with a full-scale test firing or series of test firings. Data that may result in verification comes from postfire inspection of insulation. The insulator is examined, sectioned, measured, and mapped (see below). The test performance data thus obtained can then be compared with the performance anticipated by the designer, and appropriate changes in the insulator's thickness or geometry can be made.

The selection of instrumentation required to define adequately the rocket-motor-chamber heating environment and insulator exposure time normally is made well in advance of the motor test firing. For testing, the instruments are installed carefully at locations that will best provide verification data (e.g., insulator and case-wall temperature profiles, insulator/case interface temperatures, insulator exposure time, and chamber heat flux) (ref. 77).

Before it is possible to carry out the postfire hardware examination, there must be preliminary planning to provide the prefiring insulation thickness measurements taken at locations that can be identified and remeasured after firing. This practice makes it possible to determine the amount of material charred and eroded and the amount of virgin material remaining. Measurement locations are planned to include areas where the most severe char and erosion are expected to occur; e.g., at the bottom of propellant fins and slots, in regions of high-velocity gas flow, and in areas where exhaust-particle impingement is expected to occur. Commonly, even low char and erosion rates also are measured so that insulator performance can be thoroughly assessed.

Hardware Inspection. – Hardware inspection for insulator design verification usually is conducted in keeping with procedures that preclude the loss of useful data. For example, to prevent destruction of the char by the vibration involved in cutting, the insulator is not sectioned for observation and thickness measurement before erosion-pattern mapping has been completed. To ensure an accurate determination of average ablation rate, remaining virgin material is measured only at locations where prefiring thicknesses are known. **A** general sequence for inspection is as follows: (1) obtain prefire insulator thickness measurements; **(2)** visually inspect case and insulator immediately after the motor firing, noting possible areas of excessive heating on the chamber exterior, regions of high insulator erosion, and insulator delaminations and separations; **(3)** map all erosion patterns; (4) photograph any anomalous regions of erosion for later study; and (5) obtain postfire thickness measurements of the insulation remaining at radial and circumferential positions coincident with the prefire measurement locations.

Regions of excessive ablation indicating high-velocity gas across the insulator surface and areas of particle impingement are discovered by visual observation, as are areas of delamination between insulator plies and ply separations such as those caused by blistering. Gas flow direction and flow channeling also are determined by visual observation.

Anomalous ablative patterns (refs. 100 and 101) are inspected carefully for evidence that shows flow direction or for evidence of manufacturing flaws, case-bond separations, or other possible causes of performance deviation. Areas of unusual erosion patterns or excessive particle impingement are mapped and photographed carefully to determine exact size and location of the area as an aid in the verification analysis (figs. 13 through 15).

Figure 13 is a postfire map of insulation in the forward dome of a Poseidon first-stage motor (motor **C);** a longitudinal cross section of the mapped area is shown in figure 14. Superimposed on the map of motor ***C*** are the locations of thin spots found in postfire inspection of motors A, **B,** and D also. The dotted lines at 330'' represent the location of a grain slot. Propellant burn lines are superimposed on the map to provide time of exposure to the combustion products as the burning propellant recedes. Several areas of burnthrough in the region of the grain slot show that erosion here evidently is higher than that anticipated by the designer. The grooved areas (fig. 15) are examples of localized high erosion due to excessive strain at the adapter tip. Careful inspection of the fired insulator established that the thin spots and the burnthrough were caused by a case-bond separation traceable again to the high strain in the problem area. The difficulty was solved by increasing the insulator thickness over the problem area.

Test motors programmed for postfire measurements of insulation thickness to determine the amount of ablation usually are water quenched at the end of motor operation to eliminate the additional insulator ablation that occurs during motor tailoff and cooldown. If tailoff and cooldown ablation is not prevented by quenching, the measured thickness loss will be in error.

Techniques employed in measuring prefire and postfire insulator thickness vary with the method used to manufacture the insulator and the type of motor case in which the insulator is installed. Laidup-insulator thickness is measured in one or more of the following ways: (1) summing the thicknesses of plies laid into the case; (2) using rigid templates with depths gauged from a referenced position; (3) making tangential X-rays; (4) obtaining eddy-current meter readings (refs. 102 and 103). The last method is effective only on electrically conductive materials (metal cases).

Premolded insulator thicknesses usually are measured by standard direct methods before the insulator is installed in the motor case; but once installed, insulators of this type can also be measured by any of the methods listed above for the laidup insulator except that of ply summation.

Postfire measurements of insulator thickness are made after motor sectioning. The case domes usually are cut first at the line tangent to the cylindrical section. Most often, four longitudinal cylinder sections are cut, and from four to eight dome sections are cut parallel to the longitudinal axis of the motor (fig. 16). Axial sections are measured at 8 to 12 stations along their length to provide a data sample of sufficient size to allow a statistical analysis.

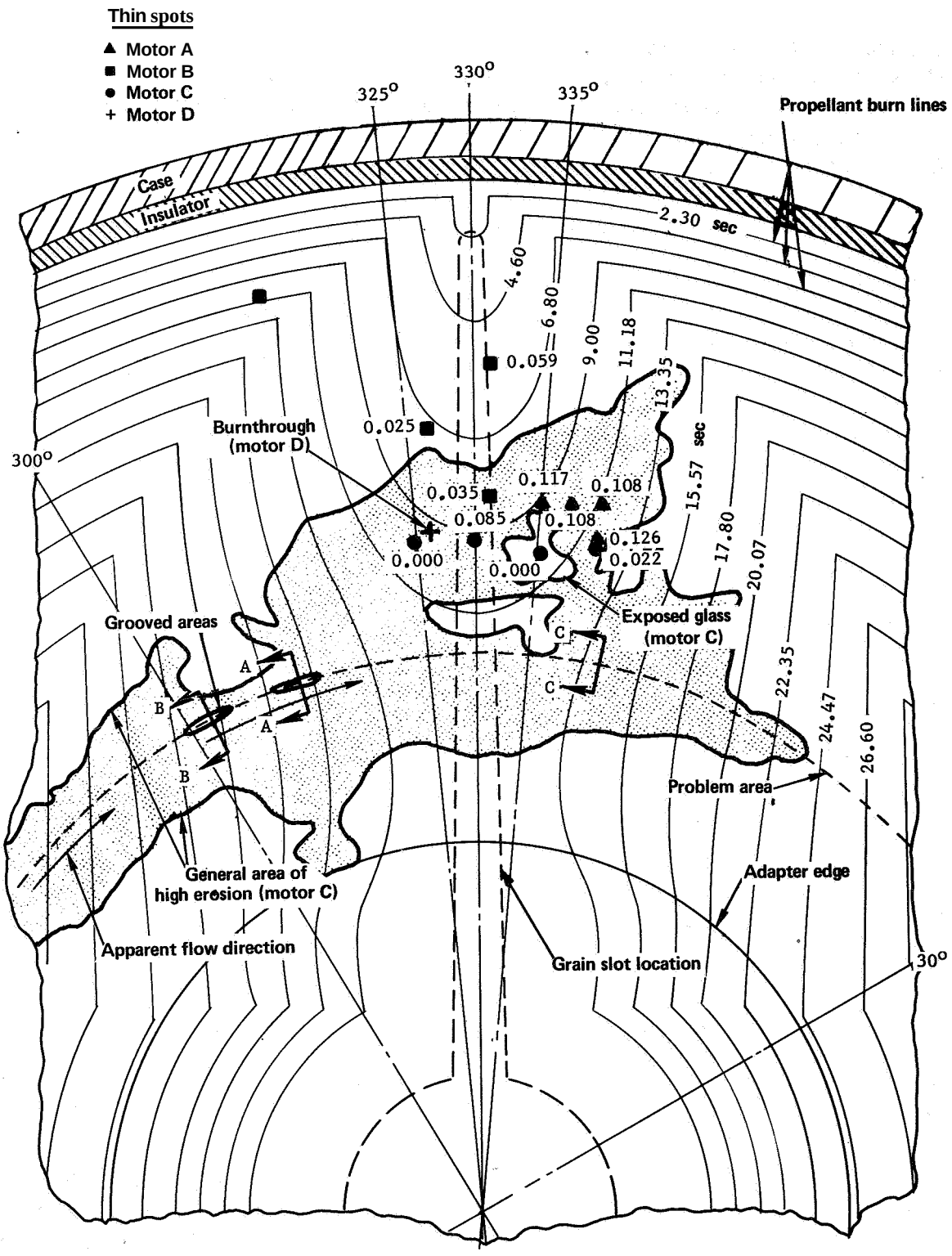

Figure 13. – Illustration of erosion-pattern mapping.

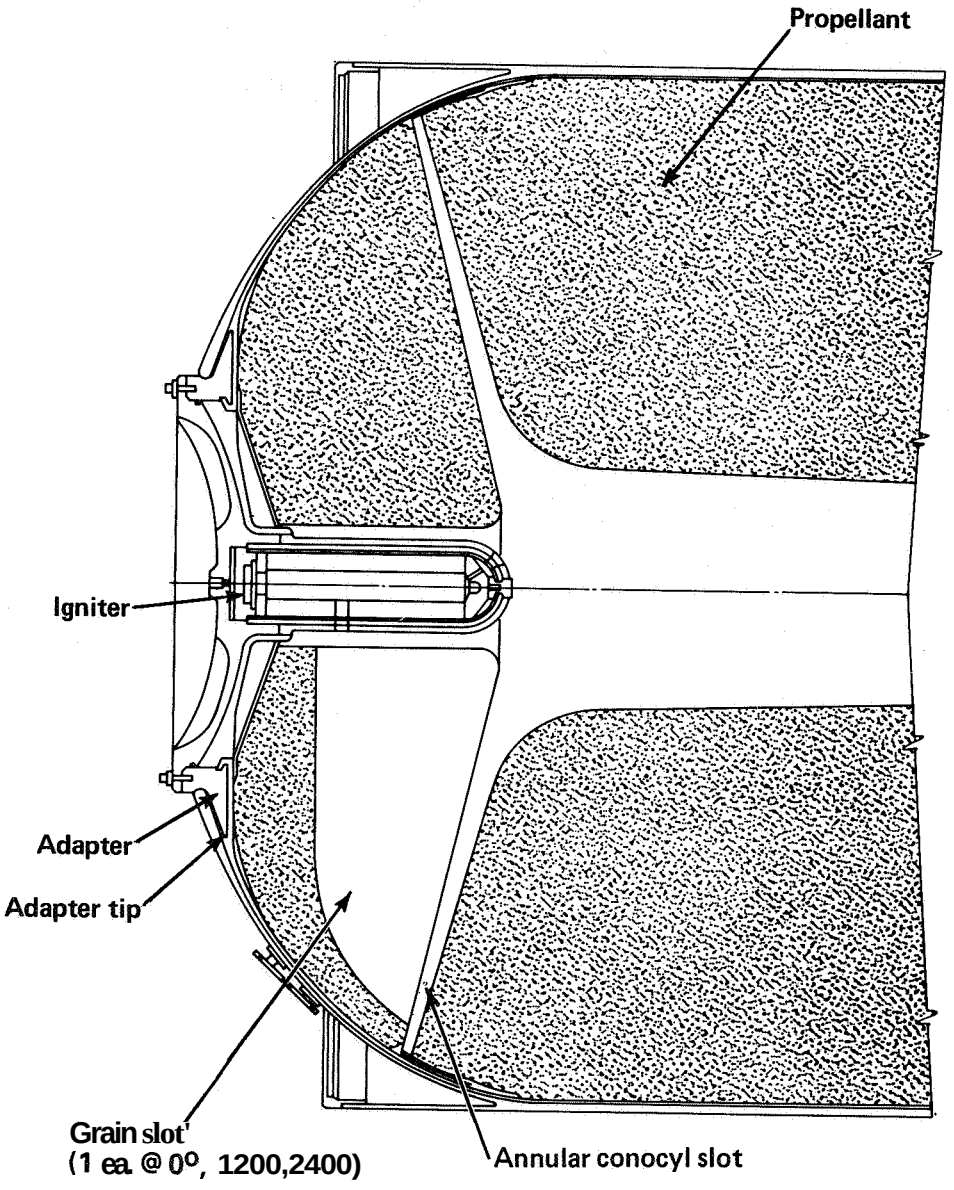

Figure 14. – Longitudinal cross section of motor area mapped in figure 13.

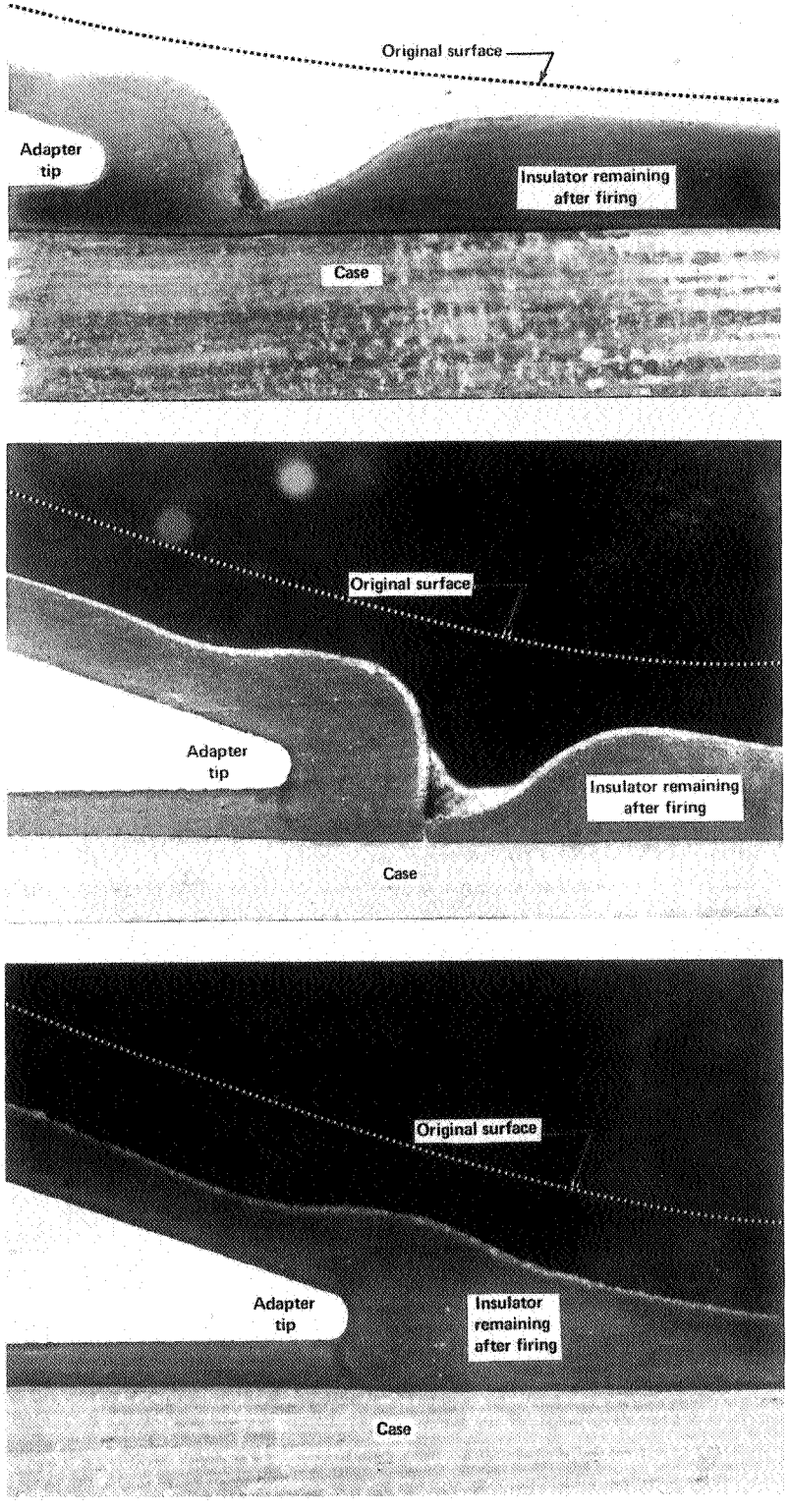

(a) Section AA through insulator groove at adapter tip

(b) Section BB through insulator groove at adapter tip

(c) Section CC through insulator at adapter tip

Figure 15. – Photographs of cross sections of insulator of figure 13 showing increased erosion near adapter tip.

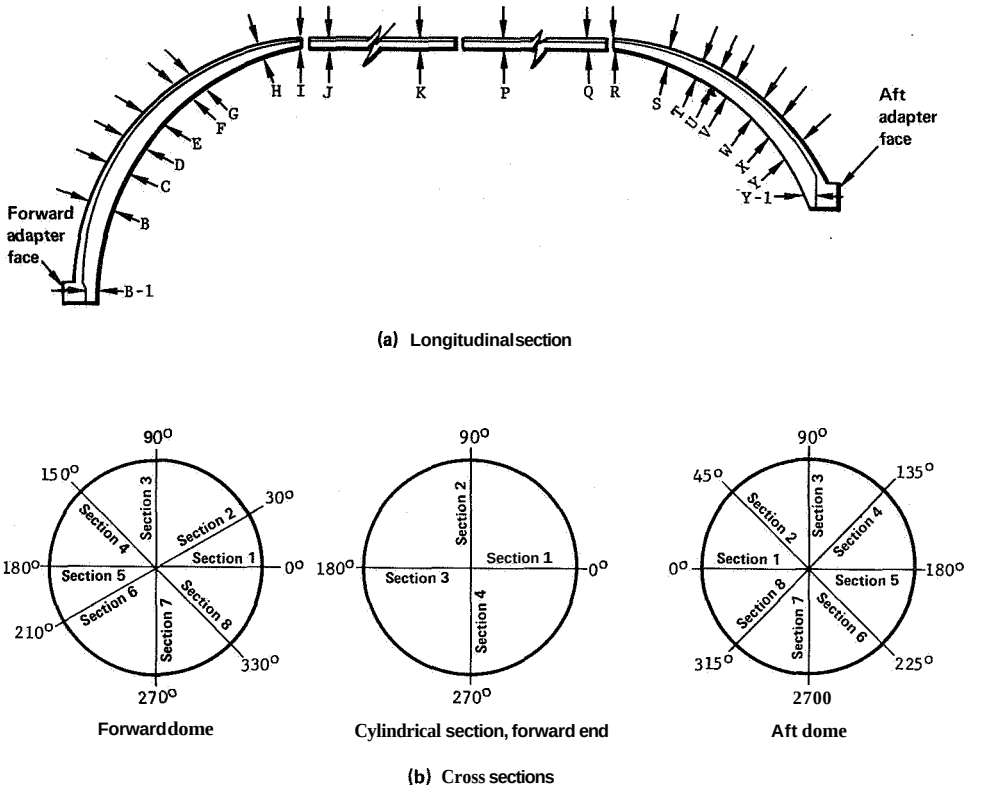

Figure 16. – Typical stations for measurement of insulation thickness.

Only one of the mating edges is measured. From this analysis, an average unused insulation thickness is determined after minor fluctuations in the data on insulation char and erosion have been smoothed out. When motor sectioning is completed, the charred insulator surface usually is cleaned until the decomposition zone or virgin insulation material is exposed. The remaining insulation thickness then is measured on a plane normal to its exposed insulator surface. Circumferential stations are selected at points where the time of exposure to the thermal environment is known. These locations have been previously chosen for prefire measurements of insulator thickness.

If the insulation material is penetrable with a sharp instrument, the amount of insulation remaining after firing sometimes is measured with a calibrated probe. However, this method is not as accurate as the others.

Microscopic examination and photomicrographs of polished insulator and char cross sections clearly show (1) transition zones, **(2)** filler orientation, and (3) variations in char (ref. 104). All three are useful in evaluating insulation performance.

Instrumentation. – The standard instrumentation used to measure chamber thermal environment includes both thermocouples and calorimeters. Thermocouples that measure temperature change at the insulator/case interface or on the external surface of the case generally are used to verify that the case temperature has not exceeded allowable levels. It should be noted that the thermal gradient through a metal case usually is negligible, but the gradient through a glass case is not.

Complete temperature-time histories during a static test firing have been measured directly by thermocouples installed at the insulator/case interface (ref. 105). These thermocouples are installed by drilling a hole through the metal or glass case to the insulator surface and inserting the thermocouple to the insulator/case bondline surface. To minimize the effect of the thermocouple installation on the temperature field, the hole is filled with a potting material that has approximately the same thermal diffusivity as the case. Temperature-time histories of the propellant combustion products in the cavity between a stress-relief flap and an insulator surface within the motor chamber also are measured with thermocouples inserted into holes in the case (ref. 105).

Calorimeter indicators are embedded in the insulator wall to record time at which the ablating surface level arrives at a predetermined depth and to record the heating rate at the time of arrival. Calorimeters are also used to measure total heat flux to the case wall. Water or gas cooling is provided for the calorimeter over the total period of a motor firing to prevent destruction of the gage.

Thermocouples and calorimeters have been adapted to more specialized uses in determining the internal heating environment of a rocket motor chamber, as discussed in reference 106. This reference describes six basic thermal gages designed specifically to measure and define the thermal environment: (1) slug-type calorimeters; ***(2)*** circular-foil heat-flux gages to determine the radiant, convective, and total heat flux to the ablative wall; (3) surface thermocouples to measure temperature change at the ablative wall; (4) in-wall thermouples, staggered at various depths through the wall; *(5)* char detectors to determine-the time required for char formation by measuring the change in electrical conductivity that occurs on pyrolysis; and (6) erosion gages to measure the rate at which the surface is removed from the ablative material once it has been exposed to the thermal environment. Before these devices are used, the motor design is reviewed to permit selection and placement of thermal gages in areas where they will most accurately define the thermal environment by indicating elevated temperature, high heat flux, unusual flow patterns, or high ablation rates.

Evaluation of insulation performance requires a knowledge of insulator exposure time. Calculation of the location of the burning surface with time is obtainable from a

three-dimensional internal ballistic program. Location of the moving propellant flame front during a firing is extremely difficult to determine. Such methods as quenching combustion at various burn times, monitoring embedded breakwires, and cineradiography (X-ray movies) have been used to locate the burning front but with only very limited success. The most successful method of determining the location of the flame front has been achieved with the use of microwaves (refs. 107 and 108).

Data Evaluation. – The data from thermal instrumentation and hardware inspection, when compiled, correlated, and evaluated, provide a means for quantitative assessment of the insulation performance. Measured char depth, char rate, erosion depth, erosion rate, and case/insulator interface temperature range can be compared with design parameters for design verification.

The depth to which the insulator is charred and the rate at which charring occurs (ablation rate) are two of the most widely used parameters for evaluating insulator performance. Char depth and total surface regression are determined either by direct measurement with thermal instruments during the motor firing or by taking the difference between prefire and postfire insulator thicknesses. **A** char rate then is calculated from the loss of thickness and the length of time the insulator surface was exposed to the thermal environment, or the char rate is measured directly by an erosion gage. Insualtor exposure time used to calculate char or erosion rate is either measured directly by microwave methods or theoretically determined from propellant burn rate and grain geometry. The measured and calculated average char and erosion rates are compared with analytically predicted rates to verify insulator design. When valid test data and anlaytical predictions disagree, the test data are used for redesign.

Insulator thermal safety factors are calculated by dividing initial thickness by char depth for the different motor locations. The char depth is analyzed by the method of statistical inference, and a three-sigma safety factor is established for the char depth. Future performance is inferred from this type of statistical analysis, and the design is evaluated for potential burnthroughs and adequacy of safety factor. Insulator regions of excessive thickness also have been identified by this method so that inert weight can be reduced.

Design verification provides assurance that the insulator/case interface temperature requirements are met. Interface temperatures are determined by applying time-temperature histories recorded on the external surface of the chamber during a static test firing to a computer program for one-dimensional heat-transfer analysis. An insulator/case interface temperature is assumed and incorporated into the program as the inner boundary condition to the equation for heat conduction across the thickness of the case wall. The solution to the equation is equivalent to the temperature history of the external surface of the case. The solution based on the assumed interface temperature history is compared with the measured external surface temperature history, and adjustments are made in the assumed values until the calculated values for the external surface of the case agree with the measured values.

This procedure is especially suited to computer graphics techniques because the input adjustments are easily made.

The temperature at the interface of the stress-relief flap and the propellant cannot be measured directly because a thermocouple would not survive long enough to record useful data. This temperature has, however, been determined accurately by measuring the temperature-time history of the propellant combustion products in the flap cavity (ref. 105). The measured cavity temperature has then been used as a time-dependent boundary condition in a heat-transfer analysis to obtain temperature profiles across the thickness of the stress-relief flap.

3. DESIGN CRITERIA and Recommended Practices

3.1 GENERAL CONSIDERATIONS

3.1.1 Design Approach

The insulator design shall be based on conservative use of reliable data.

Use data obtained at conditions as close as possible to the anticipated operational conditions. Further, the data selected from the experimental scatter for use in char-and-erosion-rate correlations should be data that produce conservative design (i.e., the higher range of regression rates, the higher range of temperatures and pressures, the lower range of tensile strength and elongation). To ensure that conservative, reliable data are used, it is recommended that a statistical analysis of the data scatter be made. At the very least, use the conservative three-sigma values as raw material for the char-and-erosion-rate correlations (sec. 2.4.1.1.2). For a more rigorous approach, use the method of Lawrence and Vogel (ref. 109) or the more direct method of Haugen (ref. 110).

3.1.2 Motor Application

3.1.2.1 BOOSTER MOTORS

Selection of insulation for booster motors shall emphasize lowest total insulator cost.

The insulator material for a booster motor should be selected after a cost effectiveness study has been completed. The material candidates should be judged by installed cost more strongly than by thermal insulation effectiveness. All costs should be averaged over the entire program in order to amortize tooling and to take advantage of the improvement curve. When development of new materials is necessary, this cost should be included. Cost data for material selection, manufacturing processes, and installation also should be included in the insulator cost study.

Matched-metal-die compression molding is size limited by the molding capacity of the insulator manufacturer's facilities and has high initial tool cost. However, compression molding is recommended for large-volume production whenever this method can be used.

Fabrication costs are highest for hand-layup parts; however, temporary, readily fabricated, low-cost tools may be used. Product dimensional tolerance for hand layup is ± 0.050 in. minimum, but lower tolerances may be obtained by post-vulcanization machining. Hand layup is recommended for any low-volume production or for production of insulators whose design is expected to change frequently.

Mastic insulators, manufactured by rotating chamber-sweep template (ref. 9), pump extrusion (ref. 96), or spray application are recommended for motors so large that they are beyond the fabrication limits for molded insulators.

3.1.2.2 UPPER-STAGE MOTORS

Insulation for upper-stage motors shall have minimum inert weight and minimum regression rate.

It is recommended that the screening process for upperstage insulation materials segregate materials with minimum regression rate and inert weight by using as an index the product of the density and regression rate. Materials with low values for this product should be regarded as acceptable candidates for further evaluation. Care should be taken that regression rate is measured under conditions that simulate as nearly as possible the motor internal environment. Further, regression rates of materials to be compared should be measured under similar conditions. Density (or specific gravity) should be measured by a standard accepted method.

The designer should not apply the regression rate-density product index blindly, however. This method is useful only as a screening method. Before materials are chosen for the motor, heat-transfer rate, propellant compatibility, volume of insulator required, and processability should be evaluated.

3.1.2.3 THRUST-CONTROL MOTORS

3.1.2.3.1 Insulator Weight

The ablation and thermal properties of insulation for multipulse thrust control motors shall result in minimum insulation weight.

Minimum insulation weight is achieved in the multipulse thrust control motor by selecting an insulator that possesses the minimum ablation-rate characteristics (average ablation rate and its variation). These characteristics in general are obtained in a lowdensity polymeric binder with a high concentration of both carbon and hydrogen and a low concentration of oxygen (ref. 2, p. 124). The insulator should exhibit a high heat of combustion and a

tendency to form a lowdensity char. Ablative reproducibility depends on whether the char layer remains intact from pulse to pulse (as it does with reinforced plastics), is removed after every pulse (as occurs with lightly loaded elastomers), or behaves erratically, sometimes remaining intact and sometimes blowing away. Better reproducibility is found in materials that always behave the same way, either remaining intact or blowing away. Lowest regression rates usually are found in materials that retain the char layer. It is important to identify the char-layer behavior to develop a realistic thermal model, and this behavior must be demonstrated in a pulse-motor test program. **A** range of pulses from the longest to the shortest anticipated should be tested to verify that the char performance is reproducible at any specified point in the motor.

3.1.2.3.2 Insulator Postfire Characteristics

The insulation shall produce neither postfire propellant reignition nor detrimental postfire mass loss.

It is recommended that char samples be generated from motor tests of the same firing duration as the maximum pulse from the motor firing cycle. Insulators should be tested for both binder decomposition temperature and the heat capacity of the char. Thermogravimetric testing should be conducted to obtain decomposition temperature, mass loss as a function of temperature, and char specific heat.

3.1.2.4 SPACE-OPERATIONAL MOTORS

The insulation for space-operational motors shall withstand simulated sterilization cycle, space storage environment, and the multipulse operation mode without unacceptable degradation.

Insulation degradation during the space sterilization cycle, during inflight storage, and during multipulse motor operation should be assessed on a quantitative basis. The properties affected are thermal conductivity, specific heat, adhesive strength, and possibly the ablation rate.

To ascertain a degradation factor for thermal cycling, conduct standard laboratory tests at elevated temperatures. The test procedure should determine both the degree to which the insulation is degraded and to what depth in the insulator the degradation prevailes. These data for each candidate insulation material are essential both to establish a method of ranking materials and to furnish input for computer simulation of the multipulse environment.

In addition, the effect of the deep-space storage environment on thermal properties should be determined. The sterilization cycle and the space eiivironment should be determined for

a specified mission. Once these exposures have been established, the possible detrimental effects can be assessed. Both temperature extremes and vacuum storage during the mission should be simulated, or a performance projection may be made from accelerated tests. If constant-temperature soak tests are used for this purpose, the temperatures should be kept below the insulator's decomposition temperature but above the cure temperature. When possible, the criteria for stability should be established by accurate measurement of mechanical or thermal properties rather than by visual observations.

3.2 SELECTION OF MATERIALS

3.2.1 Insulators

The materials for motor internal insulation shall be proven materials for which complete and reliable data are available, unless special design considerations require other materials.

The designer should use the successful experience in previous programs whenever possible. Development programs are costly and should not be undertaken unless advancement in the state of the art is genuinely necessary. Of course, most materials that have never been used successfully must be subjected to a development program before they can demonstrate the reliability level desirable in rocket motors.

Recommended insulation materials that have been used successfully are as follows:

- Large booster ($\geqslant$ 100 in. diam.) – Silica/NBR, silica-asbestos/NBR
- Booster – Silica/NBR, silica-asbestos/NBR, asbestos/SBR
- Upper stage – Boric acid/NBR, asbestos/SBR, silica/NBR
- Thrust control – asbestos/EPDM

3.2.1.1 THERMAL PROPERTIES

Insulation thermal properties and their variability in the rocket chamber environment shall be known before the insulator is designed.

The recommended source of ablation data is full-scale motor firings, but full-scale firings are costly and time-consuming. When such expense cannot be justified or data on previous motors are not available, two methods are recommended, in order of preference: (1)

subscale motor firings that expose the insulation to the identical propellant combustion products, chamber pressure, and gas velocities to be found in the design environment; (2) plasma-arc tests of insulator candidate samples that duplicate, as nearly as possible, expected heat flux (ref. 2). Oxyacetylene-torch tests (ref. 22) of samples should be used only for preliminary screening of insulation material candidates. Correlations have been made to relate ablation rate from oxyacetylene-torch data (ref. 111) and plasma-arc data (ref. 2) to motor firing data. The designer, however, should be cautious about using plasma-arc or torch data correlations, because these tests often have produced erroneous or misleading data.

3.2.1.2 MECHANICAL PROPERTIES

Case, propellant, and insulation materials shall possess demonstrated properties acceptable for insulation structural analysis.

Case and propellant properties are needed for the structural-response model. Use of the properties in stress analysis is discussed in reference 17. Test methods for evaluating properties and securing data should be those described in the ASTM Standards (indexed in ref. 15) or those in the ICRPG manual (ref. 16).

The poker-chip test (ref. 16, sec. 4.5.5) partially simulates insulator thermal stresses that result from propellant postcure motor cooling, and is recommended for gathering structural data only in those regions that are well removed from features that cause stress concentrations. The high diameter-to-thickness ratio of the poker-chip test sample is a recommended configuration for studying the strength changes in case-bond materials caused by propellant component migration. Moreover, tensile and shear joint-evaluation tests should be employed to establish allowable design stress levels.

Peel tests should be used to compare adhesive systems for cleavage loads at grain release points. The use of peel-test results in structural analysis is not recommended, because the large deformations imposed by the test are not representative of firing conditions. However, the test is recommended for comparison of adhesives.

3.2.1.3 COMPATIBILITY OF MATERIALS

The insulation system shall not degrade because of (1) chemical incompatibility with other motor components or (2) contact with the atmosphere.

Most plastics and propellants are compounded with plasticizers. When such plasticizers are present in the motor, barrier coats should be used to limit migrations. Although epoxy, polyether polyurethanes, and chlorobutyl rubbers have been used successfully, a layer of

polyvinyl formal sprayed over a sprayed layer of neoprene is recommended. The formvar-neoprene is a more effective barrier coat than any of the others.

Oils and waxes frequently are used as protective ingredients in elastomers, but their use is not advisable when bonding of the elastomer is required, and most elastomers used in internal insulation must be bondable. Elastomers with inherent resistance to the effects of ozone and sunlight should be used in shrinkage liners or other internal insulation parts that will be exposed to the atmosphere. Ethylene-propylene, silicone, and butyl rubbers are recommended for resistance to ozone and sunlight.

When elastomers with inherent resistance to the effects of ozone and sunlight cannot be used, employ other protective measures. To prevent aging, use opaque covers that prevent air flow over the rubber surface. Consider protective coatings such as Hypalon paint. Store the insulator in wooden boxes with several pounds of cotton inside to provide a sacrificial, ozone-preventative packing. Whenever possible, store the material in a dark, ozone-free room. Moreover, to prevent accelerated aging caused by localized strains, use storage forms that eliminate the possibility of folding or stretching the insulation.

3.2.1.4 SCREENING OF MATERIALS

The method for screening candidate materials shall be suited to the purpose of the screening.

It is recommended that oxyacetylene-torch tests (ref. 22) and plasma-arc tests be used for preliminary screening or evaluating relative performance of insulators, not for final screening and selection. Subscale testing should be used for careful screening and approximate scaleup to full scale. Scaleup should not be attempted if the subscale motor is less than 9 in. in diameter. Some success has been obtained in scaleup of data from subscale motors over 9 in. in diameter, but full-scale data are much more reliable.

3.2.2 Adhesives, Liners, and Sealants

3.2.2.1 ADHESIVES

An adhesive shall provide a proven adequate margin in case-to-insulation and insulation-to-insulation bonds.

For the two general conditions – motor storage and motor ignition – determine insulation-to-insulation and case-to-insulation adhesion requirements from viscoelastic stress analysis (sec. 3.4.2.2) of the case, insulation, and propellant composite. The adhesive system

should be judged by performance in both shear and tension. For adhesivesystem screening, it is recommended that poker-chip specimens be fabricated from candidate adhesives. Then the strongest system should be selected for complete characterization. The adhesive-system strength should always be greater than the propellant cohesive strength so that propellant cohesive failures always occur first. The recommended minimum ratio of adhesive strength to propellant cohesive strength is 1.25. Aging characteristics of the adhesive must be allowed for.

To demonstrate the adhesive-system capability, use the tests discussed in section 2.2.1.2 for determination of properties for structural analysis.

3.2.2.2 LINERS

3.2.2.2.1 Bonding Method

Wherever possible, the propellant shall be capable of *being bonded directly to the insulation.*

The recommended practice for meeting liner requirements is to select, whenever possible, insulation materials and propellants that require no liner. For double-base propellants, utilize the powder-embedment case-bond method, which requires no liner. Composite propellants usually require a liner, and it is recommended that these liners be based on the same polymer as the propellants (e.g., propellants using PBAN as a binder should be bonded with a PBAN-based liner).

3.2.2.2.2 Bond Strength

The propellant-to-insulation bond shall be adequate for loads induced in storage, at ignition, and in flight at the maximum and minimum expected bondline temperatures.

Although most bond test methods are useful for screening liner formulations, the final liner selection must be based on results obtained from specimens designed and tested under conditions that may be interpreted in terms of the propellant-grain/liner stress analysis. The grain/liner stress analysis is discussed in reference 17. An assessment of the adequacy of the bond strength under motor storage conditions is particularly important and requires constant-load tensile and shear tests (ref. 16).

Bond strength margins for the motor ignition transient, flight, and test firing are determined by testing in tensile or shear modes at high strain rates under superimposed hydrostatic pressure that simulates motor operation. The allowable strain rates must include both the

rate of motor pressurization during ignition and the pressurization rate up to full operating pressure. The bond-test specimen configurations recommended for all constant-rate and constant-load shear and tensile tests are described in reference 16 (sec. 4.7).

3.2.2.2.3 Bond Deterioration

The propellant-to-insulation bond shall not be subject to excessive migration of chemical species or to deterioration of any other sort during storage.

A laboratory definition of the migration potential of chemical species in the rocket motor requires a specimen design that accurately simulates the chemical environment in the motor. The test specimen must contain all of the components of the motor and must be large enough to simulate the motor accurately. The size of the specimen is important because size affects the diffusion rate and concentration of gaseous propellant-degradation products. A diffusion path length of approximately 9 in. is necessary for simulation of a thick-web motor; small specimens such as those used for stress testing are not adequate for storage testing. Bonding-system stability can be assessed quantitatively with test specimens.

The recommended storage-test specimen for simulating thick-web motors is prepared by bonding insulation of the appropriate thickness to the bottom of a 9-in. cubical carton lined with heavy aluminum foil. The foil eliminates the short-length diffusion path. The specimen is coated with liner, cast with propellant, cured, and then stored at elevated temperature. After designated storage time, specimens are cut from the bonding interface, and the appropriate tensile and shear samples are prepared. These samples should be stored under either motor storage or accelerated aging conditions prior to test.

3.2.2.2.4 Processing Compatibility

Liner processing shall be compatible with propellant and motor processing.

Final confirmation of bonding system adequacy should be obtained by using the poker-chip specimen and by simulating as closely as possible the processing cycle of the full-scale motor. Such a process simulation should include (1) insulation preparation and drying, (2) casting or curing, (3) application of liner, and (4) accelerated aging that includes both appropriate exposure times and appropriate environments that are comparable to the proposed full-scale process.

3.2.2.3 SEALANTS

Sealing materials at insulation junctions shall possess ablative properties similar to those of the adjoining insulation materials.

Sealing materials should be evaluated by testing an appropriate configuration in the design environment (sec. 3.2.1.4). Test configurations should include a realistic configuration of insulation and sealant in an appropriately oriented flow field. The objectives of such testing are to preclude inordinately high ablation rates for the sealant. Seals and joint adhesives selected should have ablation rates that are similar to those of the adjacent insulators. This practice minimizes the probability of formation of a sharp gap or discontiauity that could cause vortex formation and attendant high ablation rates. Particular attention must be paid to the ablation characteristics of aged sealers. The uncatalyzed type of sealant is not recommended except for applications that have very short service-life requirements. Neither polyurethane nor chromate sealants are recommended for use where migration of ester-type plasticizers will occur. Chromate sealants should be used when subsequent disassembly may be required.

3.3 EVALUATION OF THERMAL ENVIRONMENT

3.3.I Cornbustion-Products Analysis

3.3.1.1 TEMPERATURE AND COMPOSITION

The combustion-products analysis shall provide accurate information on the chamber-gas/particle temperature, composition, and properties at the average pressure of *the combustion chamber.*

Equilibrium composition and temperature should be calculated for use in calculating both transport properties and surface heat transfer (fig. 3), preferably by minimizing the Gibbs free energy by the method of steepest descent (ref. 34). The computer programs for this work are called Equilibrium Thermochemistry Programs or, more commonly, Free-Energy Programs. Experimental data concerning the propellant ingredients (ref. 2) and the combustion products (refs. 32 and 33) provide the starting point for calculation. The data reservoir is vast, and the number of combustion products examined must be economically feasible and consistent with the capability of facilities available. Reduce the list of combustion products to a workable number (1) by using only those compounds whose atomic structure is a possible consequence of the propellant used, and (2) by applying experience, history, or cut-and-try methods to eliminate products whose equilibrium concentration is infinitesimal.

When the chamber pressure varies considerably during motor operation, the gas/particle composition and chamber temperature should be determined for representative pressure levels.

A summation of the weighted contribution of each species should be made to determine gas properties, including molecular weight, density, specific heat, and ratio of specific heats for the gas mixture. These calculated properties should then be used with calculated chamber temperatures for subsequent calculations of gas flow and heat transfer.

If either cost or lack of capability blocks the analysis of combustion products, the designer must interpolate or guess directly from past firing data. Such estimates should be as conservative as possible.

3.3.1.2 TRANSPORT PROPERTIES

The analysis and evaluation of chamber gas transport properties shall provide reliable and accurate values for use in calculations of *the flow field and heat transfer.*

The equilibrium composition of the chamber gases should be used with the Wilke approximation (ref. 41) to the Chapman-Enskog kinetic theory of gases to determine viscosity and thermal conductivity of the equilibrium mixture.

These properties should be determined for each chemical species by using collision integrals for the Lennard-Jones potential (ref. 37) and tabulated force parameters (ref. 38). The transport properties should then be used in the calculation of local convective-heat-transfer coefficients.

When transport properties cannot be determined, the designer must interpolate or guess directly from postfiring data. Such estimates should be as conservative as possible.

3.3.1.3 FLOW FIELD

The flow-field analysis shall provide accurate values for the velocity, Mach number, temperature, pressure, and flow angle of *the exhaust gas throughout the motor chamber.*

A two-dimensional axisymmetric or planar compressible-flow analysis using general flow equations should be made to determine the velocity, Mach number, temperature, pressure, and flow angle of the exhaust gas. **A** three-dimensional incompressible-flow analysis should be made of areas of complex geometry that cannot be defined in two dimensions.

If special problems such as complex combustion-chamber geometry or intricate flow patterns warrant the additional effort and cost, cold-flow tests should be made to determine flow properties.

The calculated flow properties should then be used for subsequent particle flow and slag accumulation analyses and for heat-transfer calculations.

When the flow field cannot be calculated, the designer must interpolate or guess directly on the basis of past experience.

3.3.2 Heat-Transfer Analysis

The description and quantitative definition of chamber heat-transfer mechanisms shall be adequate to determine the required protective insulation for the case structure.

The thermal environment within the motor chamber is defined in terms of convective, radiative, and particle impingement and deposition heat-transfer rates to the insulator surface. These rates should be determined by methods outlined in the following subsections. When surface heat transfer cannot be calculated as described, use a conservative empirical approach based on past experience.

3.3.2.1 CONVECTION

The heat-transfer analysis shall provide reliable values for convective heat transfer to all insulator surfaces that are exposed to the chamber environment.

The convective-heat-transfer coefficients should be determined by applying calculation methods outlined in section 2.2.4.1, the exact procedure depeiidiiig on motor configuration, material selection, and degree of sophistication required. The heat-transfer calculations should employ exhaust-gas transport properties and gas flow velocities determined by methods described in sections 3.3.1.2 and 3.3.1.3.

When separated flow or vortex flow occurs, as across a step, cavity, or surface discontinuity, the heat-transfer coefficient should be iiicreased to account for the increase in local velocity, as discussed in references 51, 52, and 53.

Where separated or vortex flow occurs in motor geometries involving submerged nozzle throats or multinozzle configurations, determine heat-transfer coefficients from scaling techniques based on velocity measurements from cold-flow models of the same geometry (refs. 54 and 55).

3.3.2.2 RADIATION

The heat-transfer analysis shall accurately define the thermal environment due to radiant heating within the combustion chamber.

The radiant-heating flux is found from equation (6). The gas-cloud emissivity should be determined, by procedures presented in reference 59, on the basis of gas-cloud temperature, pressure, radiant-beam path length, molecular weight of the gas, and the weight ratio of particles to gas. These controlling terms should first be determined by the methods presented in section 3.3.1. **A** range of values for radiant-heating flux for use in design and evaluation should be evolved on the basis of arbitrary values of wall temperature.

3.3.2.3 PARTICLE IMPINGEMENT AND SLAG DEPOSITION

The heat-transfer analysis shall define the particle trajectories in the motor chamber and assess the effect of impingement and slag deposition on the insulator.

If no reliable data exist, window/bomb tests (ref. 66) should be made of the propellant to determine the size distribution of the metal agglomerates. Oxide particle sizes should be determined by the methods of reference 64.

The particle trajectories should be calculated using Newton's second law of motion and Stoke's law of drag. For particles impinging on wall surfaces, determine mass, velocity, and direction of impact. Both axial and radial accelerations representative of anticipated flight conditions should be included, so that their effect upon particle trajectories can be evaluated.

Calculate the amount of slag depositing on wall surfaces by taking the sum of the individual particles impinging (ref. 65). Contributions of spin-stabilization and axial acceleration to both impingement and slag flow after impingement should be evaluated.

Calculate the energy (kinetic, thermal, chemical) available for release from the slag to the wall (refs. 68 through 71).

The calculated impingement and deposition should be used for subsequent determinations of insulator thickness. The impingement and slag deposition contribution to surface regression should be calculated by treating these phenomena as an added heat source. The added heat input of slag and particles should be included with the convective-heat-transfer contribution in calculations of required insulator thickness.

3.4 INSULATOR DESIGN

3.4.1 Thermal Design

3.4.1.1 INSULATOR THICKNESS

The insulator thickness shall be adequate to (1) protect the chamber from unacceptable heat damage throughout the motor firing and (2) limit as necessary heat radiated to associated vehicle components.

It is recommended that the insulator thickness be determined at a number of axial stations in the motor and also at a number of circumferential locations. The number of points at which the insulation thickness is calculated is arbitrary. However, when insulation thickness requirements change rapidly, thicknesses at many points should be calculated; conversely when the change is gradual, fewer need be calculated. An insulation contour should be obtained by fairing between points and smoothing out (by adding insulation) any discontinuities or depressions in the insulator internal surface.

The insulator design thickness must provide not only for the material lost by erosion, but also for a layer of material to prevent heat penetration beyond the eroded insulation surface so that the case will not overheat. The basis for establishing the amount of insulation required for this heat barrier is the specified case-wall temperature limit. Calculate the necessary thickness from a statistical-variation analysis of the insulator performance data, choosing the statistical risk involved by selecting the degree of data scatter that is to be included in the calculations.

After the insulation required for erosion and heat penetration has been determined, apply a thermal margin of safety. For well-characterized insulation materials and for motor internal flow velocities that are not unusually high or asymmetric, a thermal margin of safety of 25 to 50% is recommended, whereas for less-well-known materials and flow conditions, a thermal safety margin of 100% or more is recommended. Small motors ($<$30 in. diam.) requiring maximum utilization of volume with well-characterized materials should be given a 10% to 20% margin; those that are not well characterized should be given a 50% margin of safety.

The insulator thickness required is calculated by one of the methods set forth below.

3.4.1.1.1 Q* Analysis

Insulation thickness shall be based on the Q method when the selected insulation material does not form high-temperature chars.*

Typical materials that do not form high-temperature chars are SBR and NBR. Calculate the ablation rate for these and similar materials from the following equation, obtained by rearranging equation (7):

$$\dot{x}_a = \frac{\dot{q}_{tot}}{Q^* \rho} \tag{11}$$

The value for Q* must either be available from previous data or obtained experimentally. The thickness ablated is the product of the ablation rate and exposure time. Thus

$$x_a = \dot{x}_a t \tag{12}$$

where

x_a = thickness ablated, expressed in in. when $\dot{x}_a$ is in in./sec
t = time of exposure, sec

When $\dot{q}_{tot}$ varies significantly, the exposure time should be broken up into increments and an average $\dot{q}_{tot}$ used for each increment.

The additional insulation thickness necessary to prevent overheating of a case wall during motor operation should be determined by unsteady-state heat-transfer analysis. For the simple situation where char zones are very thin (as with silica-filled NBR and SBR insulators) and erosion rates are known, the backside temperature rise should be determined as shown in references 79 and 80. For the more complex situation where char zones are thick and an appreciable gradient through the char exists, the backside temperature rise should be determined by the finitedifference ablation analysis (sec. 2.4.1.1.3); however, the temperature may be approximated by the methods of references 79 and 80.when the highly theoretical ablation analysis cannot be employed.

3.4.1.1.2 Char and Erosion Rate Correlations

The insulation thickness shall be based on empirical char-and-erosion-rate correlations when the insulation forms high-temperature chars and when the thickness must be known accurately.

Thickness calculations based on this method should be made only in the range of operating variables in which data are sufficient to qualify the correlation. Extrapolations should not be attempted. When operating conditions, motor size, or propellant composition differ from the foundation of the correlation, additional data should be acquired. Only the data that fall

within the required confidence limits should be used to build a correlation. For the exposure time t of the insulator at a particular location, the average char rate is established from the following relation:

$$(\dot{x}_{ch})_{avg} = \frac{\int_o^{\cdot} \dot{x}_{ch}\, dt}{t} \qquad (13)$$

where $\dot{x}_{ch}$ is obtained as described in section 2.4.1.1.2.

The product of average char rate and time (i.e., the thickness charred and eroded) should then be enlarged by the desired thermal margin of safety and added to the thickness required to prevent structural damage (this thickness should be determined as described in the last paragraph of section 3.4.1.1 .1). The result is insulator thickness requirement for one location. This value should be calculated for various locations on the insulator surface and is especially important at known locations of high heat flux. As char and erosion data are obtained from full-scale motor firing, the insulator design thickness can be adjusted.

3.4.1.1.3 Ablation Analysis

The insulator thickness shall not be based primarily on ablation analysis.

The finite-difference ablation analysis is recommended primarily for use in providing confidence in the analyses previously made by Q* or by char- and erosion-rate correlations. Although some utility for this method may safely be found in detailed analysis of heating and erosion and for the extrapolation of test data, this method is highly theoretical and should be used in insulator design only when the method has been correlated with test data on a motor similar to that being designed.

3.4.1.2 STRESS-RELIEF-FLAP THICKNESS

The thickness of the stress-relief flap shall be sufficient to protect the propellant from heating to the autoignition temperature.

It is recommended that flap thickness be determined by the method outlined in reference 85. When insufficient information is available, use the perfect-gas-law method with assumed heat-transfer coefficients as discussed in section 2.4.1.2. After thickness requirements have been calculated, ultraconservative thermal margins of safety should be applied to the calculated thickness.

3.4.2 Structural Design

3.4.2.1 LOADS

The loads analysis shall evaluate the loads on the insulator from environmental, processing, and operational sources.

The insulator material should be subjected to simulated or actual environmental and processing loads in order to determine what changes occur. Where physical and thermal property changes are created by these loads, the designer should adjust, if necessary, the properties used in design calculations. Where operational loads are found to produce failure in the insulator, adjustments in thickness should be made to compensate. Occasionally, insulation material changes or extensive insulation design changes may be required, but usually only slight adjustment in thickness is sufficient. However, creep, relaxation, and slump can occur in some materials, and the need for evaluation of the potential problem exists.

3.4.2.2 STRESSES

Analysis by accepted techniques shall predict insulation stress and strain values during manufacturing and motor operation.

Preliminary stress analysis, in the form of one-dimensional analysis (ref. 86), should be performed on all insulator designs. For thermal and acceleration loads or for long motors ($L/D > 2$), the one-dimensional analysis will provide accurate, complete information. For shorter motors and for detailed analysis of stress concentrations such as bond terminations where strains exceed 2%, refined analytical techniques (ref. 89) should be used. The one-dimensional analysis often is essential in interpretation of refined analysis results and should be performed first. The analysis should be applied to loads induced by the manufacturing process as well as to operational loads.

3.4.2.3 STRENGTH ANALYSIS

The strength analysis shall verify the capability of the insulation to withstand the stress and strain values predicted by the stress analysis.

All mechanical and thermal properties used in calculations related to design should be representative of the insulator material after it has been exposed to the temperatures, stresses and strains, humidity, and aging that are associated with the motor manufacture. Cure cycles employed in fabrication of the case and the propellant grain should be

simulated. Stress and strain history of the insulator should be duplicated. When it is impossible to obtain data that were procured under these simulated conditions, a larger structural factor of safety should be used to lessen the risk.

3.4.2.3.1 Factor of Safety

The design structural factor of safety shall be adequate to provide for all uncertainties in design data.

The structural factor of safety, defined as insulator design stress at allowable strain levels divided by calculated insulator stress, should be at least 1.25. When any uncertainty exists concerning the reliability of material properties data, data being representative of processed material, or batch-to-batch variations in the material manufacturer's process, safety factors larger than 1.25 are recommended. When large factors of safety may be used at slight penalty to the weight and price of the insulator system, factors of 2 or more are recommended.

3.4.2.3.2 Margin of Safety

The structural margin of safety shall be as small as practicable.

It is recommended that design or material changes be made to reduce the structural margin of safety (eq. (10)) to zero. If it becomes impractical to do so because of cost or material limitations, then changes should be made to produce the smallest positive margin of safety attainable. The stress value used to compute the margin of safety should include the design structural factor of safety.

3.4.2.4 FAILURE MODES

Insulation shall not be subject to failure resulting from separation, cracking, or slump.

It is recommended that a thorough review of data produced by the structural analysis be made to determine whether the strain predicted is within the capability of the materials. If the strain capability of any material is exceeded, some corrective design step should be initiated to eliminate the marginal condition; for example, (1) the part should be thickened, (2) joints should be moved, or **(3)** materials should be changed. Wherever the principal strain exceeds 2 percent, adhesive joints and insulator repair should be avoided. Potting compounds, sealing compounds, or barrier coats should be selected according to ablative, mechanical, and adhesive property data. Table III indicates those areas where structural failure is most likely and identifies material properties critical to the failure mode.

Table 111. – Insulator Structural Failure Related to Location **of** Failure and Material Properties Critical to Failure

Location	Failure Mode	Critical Material Properties
Insulator/propellant interface	Separation	Insulator-propellant adhesive strain capability; barrier-coat strain capability
Insulator	Cracking	Insulator strain capability and aging resistance; barriercoat strain capability
Insulator	Flow (slump)	Barriercoat softening temperature; winding-mandrel compressive strength at case cure temperature
Insulator/flap interface	Separation	Potting-compound strain capability; barrier-coat strain capability; sealant strain capability
Insulator/case interface	Separation	Adhesive strain capability

In addition, a "volume" analysis should be conducted to determine maximum and minimum limits on sealant volume required to stay within the allowable strain of the sealant.

The recommended configuration for elastomer-to-elastomer junctions is the labyrinth joint (fig. 17(a)) filled with sealing compound. The recommended configuration for junctions of elastomer to reinforced plastic is a scarf joint, oriented **30"** to gas flow as shown in figure 17(b). It is recommended that interfaces of all types be designed to a low mean of the test values obtained for the adhesive sealant (i.e., a value somewhat lower than the average of all test values should be used for design).

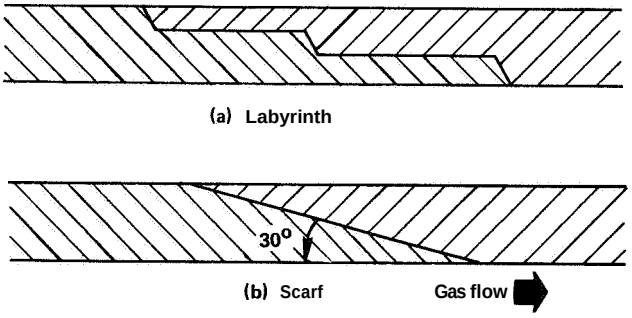

Figure 17. – Recommended designs for insulation junctions.

3.5 INSULATOR FABRICATION AND PROCESSING

3.5.1 Compounding

The insulation compounding and processing shall produce a uniform material without destroying fibrous fillers.

Recommended practice is to purchase compounded elastomer stock or molded insulator parts from a reputable, reliable supplier of insulation material. In most cases the insulation formulation is proprietary and the designer has no control of the formulation process.

Acceptance standards usually are developed from the manufacturer's recommendations (based on his own process capability) and tests of delivered material. When the designer has some control over formulation, he should specify ingredient purity, recipe accuracy, and the intended use of the material. The milling time required to produce uniformity without filler destruction should be determined by experimentation.

3.5.2 Fabricating

The method of fabricating the insulator shall be cost effective.

The method of fabricating the insulator should be matched to the size of the insulator, the quantity of insulators needed, and any special requirements imposed on the insulator. In general, as noted previously (sec. 3.1.2.1), when large quantities of small or moderate-size insulators are to be manufactured, compression molding is recommended; when production quantities are small, use hand layup. Troweling is most suitable when the insulator is too large to be handled economically by molding or machining and the cost of hand layup is prohibitive. Machining is recommended when quantities are small and accurate dimensional control is essential.

Each method is subject to constraints summarized below.

3.5.2.1 MOLDING

3.5.2.1.1 Mold Size

Compression mold design shall allow for part shrinkage.

Recommended practice is to purchase molded parts from a reputable, reliable manufacturer who is experienced in molding the insulator material chosen. Provisions should be made in the mold design to allow oversize molding that compensates for the expected shrinkage. Examples of shrinkages that must be accounted for are given below:

	NBR	SBR	EPT	Silicone
Parrallel shrinkage, %	0 to 0.8	0 to 0.9	0.3	2 to 7
Perpendicular shrinkage, %	1.3 to 2.5	1.3 to 2.3	1.2	2 to 7

3.5.2.1.2 Molding Variables

Control of *molding variables shall be adequate to produce optimum performance* of *the insulation.*

It is recommended that strict process controls be exercised over the molding variables such as time, temperature, pressure, and mold charge. Molding variables should be determined by skilled personnel with accurate equipment. Where possible, quality control tabs or "runoffs" should be included in the mold design to permit destructive tests for molding and cure quality. **A** permanent record of the molding variables should be maintained by operating personnel; the record may be a chart produced by automatic recording equipment or a written record of observations. Each of the molding-variable records should be examined by management representatives or quality-control personnel before the molded insulator section is permitted to move to the next assembly step.

When insulators are manufactured from materials that degrade at temperatures within the probable atmospheric temperature range, it is recommended that appropriate air conditioning or heating be provided for all shipping, storage, aiid processing areas. When insulators are manufactured from materials that degrade under exposure to sunlight and ozone, protect the insulator from such exposure by storing in a cool, dry, dark place and by sealing the material so that air cannot reach it.

3.5.2.2 LAYUP

The solvent content of *insulators fabricated by hand layup shall be below the level that will degrade insulator performance.*

An air dry at room temperature and humidity for thirty minutes should be allowed between application of plies in manufacture of hand-layup insulators.

3.5.2.3 TROWELING

The troweled mastic insulator shall be free from (1) voids and inclusions and (2) unacceptable degree of slump.

Pumpextrusion techniques are recommended in fabrication of mastic insulation because such techniques minimize the number and size of the voids. Limits on void shape, size, and dispersion should be established by test firings. Vacuum cycles and nondestructive test techniques should be used to locate any voids present in a finished insulator. Located voids should be reworked by filling either with uncured insulation material or with a suitable potting material.

Maximum acceptable slump should be determined from thickness calculations outlined in section 3.4.1.1. The use of thixotropic agents, binder systems with short pot life, or application of material in layers that do not slump before cure are recommended, both individually and in concert, as methods of eliminating slump from the insulator. The best of the three methods should be determined from analysis of the insulation process and materials used.

3.5.2.4 MACHINING

The machining method used to bring the insulator to design thickness and contour shall be suited to the special needs of the insulator.

The layup-grind method, in which the insulator is laid up on a male mandrel to an oversize configuration and then ground to final dimensions, is generally recommended. The designer however should make a cost analysis of the proposed manufacturing methods, including dimensional capabilities and the number of insulator units to be made. The machining method should then be chosen by selecting the method acheiving lowest cost for the required part throughout the entire manufacturing run.

3.5.3 Processing

3.5.3.1 BOND DEGRADATION

The case/insulator/propellant bond system shall not be degraded by moisture during processing and storage.

The recommended method of preventing bond degradation by moisture is to select primers, adhesives, and insulation materials that are relatively unaffected by moisture. Adhesives that possess good moisture resistance are epoxies, nitrile-phenolics, neoprene-phenolics, and epoxy-phenolics. When it is necessary to use moisture-sensitive materials, the insulator and case should be dried before bonding, and the insulator/case assembly should be dried before propellant casting. The drying periods must be based on comparable experience or determined by simulated processing tests.

3.5.3.2 INSULATOR DEGRADATION

Insulator handling procedures shall prevent exposure to ambient conditions that degrade the insulator material.

Ozone, sunlight, moisture, and high temperatures should be avoided in the storage and processing of elastomeric insulators. Opaque, air-tight packaging is recommended. Storage should be in areas cool and dry enough to prevent damage to insulators.

3.6 DESIGN VERIFICATION

3.6.1 Full-scale Testing and Evaluation

When any design uncertainty exists, full-scale test firings and postfire evaluation shall verify the insulator design adequacy.

The thermal performance of the insulator should be evaluated in full-scale test firings. Provide for acquisition of (1) physical thickness measurements before and after firing (fig. 16), (2) case/insulator interface temperature versus time during firing, (3) chamber heat flux, (4) insulator and case wall temperature profiles versus time during firing, and (5) insulator exposure time. Case/insulator interface temperatures should be measured by drilling holes through the case to the interface, implanting thermocouples, and potting the hole with a material having approximately the same thermal diffusivity as the case. Chamber heat flux should be measured by slug-type calorimeters or circular-foil heat-flux gages. Temperature at the ablative wall should be measured by surface thermocouples. Temperature profiles of the insulator and case wall should be measured by thermocouples embedded at successively deeper locations. Insulator exposure times should be obtained from event gages (e.g., embedded breakwires) or char detectors (e.g., electical conductivity gages). Progression of the flame front should be measured by microwave techniques (refs. 101 and 102). After the testing, evaluate the insulation performance, and if insulation performance margins are substantially less than or greater than desired, adjust the design accordingly.

Hardware inspection. – The postfire inspection of insulation should be planned to preclude destruction of test hardware by either cutting or measurement operations until all data and anomalies have been inspected and recorded. It is recommended that thickness measurements be obtained at locations of highest anticipated insulator erosion and that visual inspection of case and insulator be made after firing and before removal of the case from the test stand. Areas of excessive external case heating should be noted, as should those of high insulator erosion and insulator delaminations and separations. All unusual erosion patterns should be mapped (fig. 13) and the case sectioned. Postfire insulation thicknesses should be measured at locations coincident with those of prefire measurements.

Instrumentation. – Insulation instrumentation should be used for material evaluation motors and for full-scale development motors but should not be used in operational motors. The risk inherent in instrumenting insulators, which often involves practices such as drilling holes through the chamber wall into the insulator, should not be imposed on operational motors. When instrumentation must be used, the risk should be minimized by running many wires through the same hole or by making multiple use of instrument taps.

Data Evaluation. – Prefire measurements of insulator initial thickness and postfire measurements of insulator char and erosion should be obtained by reliable and repeatable methods and should be evaluated statistically. Measurements of insulator thickness before and after firing using a mechanical template and standard measuring instruments is recommended in order to provide repeatability. When measurements are determined from X-ray methods, the possibility of parallax should be precluded to avoid erroneous measurements. Prefiring and postfiring measurements should be taken in sufficiently large quantities that an accurate statistical inference may be taken from the data acquired. Statistical techniques of regression analysis are recommended for processing these thickness measurements. The char depth recorded for a measurement station should be the maximum char at any of the circumferential locations at that station.

APPENDIX A

Conversion of U.S. Customary Units to SI Units

Physical quantity	U.S. customary unit	SI unit	Conversion factor[a]
Density	lbm/ft^3	kg/m^3	1.602×10^1
Energy	Btu	J	1.054×10^3
Force	lbf	N	4.448
Heat flux	$Btu/(ft^2\text{-sec})$	$J/(m^2\text{-sec})$	1.135×10^4
Heat of ablation	Btu/lbm	J/kg	2.324×10^3
Heat-transfer coefficient	$\frac{Btu}{ft^2\text{-sec-}^\circ F}$	$\frac{J}{m^2\text{-sec-K}}$	2.043×10^4
Length	ft	m	3.048×10^{-1}
	in,	cm	2.54
	mil	μm	2.54×10^1
Mass	lbm	kg	4.536×10^{-1}
Mass diffusivity	ft^2/hr	m^2/hr	9.29×10^{-2}
Pressure	psi $(lbf/in.^2)$	N/cm^2	6.895×10^{-1}
Specific heat	$Btu/(lbm\text{-}^\circ F)$	J/(kg-K)	4.184×10^3
Stefan-Boltzmann constant	$\frac{Btu}{hr\text{-}ft^2\text{-}^\circ R^4}$	$\frac{J}{sec\text{-}m^2\text{-}K^4}$	$3.310 \times 10'$
Temperature	°F	K	$K = \frac{5}{9}(^\circ F + 459.67)$
	°R	K	$K = \frac{5}{9}(^\circ R)$
Temperature difference	°F	K	$K = \frac{5}{9}(^\circ F)$
	°R	K	$K = \frac{5}{9}(^\circ R)$

(continued)

Conversion of U.S. Customary Units to SI Units (concluded)

Physical quantity	U.S. customary unit	SI unit	Conversion factor[a]
Thermal conductivity	$\frac{\text{Btu}}{\text{sec-ft-}^\circ\text{F}}$	$\frac{\text{J}}{\text{sec-m-K}}$	6.227×10^{3}
Thermal diffusivity	ft^2/hr	m^2/hr	9.29×10^{-2}

[a]Multiply value given in U.S. customary unit by conversion factor to obtain equivalent value in SI units. For a complete listing of conversion factors for basic physical quantities, see Mechtly, E. A.: The International System of Units. Physical Constants and Conversion Factors. Second Revision, NASA SP-7012, 1973.

APPENDIX B

GLOSSARY

Term or Symbol	Definition
a,b,c,d,e,f	empirical constants fitted to data for Luikov number
ablation cooling	cooling mechanism in which a material on a rocket chamber wall chars, evaporates, sublimes, and erodes during motor firing and thereby absorbs exhaust-gas heat and prevents it from reaching the chamber Wall
ambient temperature	temperature of the environment surrounding a system or a component
autoclave	apparatus for curing materials under heat and pressure
ballistics (internal)	combustion characteristics of the solid propellant grain, especially those related to thrust- and pressure-time curves for the motor
Biot number (Bi)	dimensionless group relating temperature conditions in the exhaust gas to the temperature distribution in the insulator ($Bi = \frac{hr}{k}$)
bleeder cloth	an open-weave cloth used to facilitate complete removal of air in vacuum-bag processing of reinforced-plastic parts
C_1, C_2	empirical constants for data correlations
C_p	specific heat at constant pressure
conocyl	acronym for "cone in cylinder''
cracking	thermal decomposition of heavy hydrocarbons into lighter and simpler hydrocarbons and other products
elastomer	polymeric material that at room temperature can be stretched to approximately twice its original length and on release return quickly to its original length
factor of safety	see "safety factor"
Fourier number (Fo)	dimensionless group relating rate of change of temperature conditions in the exhaust gas to rate of change of temperature distribution in the insulator ($Fo = \frac{\chi t}{r^2}$)

Term or Symbol	Definition
h	heat-transfer coefficient
k	thermal conductivity
Q	radiant-beam path length
L/D	length-to-diameter ratio of propellant grain
Luikov number (Lu)	dimensionless group relating insulator mass diffusivity to thermal diffusivity ($Lu = \frac{\dot{x}_{ch} r_j}{\chi}$)
Mach number	ratio of the speed of flow of a fluid to the speed of sound in the fluid
margin of safety (MS)	fraction by which the allowable load on stress exceeds the applied load or stress, $MS = \frac{1}{R} - 1$
NDT	nondestructive testing
P	pressure
partition equilibrium	the condition in which, for a chemical species distributed between two fluids in contact at definite temperature, the ratio of the equilibrium concentrations in the fluids is constant
potential flow	flow with the effects of viscosity not considered
potting compound	inert material used to fill in or surround a part or component
Pr	Prandtl number, ratio of momentum transport to heat transport in fluid flow ($Pr = C_p \mu/k$)
pyrolysis	chemical decomposition by heat
Q*	effective heat of ablation
$\dot{q}$	heat flux
R	design stress/allowable stress
r	radius of flow channel (i.e., radius of combustion chamber at a given station)
regression line	term used in the mathematical technique of regression analysis

Term or Symbol	Definition
Reynolds number (Re)	ratio of momentum forces to viscous forces in fluid flow $\left(\mathrm{Re} = \frac{\rho v r}{\mu}\right)$
safety factor	an arbitrary multiplier greater than 1 applied in design to allow for uncertainties in design data
Stanton number	ratio of the heat transmissions perpendicular to and parallel to the direction of flow
slump	flow or sag of a material (mastic) after it has been applied to the chamber wall
spallation	chunking out of insulation material by shear forces and operational stresses
submerged nozzle	nozzle in which the nozzle entry, throat, and part or all of the exit are cantilevered into the combustion chamber
sweep template	contoured device used to control thickness of mastic as it is applied to chamber wall
T	temperature
t	time
thixotropic agent	an additive material that does not alter flow properties when the base material is being applied to a surface but hastens gelation when the material is allowed to stand; used to prevent slump in mastics
transpiration cooling	cooling of a chamber wall by flow of coolant gases through porous material on the wall
v	local gas velocity
wash coat	thin layer of curing agent for the liner that is applied to surface of propellant or insulator to enhance liner adhesion
x	insulator thickness
	Greek
α	gas-cloud emissivity parameter that is a function of particle size, concentration, and density

Term or Symbol	Definition
A	incremental change in a quantity
ε	emissivity
μ	absolute viscosity
ρ	density
σ	Stefan-Boltzmann constant, 0.1713×10^{-8} Btu/(hr-ft^2-°R^4)
χ	thermal diffusivity

Subscripts

a	ablation
avg	average
ch	char
cl	gas/particle cloud
cl-w	pertaining to interchange between gas/particle cloud and wall
con	convective
g	exhaust gas (combustion products)
i	insulator
par	pertaining to impingement and deposition of particles
rad	radiant
tot	total
w	wall (insulator)

Material	Identification
antioxidant	organic compound added to a material to retard oxidation, deterioration, and rancidity

Material	Identification
butyl rubber	copolymer of 97% isobutene and 3% isoprene or butadiene
CA	cellulose acetate, a cellulose ester in which the cellulose is not completely esterified by acetic acid
CMDB	composite-modified double-base propellant; modification is by addition of oxidizer such as ammonium perchlorate and/or fuel such as aluminum powder
cresol	methyl phenol
CTPB	carboxy-terminated polybutadiene
DB	double-base propellant
epoxy	thermosetting resin widely utilized as an adhesive and as a binder in the fabrication of glass-filament/resin composites
ethylene-propylene rubber (EPR)	an elastomer, a copolymer of ethylene and propylene
ethylene-propylene terpolymer (EPT, EPDM)	an elastomer based on linear terpolymers of ethylene, propylene, and small amounts of a diene
HTPB	hydroxyl-terminated polybutadiene
Hypalon	trademark of E.I. du Pont de Nemours & Co. (Wilmington, DE) for chlorosulfonated polyethylene
mastic	filed elastomer that is cast or troweled in place and cured at or near room temperature and pressure
NBR, Buna N, nitrile	copolymer of butadiene and acrylonitrile
neoprene	polychloroprene
NG	nitroglycerin
PBAA	butadiene-acrylic acid polymer
PBAN	butadiene-acrylic acid-acrylonitrile polymer
phenolic	short term for a family of phenol-aldehyde thermosetting resins

Material	Identification
polysulfide	short term for NBR-polysufide-epoxy
RTV silicone	organosiloxane polymer that vulcanizes at room temperature
SBR	copolymer of styrene and butadiene
silicone	organosiloxane polymer; may be an oil or an elastomer, depending on degree of polymerization
urethane	polyurethane diisocyanate copolymer

ABBREVIATIONS

Abbreviation	Identification
ABL	Allegany Ballistics Laboratory
AFRPL	Air Force Rocket Propulsion Laboratory
AGARD	Advisory Group on Aerospace Research and Development
AIAA	American Institute of Aeronautics and Astronautics
AIChE	American Institute of Chemical Engineers
ARPA	Advanced Research Projects Agency
ARS	American Rocket Society
ASME	American Society of Mechanical Engineers
ASTM	American Society for Testing and Materials
CPIA	Chemical Propulsion Information Agency
GALCIT	Guggenheim Aeronautical Laboratory (California Institute of Technology)
IAS	Institute of the Aeronautical Sciences
ICRPG	Interagency Chemical Rocket Propulsion Group
JANAF	Joint Army-Navy-Air Force

Abbreviation	Identification
SAMPE	Society of Aerospace Material and Process Engineers
SRSIA	Solid Rocket Structural Integrity Abstracts
SSD	Space Systems Divison (USAF)

REFERENCES

1. Toscano, C.; and Hribar, V. F.: Critique of Internal Insulation Materials for Solid Propellant Rocket Motors and Their Effect on Missile Performance. SSD-TDR-64-266 (AD-459371), Aerospace Corp., Jan. 15,1965.

2. Bradley, W.; et al.: Investigation and Evaluation of Motor Insulation for a Multiple Restart Application. AFRPL-TR-67-287 (AD-824877), Aerojet-General Corp., November 1967.

3. Jaffe, L. D.: Effects of Space Environment Upon Plastic and Elastomers. Tech. Rep. 32-176, Jet Propulsion Lab., Calif. Inst. Tech., Nov. 16, 1961.

4. Rivera, M.; Fassell, W. M.; and Carson, W. Q.: Characteristics of Some Elastomers in the Space Environment. Minutes of 7th SAMPE Symposium (Los Angeles, CA, May 20-22, 1964), SAMPE, 1964.

5. Orchon, J.: Behavior of Solid Rocket Organic Materials in Space and Re-Entry Environments. Rep. RA/SA BSR, Aerojet-General Corp., Feb. 23,1967.

6. Hayden, H. W.; Moffatt, W. G.; and Wulff, J.: The Structure and Properties of Materials. Vol. III: Mechanical Behavior. John Wiley & Sons, Inc. (New York), 1965.

7. Anon.: 260-SL-3 Motor Program. Vol. I: 260-SL-3 Motor Internal Insulation System. NASA CR-72228, Aerojet-General Corp., April 28, 1967.

8. Anon.: 260-Inch Motor Demonstration and 156-Inch Motor Nozzle Test Program. RPL-TDR-64-58, Thiokol Chemical Corp., March 31,1964.

9. Anon.: 156-Inch Diameter Motor Liquid Injection TVC Program (Test Results, Motor 156-5) (U). Vol. II, Final Report, AFRPL-TR-66-109, Lockheed Propulsion Co., July 1966. (CONFIDENTIAL)

10. Lyons, C. S.; and Lawson, D. D.: Ablative Characteristics of Reinforced Plastics in Nozzles and Thrust Chambers for Varying Environments. Applications of Plastic Materials in Aerospace, Chem. Eng. Prog. Symposium Series, no. 40, vol. 59, AIChE, 1963, pp. 33-38.

11. Anon.: Solid Rocket Motor Nozzles. NASA Space Vehicle Design Criteria Monograph, NASA SP-8115, June 1975.

12. Anon.: Liquid Rocket Engine Self-Cooled Combustion Chambers. NASA Space Vehicle Design Criteria Monograph, NASA SP-8124 (to be published).

13. McAdams, W. H.: Heat Transmission. Third ed., McGraw-Hill Book Co., Inc. (New York), 1954.

14. Schwartz, H. S.: Laboratory Techniques for Studying Thermally Ablative Plastics. Applications of Plastic Materials in Aerospace, Chem. Eng. Prog. Symposium Series, no. 40, vol. 59, AIChE, 1963, pp. 64-80.

15. Anon.: Index to ASTM Standards. Part 33, Annual Book of ASTM Standards (revision issued annually). Am. Soc. for Testing and Materials (1619 Race Street, Philadelphia, PA 19103).

16. Anon.: ICRPG Solid Propellant Mechanical Behavior Manual. CPIA Publ. 21, Chem. prop. Information Agency (Johns Hopkins Univ., Silver Spring, MD), September 1963.

17. Anon.: Solid Propellant Grain Structural Integrity Analysis. NASA Space Vehicle Design Criteria Monograph, NASA SP-8073, June 1973.

18. Dickinson, L. A.; Altschuler, M. H.; McClay, H. B.; and Tice, H. B.: Case Bonding Technology – A Review of Selected Applications (U). CPIA Publ. 159, Insulation and Case Bonding Symposium (Sept. 12-13, 1967, Wayne, NJ), November 1967, pp. 143-151. (CONFIDENTIAL)

19. Myers, J. L.; Moon, E. L.; and Allen, L. R.: Final Report, Solid Rocket Motor Component Aging Study: A State of the Art Survey (U). AFRPL-TR-11(AD-378814), Systems Group, TRW, Inc., January 1967. (CONFIDENTIAL)

20. Pickett, A. G.; and Lemcoe, M. M.: Handbook of Design Data on Elastomeric Materials Used in Aerospace Systems. ASD-TR-61-234(AD-273880), Southwest Research Institute, January 1962.

21. Anon.: Rubber and Rubber-Like Materials. Military Standardization Handbook, MIL-HDBK-149A, Dept. of Defense, June 30, 1965.

22. Anon.: Oxyacetylene Ablation Testing of Thermal Insulation Materials. ASTM Standard E 285-70, ASTM.

23. Skeist, I.: Modern Structural Adhesives for Use in the Building Industry. Adhesives Age, vol. 7, no. 4, April 1964, pp. 21-26.

24. Malis, M. F.: High Expansion Ratio Motors Using High Energy Force Propellant (U). AFRPL-TR-66-120 (AD-373359), Lockheed Propulsion Co., Jan. 17, 1966. (CONFIDENTIAL)

25. Delmonte, J.; Hartry, D.; and Fullerton, R.: Influence of Application Variables on Properties of an Epoxy Adhesive. Structural Adhesive Bonding, Applied Polymer Symposia, No. 3, Interscience Publishers, Div. of John Wiley & Sons, Inc., 1966, pp. 397403.

26. Bryant, R. W.; and Dukes, W. A.: The Effect of Joint Design and Dimensions on Adhesive Strength. Structural Adhesives Bonding, Applied Polymer Symposia, No. 3, Interscience Publishers, Div. of John Wiley & Sons, Inc., 1966, pp. 81-98.

27. Rogers, C. J.; Smith, P. L.; Bills, K. W.; and Dixon, J. D.: Development and Selection of Liners for Case-Banded Motors (U). CPIA Publ. 49, vol. II, 20th Interagency Solid Propulsion Meeting, July 13-15, 1964 (Philadelphia, PA), May 1964, pp. 223-246. (CONFIDENTIAL)

28. Anon.: Solid Propellant Structural Integrity Investigations: Propellant-Liner Bond Studies (U). Final Report AGC 0752-81F, Aerojet-General Corp., March 25, 1964. (CONFIDENTIAL)

29. Anon.: Solid Propellant Processing Factors in Rocket Motor Design. NASA Space Vehicle Design Criteria Monograph, NASA SP-8075, October 1971.

30. Greever, W. L.: An Extended-Temperature-Range Case Bond System for CMDB Propellants (U). CPIA Publ. 196, vol. II, 26th JANAF Solid Propulsion Meeting (July 14-16, 1970, Washington, DC), pp. 179-196. (CONFIDENTIAL)

31. Anderson, **S. E.;** and Thompson, B. L.: Evaluation of Motor Case Insulation Materials for Low Signature Applications (U). CPIA Publ. 159, Insulation and Case Bonding Symposium (Sept. 12-13, 1967, Wayne, NJ), November 1967. (CONFIDENTIAL)

32. Justice, B. H.; and Carr, I. **H.:** The Heat of Formation of Propellant Ingredients (U). AFRPL-TR-67-311, Thermal Research Lab., Dow Chemical Co., December 1967. (CONFIDENTIAL)

33. Anon.: JANAF Thermochemical Tables. Thermal Research Lab., Dow Chemical Co., updated periodically.

34. White, W. B.; Johnson, **S.** C.; and Dantzig, G. B.: Chemical Equilibrium in Complex Mixtures. J. Chem. Phys., vol. 28, no. 5, May 1958, pp. 751-755.

35. Gordon, **S.;** and McBride, B. J.: Computer Program for Calculation of Complex Chemical Equilibrium Compositions, Rocket Performance, Incident and Reflected Shocks, and Chapman-Jouguet Detonations. NASA SP-273, 1971.

36. Cruise, D. R.: Notes on the Rapid Computation of Chemical Equilibria. J. Phys. Chem., vol. 68, no. 12, December 1964, pp. 3797-3802.

37. Itean, E. C.; Glueck, H. R.; and Svehla, R. A.: Collision Integrals for a Modified Stockmayer Potential. NASA TN-D-491, 1961.

38. Svehla, R. A.: Estimated Viscosities and Thermal Conductivities of Gases at **High** Temperatures. NASA TR-R-132, 1962.

39. Chapman, **S.;** and Cowling, T. G.: Mathematical Theory of Non-Uniform Gases. Seconded., Cambridge University Press, 1951.

40. Curtiss, C. F.; and Hirschfelder, J. **O.:** Transport Properties of Multicomponent Gas Mixtures. J. Chem. Phys., vol. 17, no. 6, June 1949, pp. 550-555.

41. Wilke, C. R.: A Viscosity Equation for Gas Mixtures. J. Chem. Phys., vol. 18, no. 4, April 1950, pp. 517-519.

42. Brokaw, R. **S.:** Alignment Charts for Transport Properties, Viscosity, Thermal Conductivity, and Diffusion Coefficient for Non-Polar Gases and Gas Mixtures of Low Density. NASA TR-R-81, 1961.

43. Shapiro, A. H.: The Dynamics and Thermodynamics of Compressible Fluid Flow. The Ronald Press Co. (New York), 1953, pp. 284-297.

44. Bartz, D. R.: A Simple Equation for Rapid Estimation of Rocket Nozzle Convective Heat Transfer Coefficients. Jet Propulsion, vol. 27, no. 1, January 1957, pp. 49-51.

45. Welsh, W. E., Jr.; and Witte, A. B.: A Comparison of Analytical and Experimental Local Heat Fluxes in Liquid Propellant Rocket Thrust Chambers. Tech. Rep. 3243, Jet Propulsion Lab., Calif. Inst. Tech., Feb. 1, 1961.

46. Witte, A. B.; and Harper, E. Y.: Experimental Investigation of Heat Transfer Rates in Rocket Thrust Chambers. AIAA J., vol. 1, no. 2, February 1963, pp. 443-451.

47. Elliot, D. G.; Bartz, D. R.; and Silver, S.: Calculation of Turbulent Boundary-Layer Growth and Heat Transfer in Axisymmetric Nozzles. Tech. Rep. 32-387, Jet Propulsion Lab., Calif. Inst. Tech., February 1963.

48. Price, F. C.; et al.: Detail Design Optimization of Solid Propellant Rocket Motor, Aft Closure Nozzle Combinations. Vol. I, Publ. C-1809, Aeronutronics Div., Ford Motor Co., Oct. 30, 1962.

49. Culick, F. C. C.; and Hill, J. A. F.: A Turbulent Analog of the Stewartson-Illingsworth Transformation. J. Aeron. Sci., vol. 25, no. 4, April 1958, pp. 259-262.

50. Truckenbrodt, E.: A Method of Quadrature for Calculation of the Laminar and Turbulent Boundary Layer in Case of Plane and Rotationally Symmetrical Flow. NASA TM 1379, 1955.

51. Emergy, A. F.; Sadunas, J. A.; and Loll, M.: Heat Transfer and Pressure Distribution in Open Cavity Flow. J. Heat Transfer, Trans. ASME, Series C, vol. 89, 1967, pp. 103-108.

52. Haugen, R. L.; and Dhanak, A. M.: Heat Transfer in Turbulent Boundary-Layer Separation Over a Surface Cavity. J. Heat Transfer, Trans. ASME, Series C, vol. 89, 1967, pp. 335-340.

53. Charwat, A. F.; et al.: An Investigation of Separated Flows. Part II: Flow in the Cavity and Heat Transfer. J. Aerospace Sci., vol. 28, no. 7, July 1961, pp. 513-527.

54. Lund, R. K.: Final Report — Cold Flow Tests Poseidon C-3 First and Second Stage. TWR-2320, Hercules, Inc./Thiokol Chemical Corp. (A Joint Venture), February 1967.

55. Christensen, E. A.; and Haigh, W. S.: Aerodynamic Studies of the Effect of Solid-Rocket-Motor Nozzle Immersion and Entrance Shape. Tech. Memo. 212 SRP, Aerojet-General Corp., March 1963.

56. Lafazan, S.; and Turnacliff, R. D.: A Review of Rocket Engine Heat Transfer. Rocket and Missile Technology, Chem. Eng. Prog. Symposium Series, vol. 57, no. 33, AIChE, 1961, pp. 53-63.

57. Sanford, J. T.; Huson, G. R.; and Griese, R.: Design of Ablative Thrust Chambers and Their Materials. AIAA paper 64-261, First AIAA Annual Meeting (Washington, DC), June 29 – July 2, 1964.

58. Siegel, R.; and Howell, J. R.: Radiation Transfer with Absorbing, Emitting, and Scattering Media. Vol. III of Thermal Radiation Heat Transfer. NASA SP-164,1971.

59. Desmon, L. G.; et al.: Heat Transfer in Nozzle Systems **(U).** ABL/ARPA/X-143, Final Report, Allegany Ballistics Laboratory, June 30,1965. (CONFIDENTIAL)

60. Brookley, C. E.: Measurement of Heat Flux in Solid Propellant Rocketry. ABL/Z-60 (AD-432472), Allegany Ballistics Laboratory, November 1963.

61. Eckert, E. R. G.; and Drake, R. M., Jr.: Heat and Mass Transfer. Second ed., McGraw-Hill Book Co., Inc. (New York), 1959.

62. Bird, R. B.; Stewart, W. E.; and Lightfoot, E. N.: Transport Phenomena. John Wiley & Sons, Inc., 1960.

63. Marshall, R. L.; Pellett, G. L.; and Saunders, A. R.: An Experimental Study of the Drag Coefficient of Burning Aluminum Droplets. NASA TMX-59145,1966.

64. Zeamer, R. J.: Erosion Produced by High-Speed Two-Phase Flow in Solid Propellant Rocket Motors. Paper 27, AGARD Conf. Proc. 52, Reactions Between Gases and Solids, February 1970.

65. Daines, W. L.: The Effect of Acceleration Forces on the Agglomeration, Flow Trajectories, and Impingement of Aluminum Particles in the Second Stage Poseidon Motor. Rep. 17-10203/6/40-1633, Hercules, Inc., June 1970.

66. Miller, R. R.: Some Factors Affecting the Combustion of Aluminum in Solid Propellants. ICRPG 2nd Combustion Conference (Los Angeles, CA, November 1965), CPIA Publ. 105, vol. I, May 1966, pp. 331-353.

67. Davis, A.: Solid Propellants – The Combustion of Particles of Metal Ingredients. Rep. 17/R/62, Explosives Research and Development Establishment, British Ministry of Aviation, December 1962.

68. McCuen, P. A.; et al.: A Study of Solid Propellant Rocket Motor Exposed Materials Behavior. RPL-TR-64-33(AD-462331), Vidya Div., Itek Corp., February 1965.

69. Cothran, L. E.; and Barnes, S. V.: Behavior of Plastic and Refractory Materials in the Particle Impingement Areas of Solid Propellant Ducting Systems. AIAA paper 64-224, First AIAA Annual Meeting (Washington, DC), June **29** – July2,1964.

70. Allen, J. M.; et al.: An Experimental Investigation of the Deposition of Small Particles from a Moving Gas Stream. AEDC-TN-58-73, Battelle Memorial Institute, September 1958.

71. Schaefer, J. W.; et al.: Studies of Ablative Material Performance for Solid Rocket Nozzle Applications. NASA CR-72429, Rep. 68-30, Aerotherm Corp., March 1968.

72. Price, F. C.; et al.: Internal Environment of Solid Rocket Nozzles. Final Report U-2709, RPL-TDR-64-140 (AD-606393), Philco Corp. (Blue Bell, PA), July 1964.

73. Daines, W. L.: SX-0031 Failure Analysis — Dome Burnthrough Calculations. Memo. 17-10203/6/40-926, Hercules, Inc., March 1969.

74. Briggs, L. A.; et al.: Upper Stage Technology Program (U). Final Report, Vol. I, TR-68-62, Aerojet-General Corp., August 1968. (CONFIDENTIAL)

75. Anon.: Polaris Development Progress Report (U). Rep. P., Dev. 3969, Allegany Ballistics Laboratory, Nov. 25, 1963. (CONFIDENTIAL)

76. Smallwood, W. L.; et al.: Beryllium Erosion Corrosion Investigation for Solid Rocket Nozzles (U). Final Report, AFRPL-TR-67-82, Space and Re-Entry Systems Div., Philco-Ford Corp., June 1967. (CONFIDENTIAL)

77. Anon.: Captive-Fired Testing of Solid Rocket Motors. NASA Space Vehicle Design Criteria Monograph, NASA SP-8041, March 1971.

78. Manda, L. J.: Compilation of Rocket Spin Data. NASA CR-66641, Emerson Electric Co., 1968.

79. Kordig, J. W.: Backside Temperatures of an Internal Insulator in a Solid-Propellant Motor. AIAA J., vol. 2, no. 8, August 1964, pp. 1475-1476.

80. Drechsel, P. D.: Prediction of Temperature Profiles in Virgin Material Zone of an Ablating Insulator. SPR 388, Hercules, Inc./ABL, January 1968.

81. Browning, S. C.; et al.: Structural and Thermal Analysis Report, Poseidon First Stage (U). Vol. IV: Insulator Analysis. SE025-A2A00HTJ, Hercules, Inc. (Bacchus Works, Magna, UT), April 1967. (CONFIDENTIAL)

82. Anon.: High Energy Upper Stage Rocket Motor. Phase II, Task III, Final Report: Analysis. Vol. I, Hercules, Inc., Oct. 7, 1969.

83. Moyer, C. B.; and Rindal, R. A.: Analysis of the Coupled Chemically Reacting Boundary Layer and Charring Ablator. Part II: Finite Difference Solution for the In-Depth Response of Charring Materials Considering Surface Chemical and Energy Balances. NASA CR-1061, Itek Corp., June 1968.

84. Andrepont, W. C.: Evaluation of Ablation Prediction Techniques for Solid Rocket Nozzle Materials. AFRPL-TR-68-142 (AD-839672), Rocket Propulsion Lab. (Edwards AFB, CA), August 1968.

85. McIntosh, M. J.: Heat-Transfer Solution for a Gas/Particle Mixture Losing Heat to Parallel Boundaries. J. Spacecraft Rockets, vol. 5, no. 1, January 1968, pp. 114-115.

86. Williams, M. L.; Blatz, P. J.; and Schapery, R. A.: Fundamental Studies Relating to Systems Analysis of Solid Propellants. GALCIT SM 61-5 (AD-256905), Calif. Inst. Tech. (Pasadena, CA), February 1961.

87. Anderson, J. M.: Case Bond Stress Calculations for Flapped Cylindrical Analogs of Solid Propellant Rocket Motors. AFRPL-TR-72-55, Hercules, Inc., May 1972.

88. Anderson, J. M.; Pavelka, T. D.; and Bruno, P. S.: Techniques for Assessing Case Liner-Bond Integrity in Solid Propellant Rocket Motors. AFRPL-TR-73-75, Systems Group (Wilmington, DE), Hercules, Inc., September 1973.

89. Anderson, J. M.: A Review of the Finite Element Stiffness Method as Applied to Propellant Grain Stress Analysis. Solid Rocket Structural Integrity Abstracts, vol. 6, no. 4, Oct. 1969, pp. 1-54.

90. Ferry, J. D.: Viscoelastic Properties of Polymers. Chap. 11, John Wiley & Sons, Inc. (New York), 1961.

91. Burton, J. D.; and Harbert, B. D.: Application of Fracture Mechanics in Solid Propellants. Final Report, AFRPL-TR-67-287, Rocketdyne Div., North Am. Rockwell Corp., May 1970.

92. Harris, C. P.: Experimental Study of Propellant Grain Defects. Paper presented at 28th Polaris/Minuteman/Pershing NDT Committee Meeting (Magna, UT), July 9-10, 1963.

93. Soderholm, L. G.: Elastomers – Tailor-Made Design Materials. A Design News Supplement, vol. 20, no. 7, March 31, 1965, pp. 2-24.

94. Anon.: GEN-GARD Technical Bulletin K2(a). General Tire and Rubber Company.

95. Anon.: GEN-GARD Process Specification 1782B. General Tire and Rubber Company

96. Anon.: 260-Inch Motor Demonstration and 156-Inch Motor Nozzle Test Program. Tech. Note No. RPL-TDR-64-139, Space Booster Div., Thiokol Chemical Corp. (Brunswick, GA), Sept. 30, 1964.

97. Simmons, B. A.; and Nachbar, D. L.: Development of Cost-Optimized Insulation System for Use in Large Solid Rocket Motors. Vol. 2, Task 2: Process Evaluation, Final Report. NASA CR-72582, Aerojet-General Corp., August 1969.

98. Anon.: 260-In.-Dia. Motor Feasibility Demonstration Program. Volume 11: 260-SL Motor Propellant Tailoring and Liner Development, Final Phase Report (U). NASA CR-54473, FPR-2, Aerojet-General Corp., Nov. 19, 1965. (CONFIDENTIAL)

99. Anon.: GEN-GARD Process Specification 1775A. Revised May 20, 1965, General Tire and Rubber Company.

100. Anon.: Subsystem Test Report Poseidon C3 First Stage Static Test FD-0007. LMSC Data Item No. SH049-A2A00HTJ, Rep. No. 3, Hercules, Inc./Thiokol Chemical Corp. (A Joint Venture), Dec. 26, 1967.

101. Anon.: Anomalous Aft Dome Insulator Erosion in the M57A1 Rocket Motor. MTO-198-67-2, Hercules, Inc., Jan. 13, 1965.

102. McMaster, Robert C.: Non-Destructive Testing, Handbook VII. The Ronald Press Company (New York), 1963.

103. Oliver, R. B.; and Comiskey, J. B.: A Comparison of Eddy Current Devices for Measuring Insulation Thickness. Paper presented at the 22nd Polaris/Minuteman/Pershing NDT Committee Meeting at Aerojet-General Corp. (Sacramento, CA), April 1962.

104. Davis, L. J.; et al.: Internal Insulation Erosion Study of Stage I Poseidon Motor, Final Report. Hercules, Inc., July 1, 1968.

105. Anon.: Subsystem Test Report Poseidon C3 Second Stage Static Test SD-0012. LMSC Data Item No. SH-49-A2A00HTJ, Report No. 8, Hercules, Inc./Thiokol Chemical Corp. (A Joint Venture), March 18,1968.

106. Brookley, C. E.: Thermal Instrumentation for the Rocket Industry. ABL/Z-78, Hercules Inc. (Cumberland, MD), November 1964.

107. Jenks, J. C.; and DeVault, J. B.: Microwave Measurements of Solid Propellant Burning Rates and Burning Profiles. Paper presented at 28th Polaris/Minuteman/Pershing NDT Committee Meeting, Hercules Powder Company (Salt Lake City, UT), July 9-10,1963.

108. Rettinger, D. W.: The Use of Microwave Deflections to Detect Burning Surfaces in Solid Propellant Rocket Motors. Paper presented at 33rd Polaris/Minuteman/Pershing NDT Committee Meeting at Hill Air Force Base (Ogden, UT), April 1965.

109. Lawrence, H. R.; and Vogel, J. M.: Some Thoughts on Reliability Estimation. Paper presented at IAS Aerospace Symposium on Systems Reliability (Salt Lake City, UT), April 16-18, 1962.

110. Haugen, E. B.: Statistical Methods for Structural Reliability Analysis. Paper presented at Tenth National Symposium on Reliability and Quality Control (Washington, DC), January 7-9, 1964.

111. Headrick, R. E.: Elastomer Research for Extreme Temperature Insulation and Ablative Materials. ML-TDR-64-287 (AD-456968), Air Force Materials Laboratory, December 1964.

NASA SPACE VEHICLE DESIGN CRITERIA
MONOGRAPHS ISSUED TO DATE

ENVIRONMENT

SP-8005	Solar Electromagnetic Radiation, Revised May 1971
SP-8010	Models of Mars Atmosphere (1974), Revised December 1974
SP-8011	Models of Venus Atmosphere (1972), Revised September 1972
SP-8013	Meteoroid Environment Model—1969 (Near Earth to Lunar Surface), March 1969
SP-8017	Magnetic Fields—Earth and Extraterrestrial, March 1969
SP-8020	Surface Models of Mars (1975), Revised September 1975
SP-8021	Models of Earth's Atmosphere (90 to 2500 km), Revised March 1973
SP-8023	Lunar Surface Models, May 1969
SP-8037	Assessment and Control of Spacecraft Magnetic Fields, September 1970
SP-8038	Meteoroid Environment Model—1970 (Interplanetary and Planetary), October 1970
SP-8049	The Earth's Ionosphere, March 1971
SP-8067	Earth Albedo and Emitted Radiation, July 1971
SP-8069	The Planet Jupiter (1970), December 1971
SP-8084	Surface Atmospheric Extremes (Launch and Transportation Areas), Revised June 1974
SP-8085	The Planet Mercury (1971), March 1972
SP-8091	The Planet Saturn (1970), June 1972
SP-8092	Assessment and Control of Spacecraft Electromagnetic Interference, June 1972

SP-8103	The Planets Uranus, Neptune, and Pluto (1971), November 1972
SP-8105	Spacecraft Thermal Control, May 1973
SP-8111	Assessment and Control of Electrostatic Charges, May 1974
SP-8116	The Earth's Trapped Radiation Belts, March 1975
SP-8117	Gravity Fields of the Solar System, April 1975
SP-8118	Interplanetary Charged Particle Models (1974), March 1975
SP-8122	The Environment of Titan (1975), July 1976

STRUCTURES

SP-8001	Buffeting During Atmospheric Ascent, Revised November 1970
SP-8002	Flight-Loads Measurements During Launch and Exit, December 1964
SP-8003	Flutter, Buzz, and Divergence, July 1964
SP-8004	Panel Flutter, Revised June 1972
SP-8006	Local Steady Aerodynamic Loads During Launch and Exit, May 1965
SP-8007	Buckling of Thin-Walled Circular Cylinders, Revised August 1968
SP-8008	Prelaunch Ground Wind Loads, November 1965
SP-8009	Propellant Slosh Loads, August 1968
SP-8012	Natural Vibration Modal Analysis, September 1968
SP-8014	Entry Thermal Protection, August 1968
SP-8019	Buckling of Thin-Walled Truncated Cones, September 1968
SP-8022	Staging Loads, February 1969
SP-8029	Aerodynamic and Rocket-Exhaust Heating During Launch and Ascent, May 1969
SP-8030	Transient Loads From Thrust Excitation, February 1969
SP-8031	Slosh Suppression, May 1969

SP-8032	Buckling of Thin-Walled Doubly Curved Shells, August 1969
SP-8035	Wind Loads During Ascent, June 1970
SP-8040	Fracture Control of Metallic Pressure Vessels, May 1970
SP-8042	Meteoroid Damage Assessment, May 1970
SP-8043	Design-Development Testing, May 1970
SP-8044	Qualification Testing, May 1970
SP-8045	Acceptance Testing, April 1970
SP-8046	Landing Impact Attenuation for Non-Surface-Planing Landers, April 1970
SP-8050	Structural Vibration Prediction, June 1970
SP-8053	Nuclear and Space Radiation Effects on Materials, June 1970
SP-8054	Space Radiation Protection, June 1970
SP-8055	Prevention of Coupled Structure-Propulsion Instability (Pogo), October 1970
SP-8056	Flight Separation Mechanisms, October 1970
SP-8057	Structural Design Criteria Applicable to a Space Shuttle, Revised March 1972
SP-8060	Compartment Venting, November 1970
SP-8061	Interaction with Umbilicals and Launch Stand, August 1970
SP-8062	Entry Gasdynamic Heating, January 1971
SP-8063	Lubrication, Friction, and Wear, June 1971
SP-8066	Deployable Aerodynamic Deceleration Systems, June 1971
SP-8068	Buckling Strength of Structural Plates, June 1971
SP-8072	Acoustic Loads Generated by the Propulsion System, June 1971
SP-8077	Transportation and Handling Loads, September 1971

SP-8079	Structural Interaction with Control Systems, November 1971
SP-8082	Stress-Corrosion Cracking in Metals, August 1971
SP-8083	Discontinuity Stresses in Metallic Pressure Vessels, November 1971
SP-8095	Preliminary Criteria for the Fracture Control of Space Shuttle Structures, June 1971
SP-8099	Combining Ascent Loads, May 1972
SP-8104	Structural Interaction With Transportation and Handling Systems, January 1973
SP-8108	Advanced Composite Structures, December 1974

GUIDANCE AND CONTROL

SP-8015	Guidance and Navigation for Entry Vehicles, November 1968
SP-8016	Effects of Structural Flexibility on Spacecraft Control Systems, April 1969
SP-8018	Spacecraft Magnetic Torques, March 1969
SP-8024	Spacecraft Gravitational Torques, May 1969
SP-8026	Spacecraft Star Trackers, July 1970
SP-8027	Spacecraft Radiation Torques, October 1969
SP-8028	Entry Vehicle Control, November 1969
SP-8033	Spacecraft Earth Horizon Sensors, December 1969
SP-8034	Spacecraft Mass Expulsion Torques, December 1969
SP-8036	Effects of Structural Flexibility on Launch Vehicle Control Systems, February 1970
SP-8047	Spacecraft Sun Sensors, June 1970
SP-8058	Spacecraft Aerodynamic Torques, January 1971
SP-8059	Spacecraft Attitude Control During Thrusting Maneuvers, February 1971

SP-8065	Tubular Spacecraft Booms (Extendible, Reel Stored), February 1971
SP-8070	Spaceborne Digital Computer Systems, March 1971
SP-8071	Passive Gravity-Gradient Libration Dampers, February 1971
SP-8074	Spacecraft Solar Cell Arrays, May 1971
SP-8078	Spaceborne Electronic Imaging Systems, June 1971
SP-8086	Space Vehicle Displays Design Criteria, March 1972
SP-8096	Space Vehicle Gyroscope Sensor Applications, October 1972
SP-8098	Effects of Structural Flexibility on Entry Vehicle Control Systems, June 1972
SP-8102	Space Vehicle Accelerometer Applications, December 1972

CHEMICAL PROPULSION

SP-8089	Liquid Rocket Engine Injectors, March 1976
SP-8087	Liquid Rocket Engine Fluid-Cooled Combustion Chambers, April 1972
SP-8113	Liquid Rocket Engine Combustion Stabilization Devices, November 1974
SP-8120	Liquid Rocket Engine Nozzles, July 1976
SP-8107	Turbopump Systems for Liquid Rocket Engines, August 1974
SP-8109	Liquid Rocket Engine Centrifugal Flow Turbopumps, December 1973
SP-8052	Liquid Rocket Engine Turbopump Inducers, May 1971
SP-8110	Liquid Rocket Engine Turbines, January 1974
SP-8081	Liquid Propellant Gas Generators, March 1972
SP-8048	Liquid Rocket Engine Turbopump Bearings, March 1971
SP-8101	Liquid Rocket Engine Turbopump Shafts and Couplings, September 1972
SP-8100	Liquid Rocket Engine Turbopump Gears, March 1974

SP-8088	Liquid Rocket Metal Tanks and Tank Components, May 1974
SP-8094	Liquid Rocket Valve Components, August 1973
SP-8097	Liquid Rocket Valve Assemblies, November 1973
SP-8090	Liquid Rocket Actuators and Operators, May 1973
SP-8119	Liquid Rocket Disconnects, Couplings, Fittings, Fixed Joints, and Seals, September 1976
SP-8112	Pressurization Systems for Liquid Rockets, October 1975
SP-8080	Liquid Rocket Pressure Regulators, Relief Valves, Check Valves, Burst Disks, and Explosive Valves, March 1973
SP-8064	Solid Propellant Selection and Characterization, June 1971
SP-8075	Solid Propellant Processing Factors in Rocket Motor Design, October 1971
SP-8076	Solid Propellant Grain Design and Internal Ballistics, March 1972
SP-8073	Solid Propellant Grain Structural Integrity Analysis, June 1973
SP-8039	Solid Rocket Motor Performance Analysis and Prediction, May 1971
SP-8051	Solid Rocket Motor Igniters, March 1971
SP-8025	Solid Rocket Motor Metal Cases, April 1970
SP-8115	Solid Rocket Motor Nozzles, June 1975
SP-8114	Solid Rocket Thrust Vector Control, December 1974
SP-8041	Captive-Fired Testing of Solid Rocket Motors, March 1971

NASA-Langley, 1977